

Applications of 3 Tesla CMR in acute coronary syndromes (ACS)

Erica Dall'Armellina, MD

St Catherine's College, University of Oxford

Department of Cardiovascular Medicine

Oxford Centre for Clinical Magnetic Resonance Research (OCMR)

Thesis submitted for the degree of Doctor in Philosophy

Hilary Term 2012

Table of Contents

Table of Contents **3**

Acknowledgments **5**

Manuscripts and abstracts arising from this work **8**

Declaration **12**

Abbreviations **13**

Abstract **14**

Chapter 1: Introduction **17**

1.1 Clinical challenges in the Emergency Department: the potential role of CMR 18

1.2 CMR techniques: direct representation of the "ischemic cascade" 19

1.2.1 Acute ischemic injury *22*

1.2.2 Global and segmental function *27*

1.2.3 Myocardial necrosis and fibrosis *28*

1.2.4 Microvascular obstruction and post reperfusion myocardial hemorrhage *30*

1.3 Applications in Acute Coronary Syndromes 34

1.3.1 Non ST elevation acute coronary syndromes *34*

Diagnosis of non ST-elevation acute coronary syndrome in the emergency department *34*

1.3.2 ST elevation acute coronary syndromes *35*

Assessment of salvaged myocardium: a potential way to monitor treatment effects *35*

1.4 Clinical challenges for application of CMR in acute settings 36

1.5 The controversies and the need for new techniques to characterize myocardial tissue: T1 and T2 mapping 37

1.6 Conclusions 40

1.7 Study aims and Hypothesis 40

Chapter 2: Methods **43**

2.1 Patient population 43

2.2 Study protocol 44

2.3 CMR protocol 46

2.3.1 Functional imaging *50*

2.3.2 T2Prep-SSFP *50*

2.3.3 T1-mapping *52*

2.3.4 Late gadolinium enhancement (LGE) imaging *52*

2.4 Post processing 53

Chapter 3. Validation and reproducibility of T2W images analysis. **60**

3.1 Introduction 60

3.2 Aims 63

3.3 Methods 64

3.4 Results 67

3.5 Discussion 78

3.6 Conclusions 80

Chapter 4: Dynamic changes of oedema and late gadolinium enhancement after ST elevation acute myocardial infarction and their relationship to functional recovery and salvage index 81
4.1 Introduction 81
4.2. Aims 82
4.3 Methods 83
4.4 Results 86
4.5 Discussion 103
4.6 Limitations 108
4.7 Conclusions 109

Chapter 5: 3T CMR depict myocardial injury downstream remote coronary plaques in patients presenting with acute myocardial infarction 110
5.1 Introduction 110
5.2. Aims 111
5.3 Methods 112
5.4 Results 119
5.5 Discussion 137
5.6 Limitations 140
5.7 Conclusions 141

Chapter 6: Cardiovascular magnetic resonance by non contrast T1 mapping allows assessment of severity of injury in acute myocardial infarction 142
6.1 Introduction 142
6.2 Aims 145
6.3. Methods 145
6.4 Results 150
6.5 Discussion 167
6.6 Limitations 172
6.7 Conclusions 173

Chapter 7: General conclusions and outlook 174

References 178

Index of Figures 195

Index of Tables 202

Appendix A 203
Ethical approval 203

Appendix B 216
PIL for patients 216

Appendix C 233
Consents Forms 233

Acknowledgments

These last years of research have been special thanks to the people I had the opportunity to work with: they all taught me the love for science and that the greatness of a scientific idea lays in its simplicity.

Professor Robin Choudhury has been a brilliant enthusiastic supervisor, he has always been very supportive and he encouraged me through the past years; he always valued my work and he showed me the way in academia.

Thanks to Professor Stefan Neubauer I had the opportunity to work in a stimulating environment and to grow in the field of research; he taught me qualities such as thoroughness and persistence; he gave me a fantastic opportunity.

I am sincerely grateful to both for their mentorship and support in these years: they have been of great inspiration in deciding my future path.

Thanks to all my colleagues in OCMR, AVIC and "Level 6": they have all been, very supportive and they made the days enjoyable even during the hardest times. A special thanks to my closest collaborators and friends: Dr. Vanessa Ferreira for her continuous help and for making the AHA meeting 2011 " memorably psychic", Dr Sacha Bull for introducing me to the Oxford University Choir and for making my hours outside work "fun" and entertaining (she will always be remembered as the "best of the best" and the president of the OCMR running and fine dining club), Dr. Cameron Holloway for his support, advise and for showing me how not to take things too seriously, Dr. Ntobeko Ntusi: I will always remember his morning greeting "buongiorno principessa", Dr. Sairia Dass for her optimism and her energy.

To my parents for believing in my choices and for being always there for me with a big smile and lots of encouragement. Being apart is not always easy but with their support they made this possible.

Last but not least, thanks to my Jürgen, for being always proud of me and for being at my side in every step of my career. To Jürgen, a righteous man and a man of science.

My research was possible thanks to the Oxford Biomedical Research Centre who funded me.

“When bad things happened, we just calmly laid out all the options, and failure was not one of them.”
Apollo 13 FDO Flight Controller Jerry Bostick

“If I have seen further than others, it is by standing upon the shoulders of giants.”
Isaac Newton quotes (English Mathematician and Physicist, "father of the modern science", 1642-1727)

Manuscripts and abstracts arising from this work

Manuscripts

Dall'Armellina E, Cuculi F, Choudhury RP, Neubauer S, Kharbanda RK.
Embolic myocardial infarction in atrial fibrillation: multiple territory injury revealed by cardiac magnetic resonance.
Eur Heart J. 2010 Nov; 31(21): 2624. Epub 2010 Jul 6.

Dall'Armellina E, Karamitsos TD, Neubauer S, Choudhury RP.
CMR for characterization of the myocardium in acute coronary syndromes.
Nat Rev Cardiol. 2010 Nov; 7(11): 624-36. Epub 2010 Sep 21

Dall'Armellina E, Karia N, Lindsay AC, Karamitsos TD, Ferreira V, Robson MD, Kellman P, Francis JM, Forfar C, Prendergast BD, Banning AP, Channon KM, Kharbanda RK, Neubauer S, Choudhury RP.
Dynamic changes of oedema and late gadolinium enhancement after acute myocardial infarction and their relationship to functional recovery and salvage index.
Circ Cardiovasc Imaging. 2011 May 1; 4 (3): 228-36. Epub 2011 Mar 29

Dall'Armellina E, Choudhury RP.
The Role of Cardiovascular Magnetic Resonance in Patients With Acute Coronary Syndromes
Progress in Cardiovascular Diseases 2011 November-December; 54 (3) 230-239

Dall'Armellina E. Piechnik S.K.; Ferreira V.M.; Le Si Q., Robson D.M.; Francis JM.; Cuculi F.; Kharbanda R.K; Banning A.P.; Choudhury R.P.; Karamitsos T.D., Neubauer S.
Cardiovascular magnetic resonance by non contrast T1 mapping allows assessment of severity of injury in acute myocardial infarction
JCMR 2012: 14 (1) 15

Abstracts

T1-Mapping is Superior to T2-Weighted Cardiovascular Magnetic Resonance Imaging for the Detection of Acute Reversible Myocardial Injury
Vanessa M Ferreira, Stefan K Piechnik, **Erica Dall'Armellina**, Theodoros D Karamitsos, Jane M Francis, Robin P Choudhury, Matthias G Friedrich, Matthew D Robson, and Stefan Neubauer
Circulation. 2011; 124:A16312, presented at the America Heart Association (AHA) Scientific Sessions in Orlando Florida US, in November 2011

CMR T1 Mapping at 3T characterizes the Extent of Acute Ischemic Myocardial Injury: Comparison to Standard Techniques
Erica Dall'Armellina, Stefan Piechnik, Vanessa Ferreira, Theodoros D Karamitsos, Jane M Francis, Florim Cuculi, Colin Forfar, Bernard D Prendergast, Adrian P Banning, Keith M Channon, Rajesh K Kharbanda, Matthew D Robson, Robin P Choudhury, and Stefan Neubauer
Circulation. 2011; 124: A10659, presented at the America Heart Association (AHA) Scientific Sessions in Orlando Florida US, in November 2011

Non-Contrast T1-Mapping is a Novel Diagnostic Tool for Acute Myocarditis on Cardiovascular Magnetic Resonance Imaging
Vanessa M Ferreira, Stefan K Piechnik, **Erica Dall'Armellina**, Theodoros D Karamitsos, Jane M Francis, Robin P Choudhury, Attila Kardos, Matthias G Friedrich, Matthew D Robson, and Stefan Neubauer
Circulation. 2011; 124: A16486, presented at the America Heart Association (AHA) Scientific Sessions in Orlando Florida US, in November 2011\

Early Dynamic Changes in 'Salvaged Area at Risk' Assessed by Serial MRI at 3t in Patients With Acute Coronary Syndrome
Erica Dall'Armellina, Alistair C Lindsay, Matthew D Robson, Theodore Karamitsos, Jane M Francis, Keith M Channon, Adrian P Banning, Rajesh Kharbanda, Stefan Neubauer, and Robin P Choudhury
Circulation. 2009;120: S370, presented at the America Heart Association (AHA) Scientific Sessions in Orlando Florida US, in November 2009

Characterization of acute myocardial infarction by pre-contrast T1 mapping
Erica Dall'Armellina, Stefan K Piechnik, Vanessa Ferreira, Jane M Francis, Matthew D Robson, Florim Cuculi, Rajesh Kharbanda, Adrian P Banning, Robin P Choudhury, Theodoros Karamitsos, Stefan Neubauer

Journal of Cardiovascular Magnetic Resonance 2012, **14**(Suppl 1): P28 (1 February 2012), presented at the 15th Annual SCMR (Society of Cardiovascular Magnetic Resonance) Scientific Sessions in Orlando Florida US, in February 2012

Quantification of acute myocardial injury in STEMI patients post revascularization at 3Tesla. Comparison of T1-mapping, late gadolinium and oedema imaging
Dall'Armellina Erica, Stefan K Piechnik, Vanessa M Ferreira, Theodoros D Karamitsos, Jane M Francis, Matthew D Robson, Robin P Choudhury, Stefan Neubauer

Journal of Cardiovascular Magnetic Resonance 2011, **13**(Suppl 1):P146 (2 February 2011) presented at the 14th Annual SCMR (Society of Cardiovascular Magnetic Resonance) Scientific Sessions in Nice, France, in February 2011

Gaussian modelling for operator-independent and threshold-free volumetric segmentation of phase sensitive inversion recovery late gadolinium enhanced images
Stefan K Piechnik, **Erica Dall'Armellina**, Vanessa M Ferreira, Matthew D Robson

Journal of Cardiovascular Magnetic Resonance 2011, **13**(Suppl 1):P43 (2 February 2011) presented at the 14th Annual SCMR (Society of Cardiovascular Magnetic Resonance) Scientific Sessions in Nice, France, in February 2011

Quantification of acute myocardial injury by ShMOLLI T1-Mapping, T2-weighted and late gadolinium imaging in patients presenting with chest pain, positive troponins and non-obstructive coronary arteries
Vanessa M Ferreira, Stefan K Piechnik, **Erica Dall'Armellina**, Theodoros D Karamitsos, Jane M Francis, Matthias G Friedrich, Matthew D Robson, Stefan Neubauer

Journal of Cardiovascular Magnetic Resonance 2011, **13**(Suppl 1):P16 (2 February 2011) presented at the 14th Annual SCMR (Society of Cardiovascular Magnetic Resonance) Scientific Sessions in Nice, France, in February 2011

Differentiation of acutely infarcted myocardium by quantitative differences in T1 relaxation times using Shortened Modified Look-Locker Inversion Recovery (ShMOLLI) in 3T.
Erica Dall'Armellina, Stefan K Piechnik, Vanessa M Ferreira, Stefan Neubauer, Matthew D Robson

Journal of Cardiovascular Magnetic Resonance 2010, **12**(Suppl 1):P172 (21 January 2010) presented at the 13th Annual SCMR (Society of Cardiovascular Magnetic Resonance) Scientific Sessions in Phoenix, AZ, USA, in February 2010

Time course of myocardial oedema in acute coronary syndrome assessed at 3 T using a bright blood T2-prepared SSFP sequence
Erica Dall'Armellina, Alistair C Lindsay, Matthew D Robson, Theodoros D Karamitsos, Jane M Francis, Keith M Channon, Adrian P Banning, Rajesh Kharbanda, Robin P Choudhury, Stefan P Neubauer

Journal of Cardiovascular Magnetic Resonance 2010, **12**(Suppl 1):P149 (21 January 2010) presented at the 13th Annual SCMR (Society of Cardiovascular Magnetic Resonance) Scientific Sessions in Phoenix, AZ, USA, in February 2010

Pre-contrast T1 mapping allows assessment of severity of acute ischaemic myocardial injury
E Dall'Armellina, S Piechnik, V M Ferreira, M D Robson, J M Francis, F Cuculi, R K Kharbanda, A P Banning, R P Choudhury, T D Karamitsos, S Neubauer

Heart 2012; **98**: Suppl 1 A52 doi:10.1136/heartjnl-2012-301877b.90, presented at the BCS (British Cardiac Society) Annual Conference in Manchester, UK, in May 2012

Dynamic changes of oedema and late gadolinium enhancement after acute myocardial infarction and their relationship to functional recovery and salvage index
E Dall'Armellina, N Karia, A Lindsay, T D Karamitsos, V Ferreira, M D Robson, P Kellman, J M Francis, C Forfar, B Prendergast, A P Banning, K Channon, R J Kharbanda, S Neubauer, R P Choudhury

Heart 2011; **97:Suppl** 1 A12-A13 doi: 10.1136/heartjnl-2011-300198.14, presented at the BCS (British Cardiac Society) Annual Conference in Manchester, UK, in June 2011

Declaration

I declare that the work presented in this thesis is my own and has not been submitted for any other degree in this or any other University or Institute of learning.

I participated in the design of the study and I wrote the ethics; I organised and coordinate adequate premises in order to be able to scan the acute patients in a safe environment and guarantee adequate monitoring. In order to guarantee the safety of the patients I coordinated a team of people who were familiar with the protocol and with the standard operating procedures. On a daily basis, I screened new admission for primary PCI and chest pain in coronary care unit, emergency department, and wards. I consented and recruited the patients; I performed the acute scans. I organised, coordinated and performed the follow up visits and scans.

Dr. A.Lindsay, Dr. V. Ferreira and Mrs. Jane Francis were part of the " acute scanning team " and provided support during the scans. They also performed a few follow up scans when I was not available.

Prof. A. Arai and Dr. P. Kellman from the NIH Institute, Bethesda, US provided the unit with the T2Prep SSFP sequence for T2 W imaging.

Dr. M. Robson and Dr. S. Piecknick provided physics support for the T1 mapping / SHMOLLI work leading of the results of chapter 6. I analysed the imaging data and performed statistical analyses. I wrote the manuscripts and the thesis.

Abbreviations

ACS, acute coronary syndrome

AHA, American Heart Association

CABG, coronary artery by-pass

CMR, cardiovascular magnetic resonance

EDV, end-diastolic volume

EF, Ejection fraction

ESV, end-systolic volume

ECG, electrocardiogram

LAD, Left Anterior Descending

LCx, Left Circumflex

LGE, late gadolinium enhancement;

LV, left ventricle

MI, myocardial infarction

MO, microvascular obstruction

NSTE-ACS, Non ST elevation acute coronary syndrome

NSTEMI, Non ST elevation myocardial infarction

PCI, percutaneous coronary intervention

RCA, Right Coronary Artery

STE-ACS, ST elevation coronary syndrome

STEMI, ST elevation myocardial infarction

T2W, T2-weighted

SV, stroke volume

WMSI, wall motion score index.

Abstract

Applications of 3T CMR in acute coronary syndromes (ACS)

Erica Dall'Armellina, MD, St Catherine's College, DPhil, Hilary Term 2012

Introduction

There is a pressing clinical need to treat patients with acute coronary syndrome (ACS) timely and efficiently in order to improve their prognosis. Standard tools available in ED, while useful, do not comprehensively characterize ACS for either diagnosis or risk stratification. The role of CMR in ACS is emerging because it allows assessment of both myocardial composition and function. Newer CMR techniques such as: a) T2 W imaging for assessing myocardial oedema and area at risk B) pre contrast T1 mapping techniques for quantitative characterization of the tissue composition, are adding further utility for CMR in ACS. At present the clinical use of these techniques is still limited and further investigations are needed to assess their clinical applicability in ACS patients.

Aims

The aims of this thesis were several. Firstly we sought to establish a CMR protocol for imaging ACS patients on a 3T CMR scanner. In order to do so, we validated a novel T2 W technique for oedema imaging (T2 prep SSFP) at 3T. Second, we aimed to perform a detailed study of the time course of oedema in ACS patients in order to establish the appropriate imaging time for the assessment of area at risk. Third, by applying T2W acute oedema imaging, we sought to investigate the functional and pathological meaning of complicated remote plaques in patients with multivessel disease. Finally, we aimed to establish whether, in comparison to standard CMR techniques, novel precontrast T1

mapping allows better characterisation of the acutely injured myocardium and whether it can predict long-term functional recovery.

Methods

The research studies were all performed on a 3T Trio Siemens scanner. In the initial stage of the research, we validated the T2 W technique performing phantom work and scanning both volunteers and patients to assess the uniformity of signal intensity in the myocardium and to establish a threshold based method to post process the images. We then established a CMR protocol for ACS including oedema imaging, T1 mapping imaging, perfusion, functional and late gadolinium enhancement imaging. Patients with acute myocardial infarction (both ST elevation myocardial infarction (STEMI) and non STEMI) were scanned at 4 different time points after the acute event (3 scans within 2 weeks and one at 6 months). All STEMI patients underwent primary percutaneous coronary intervention (PCI) while the non-STEMI patients underwent coronary angiography and /or PCI.

Results

We validated the T2prep SSFP technique at 3T, highlighting its limitations and establishing a threshold of mean ± 2SD to assess myocardial oedema. We found that the optimal imaging window to assess the maximal expression of myocardial oedema was within 1 week from the acute event in patients with ST elevation MI. Also, our results showed a reduction of LGE over time (from acute to chronic) in segments which also showed improvement in contractile function indicating that even segments with transmural LGE assessed in the early hours post event could be viable. By applying these techniques in acute patients with bystander disease undergoing percutaneous coronary

intervention, we found that: 1) T2W imaging can detect myocardial injury downstream from a vessel identified as “non culprit” 2) in 20% of NSTEMI patients, the angiographic assessment alone failed to identify the culprit vessel.

Finally, we found that the diagnostic performance of acute pre-contrast T1-mapping was at least as good as that of T2W CMR for detecting myocardial injury. There was a significant relationship between the segmental damaged fraction assessed by either by LGE or T2W, and mean segmental T1 values and the likelihood of improvement of segmental function at 6 months decreased progressively as acute T1 values increased.

Conclusions

In summary, we defined a stable imaging window for the retrospective evaluation of area at risk and we also indicated that acutely detected LGE does not necessarily equate with irreversible injury and may severely underestimate salvaged myocardium. Furthermore, in NSTEMI patients with multivessel disease, by revealing acute myocardial damage in territories pertaining to vessels not treated acutely, we raised the issue of the need for better tools for the correct identification of the culprit vessel and to stratify patients rather than by angiographic assessment alone.

Finally, we demonstrated how pre-contrast T1 mapping allows for assessment of the extent of myocardial damage and how T1 mapping might become an important complementary technique to LGE and T2W for the identification of reversible myocardial injury and the prediction of functional recovery in acute MI.

Chapter 1: Introduction

While treatment of acute coronary syndromes (ACS) has advanced rapidly in the past 20 years, the diagnostic tools at the point of presentation remain the electrocardiogram (ECG), blood biomarkers and ultrasound [Sabia 1991] which give only a partial insight into a complex process. Even when clinical findings clearly demonstrate myocardial ischemia or infarction (MI) in progress, current investigations yield very little information on the extent or stage of evolution of infarction or, critically, on the potential for recovery with reperfusion or other interventions. New clinical tools for more accurate diagnosis and risk stratification are needed.

Because of its ability to characterize soft tissue, cardiovascular magnetic resonance (CMR) has the versatility to evaluate a range of states of the myocardium that are of potential importance in enhancing diagnostic complexity. Established CMR techniques (such as SPSS cine imaging, FLASH first pass perfusion imaging and LGE scar imaging) already widely applied in the assessment of stable syndromes, provide accurate assessment of left ventricular function, perfusion and myocardial viability for a comprehensive assessment of status of the myocardium, which may inform decisions on the appropriateness and nature of revascularization. Recently, new applications (such as T2 W oedema imaging and T2/T1 mapping) are emerging to further characterize changes in myocardial tissue and identify acute ischemic events [Aletras 2008, Kellman 2007]. The clinical application of new sequences for T2W and T1mapping in patients with ACS have been investigated in this thesis to obtain new details on the acute CMR features compared to the traditional standard techniques to assess acute myocardial injury. In this chapter as introduction to my thesis, I will explain the challenges faced in clinical

practice, the limitations of current diagnostic approaches and I will introduce the innovative CMR applications which will be investigated in this thesis. In order to understand fully the mechanistic insights that could be obtained from the CMR findings in relation to the underlying pathophysiology, I will also relate the features on the CMR images to the pathologic changes happening in the ischemic myocardium.

1.1 Clinical challenges in the Emergency Department: the potential role of CMR

Diagnosis and stratification of patients with chest pain is crucial to address optimal treatment. In ACS time can be a critical factor, as persistently ischemic myocardium risks irreversible injury, which an early intervention may abort. Standard clinical tools such as ECG, or blood biomarkers may detect changes in the myocardium due to acute ischemia. However, two major challenges are commonly experienced: 1) the tools available are often normal or negative at the time of presentation, delaying diagnosis and treatment; 2) even when ECG or biomarkers show alterations indicative of myocardial injury due to ACS, the information that can be derived is limited and often not precise for (i) assessing the extent of the area at risk and (ii) establishing the evolutionary stage of the ischemic injury from early reversible stages to more severe and irreversible changes. Information regarding location of the culprit coronary lesion, distribution and extent of the ischemic injury/area at risk, viability of the myocardium downstream, presence of microvascular impairment cannot be fully or accurately derived from ECG or blood biomarkers or bedside echocardiogram.

1.2 CMR techniques: direct representation of the “ischemic cascade”

CMR techniques potentially offer a way to “display” the changes happening in the myocardium at the different steps of the ischemic cascade. In fact the cessation of blood flow due to ‘upstream’ epicardial artery obstruction and the consequent diminished perfusion ‘downstream’, initiates a pathophysiological cascade of progressive myocardial injury. These changes are initially reversible and, later, irreversible. Within minutes of ischemia, intracellular hypoxia causes a drop of available high-energy phosphates and conformational changes of proteins with subsequent contractile dysfunction. With on-going ischemia, intracellular oedema (within 20-40 minutes) is followed by irreversible injury to cardiomyocytes (starting from the subendocardium around 30-60 minutes) and vascular endothelial cells (after about 60-90 minutes).

Complementary CMR techniques (Table 1) can be used in a single examination to characterize the changes in myocardial tissue composition from early ischemia through to necrosis and to assess the consequent changes in myocardial function.

Table 1.1 Summary of imaging techniques used in cardiac magnetic resonance to assess myocardial tissue changes and function.

Clinical indication	Imaging technique	Application	Target
STANDARD			
LV Function	**Cine (SSFP)**	Functional / Cine imaging	Volumes, regional systolic and diastolic wall motion abnormalities
Myocardial Infarction / viability	**Late Gadolinium Enhancement (LGE)**	Late gadolinium enhancement	Infarct size Microvascular obstruction
NEW			
acute ischemic injury	**Oedema Imaging (STIR/T2W)**	myocardial oedema	Extent of reversible injury
Myocardial salvage	**T2W imaging and LGE**		
RESEARCH			
Ischemia/reperfusion	**T1-T2 mapping**	Tissue composition: myocardial oedema	Salvageable myocardium Myocardial stunning

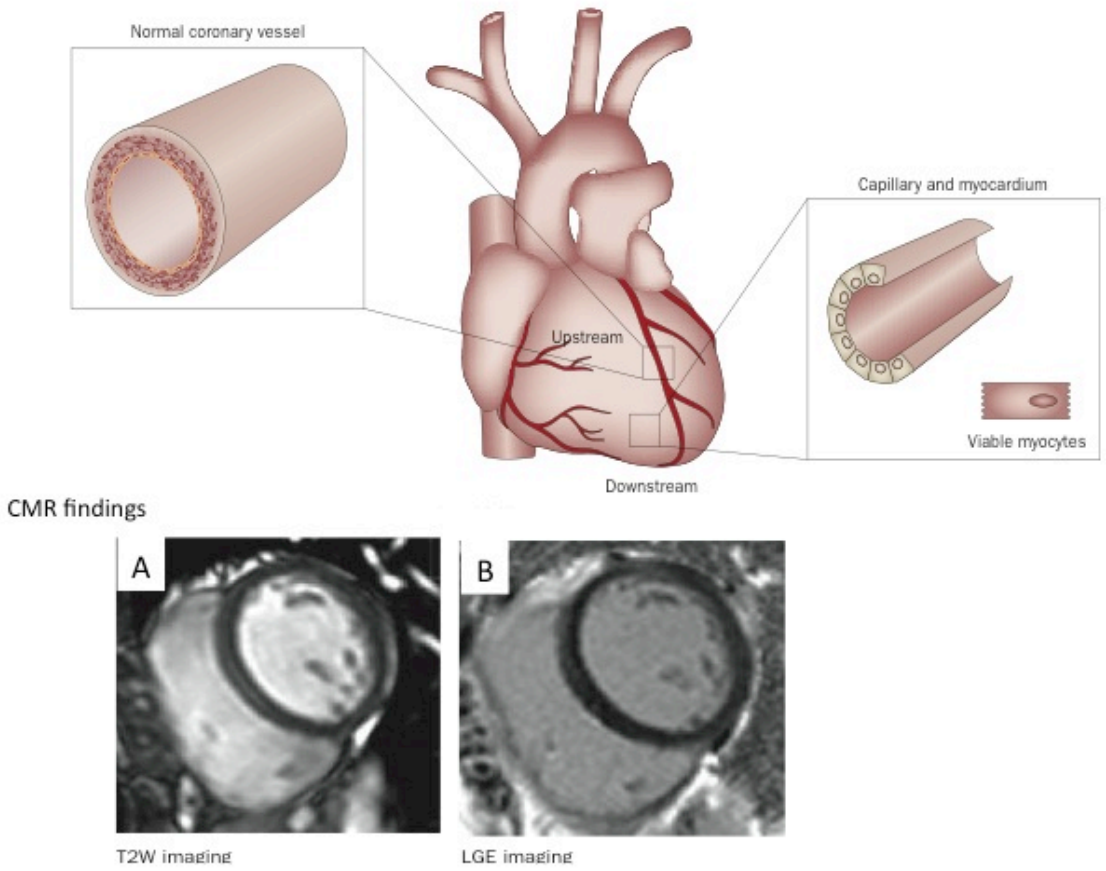


Figure 1.1. Normal CMR findings in the absence of a flow-limiting coronary stenosis. The figure shows a normal coronary vessel, a microvessel, and myocardium. CMR images representing normal findings are shown for a | T2W imaging, and b | LGE imaging. [Dall'armellina 2010]

1.2.1 Acute ischemic injury

The appearance of healthy myocardium on CMR (Figure 1.1) differs from that of ischemic tissue, in which imaging findings correlate with the underlying pathology (Figures 1.2-1.4) Acute changes in the myocardium after coronary occlusion can be assessed using recently developed CMR techniques that depict increased tissue water content (Figure 1.2) In the first 10 minutes following coronary occlusion, the lack of blood supply leads to intracellular metabolic and molecular changes with accumulation of osmotically active substances within the myocytes [Reimer 1983]. At this stage, the increase of intracellular water will be mild and mainly due to a change of binding status leading to release of water from protein bindings [Friedrich 2010]. Ultrastructural changes including mitochondrial swelling may follow by 20-40 minutes [Steenbergen 1985].

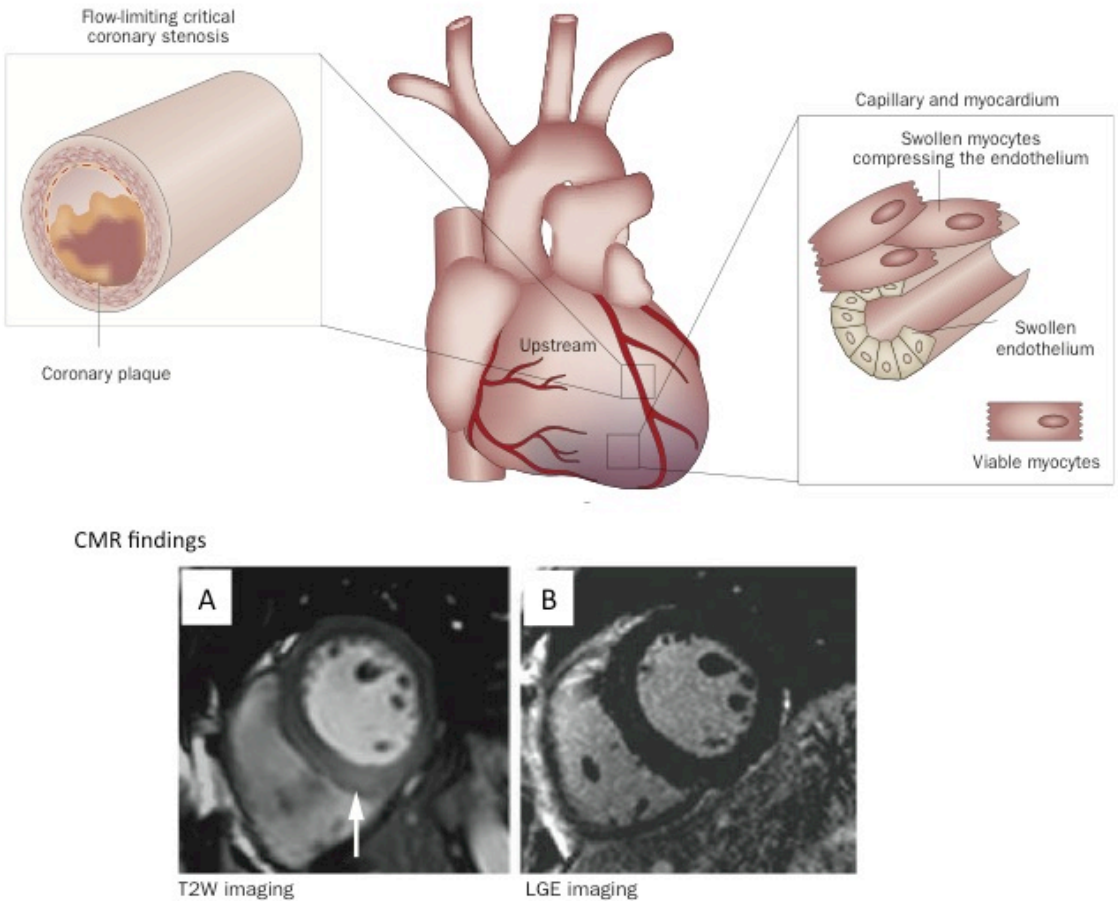


Figure 1.2. CMR findings in the presence of a flow-limiting coronary stenosis. A flow-limiting stenosis leads to downstream microvessel and myocardial changes, including swollen myocytes and initial swelling of endothelial cells. a| As a result of ischemia, initial changes in the myocardium owing to increased myocardial oedema (arrow) are shown on T2W imaging. b| No sign of irreversible damage is depicted by LGE imaging. [Dall'armellina 2010]

At this point, swelling and disruption of the cell membrane in the myocytes may also occur. (Figure 1.3) Following reperfusion, the increase in vascular pressure leads to net increase of tissue water content, which accumulates mostly in the interstitium [Willerson 1977]. Changes in the myocardium were first demonstrated in experimental models of permanent versus temporary ligation with a significant increase in weight of the reperfused hearts at 40 minutes due to interstitial oedema [Willerson 1977]. The ability to assess changes in tissue composition during ischemia and reperfusion could clearly make an important contribution to clinical trials in the context of acute MI. Using the intrinsic properties of CMR to image proton density based contrast, T2-weighted CMR sequences are believed to be able to provide information related to water content [Canby 1987] (Figure 1.2 and 1.3). There is evidence that T2W imaging techniques are sensitive to an increase in water content by only 3% [Higgins 1983]. Furthermore, the change in binding status of the intracellular water during ischemia also appears to determine a relevant change in T2 relaxation time [Knight 1991] (i.e. free water has 40 times longer T2-relaxation time than bound water) [Hazlewood 1974]. Therefore it is thought that T2W imaging may be able to depict early intracellular small changes in water content before the net increase in interstitial water.

Experimental models first demonstrated that 20 to 30 minutes' ischemia followed by reperfusion leads to myocardial oedema that is detectable by CMR techniques [Abdel-Aty 2009, Aletras 2006] and therefore introduced the possibility to identify acutely ischemic myocardium and to differentiate this from chronic MI [Abdel-Aty 2004]. Several CMR sequences to assess myocardial oedema are available including turbo spin-

echo (TSE) with dark blood preparation,[Miller 2001, Wisenberg 1988] short TI inversion recovery pulse sequences and new bright blood T2-prepared SSFP sequences [Kellman 2007] or spin-echo/SSFP Hybrid (ACUT2E)[Aletras 2008]. The latter ones are T2W CMR approaches with more robust image quality as they partially overcome potential artefacts due to through plane motion [Keegan 2006], or to stationary blood [Keegan 2006]; T2-prepared SSFP sequences[Kellman 2007] or spin-echo/SSFP Hybrid (ACUT2E) are currently being tested in clinical environment. In addition, single shot free breathing sequence versions are also available[Kellman 2005] and may be particularly useful in patients who are acutely unwell. For a better quantification of the signal intensity due to a change in composition of the myocardial tissue, methods providing quantitative maps of T2 signal (T2-mapping) are currently being validated [Giri 2009]. The great advantage of T2-mapping will be to address all issues of T2W imaging related to artefacts and allow for an objective assessment of the myocardial oedema. Clinical applications of T2W sequences are described in more detail in Section 1.3.

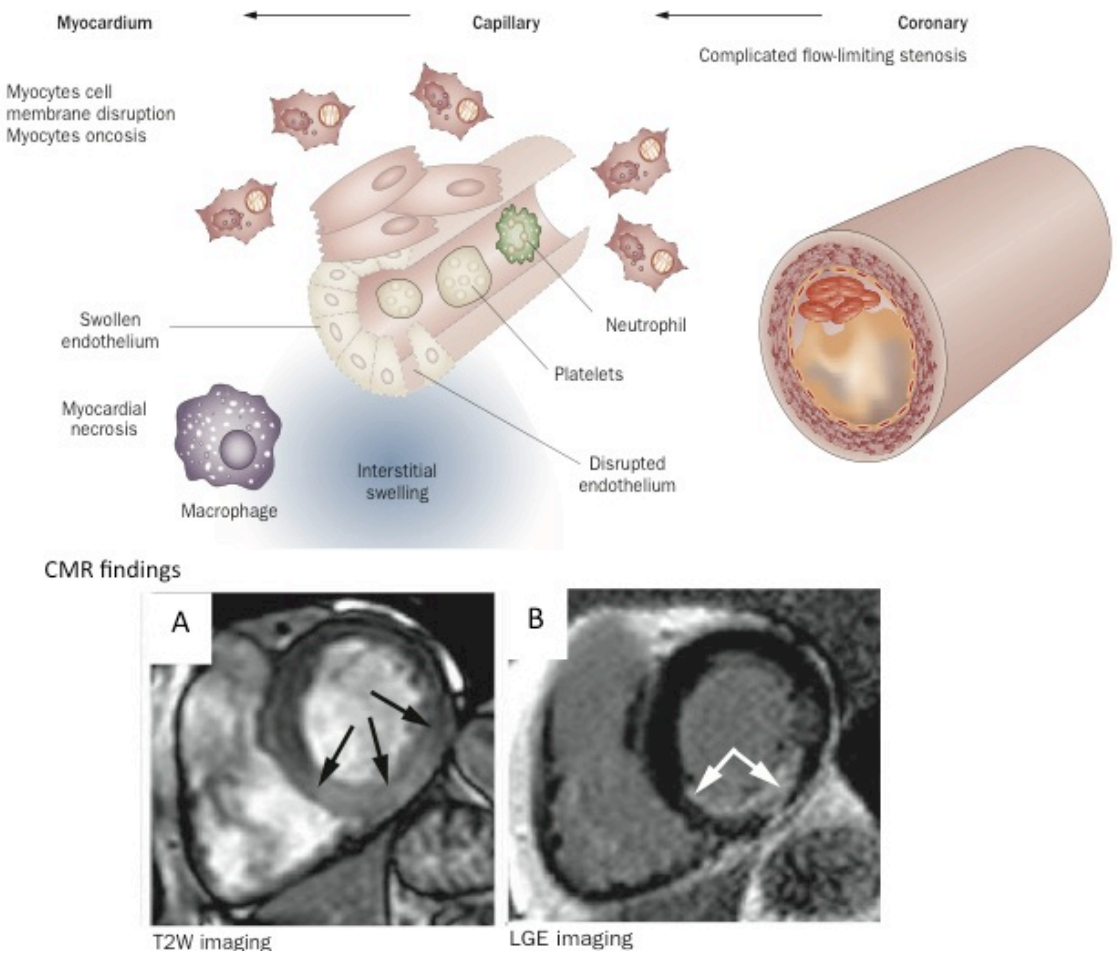


Figure 1.3 Myocardial inflammatory processes following coronary occlusion. A coronary vessel with a complicated plaque may cause long-term lack of oxygen, leading to ultrastructural changes and swelling of the endothelial cells in the capillaries and myocytes. The disruption of the endothelium in the capillaries results in increased content of interstitial water. Oncosis of the myocytes and early stages of myocardial necrosis, including inflammation and infiltration of macrophages, will also occur. a | increased signal intensity on T2W images as a result of myocardial oedema (arrows). b | Presence of myocardial scar (arrows) is revealed by LGE imaging.

1.2.2 Global and segmental function

Acute ischemia is closely followed by diastolic and systolic dysfunction of the affected myocardium due to changes in the supply and utilization of energy. Although the myocytes may still be viable, the onset of severe ischemia has almost an immediate effect on the contractility of the myocardium (stunned myocardium). [Reimer 1983] In case of prolonged ischemia leading to irreversible myocardial injury, the regional wall motion abnormalities may or may not recover post revascularization depending on the transmural extent of scar [Kim 1999]. Fast Cine CMR sequences such as SSFP are considered the gold standard to assess wall motion, volumes, ejection fraction and myocardial mass [Pennell 2004]. High signal to noise ratios (SNR), retrospective gating, rapid data acquisition and reconstruction, SSFP sequences allow acquisition of functional images of the entire cardiac cycle with high contrast between blood pool and myocardium and therefore accurate detection of endocardial border. Sensitivity of resting functional CMR for assessing myocardial injury in the acute setting has been shown to be 85% and significantly superior to: late gadolinium enhancement (LGE) (sensitivity = 62%,) perfusion (sensitivity = 77%) and T2W imaging (sensitivity = 69%). The specificity of resting functional CMR is 86%, slightly higher than LGE (84%) but significantly lower than perfusion (92%) or T2W imaging (100%) [Cury 2008]. Assessment of left ventricular wall thickness by CMR is also very accurate and adds diagnostic value to cine CMR improving sensitivity and specificity for detecting acute MI up to 100% [Cury 2008]. In addition, functional CMR techniques using low dose dobutamine (LDD) as stressor agent are also used to predict functional recovery post revascularization [Baer 1998]. However it is still controversial whether LDD yields a superior diagnostic

accuracy compared to LGE in predicting recovery of function post revascularization in those segments with intermediate severity of hyperenhancement (1-50% transmurality) [Wellnhofer 2004] [Bove 2006] [Kim and Manning 2004]. A combined approach (LGE and LDD) may be foreseen as useful in assessing viability in low risk ACS patients, but has not yet been systematically investigated. Furthermore regional wall motion at rest or under stress can be accurately quantified by strain-encoded techniques [Jung 2006, Korosoglou 2010, Neizel 2009, Rosen 2006]. Some CMR techniques allow to assessment of wall displacement over the cardiac cycle (myocardial tagging, Displacement encoding (DENSE), or they directly encode the velocity of myocardial motion into the MR signal (TPM)) or they may directly report strain (SENC). Such techniques can provide extensive information on strain, shortening and rotation and may reveal new insights in regional wall motion abnormalities in ischemic disease. Recently published data [Korosoglou 2010] show that strain rate encoding during intermediate dose of dobutamine infusion is a more sensitive marker for the detection of inducible ischemia that precedes the development of inducible wall motion abnormalities with moderate 40% to 60% coronary lesions. It remains to be seen if the application of these techniques will provide valuable additional information in the assessment of patients with ACS.

1.2.3 Myocardial necrosis and fibrosis

Prolonged ischemia (40-60 mins) leads to irreversible injury due to the disruption of the intracellular sarcolemma[Jennings 1990] followed by lysis of the myocytes after 2-8 hours (oncosis). (Figure.4) This process progresses from subendocardium towards the epicardium becoming transmural by 6 to 12 hours. [Hedstrom 2009] Interstitial oedema, along with infiltration of polymorphonuclearleukocytes (PMN) and red blood cells will

become evident and small vessels undergo necrosis. Healing mechanisms to repair the injured myocardium will then start from the periphery and include activation of inflammatory processes mediated by macrophages and followed by fibroblast expansion and eventually fibrosis (necrosis) [Go 1988]. Irreversible myocardial injury can be assessed by CMR after administration of gadolinium based contrast agents such as Gd-DTPA [Weinmann 1984]. MR contrast agents are used to induce signal intensity changes by altering magnetic properties of protons in their vicinity. Primary interstitial substances such as Gd-DTPA show a delayed washout from tissue with necrosis or fibrosis and therefore allow myocardial areas with irreversible injury to be visualised [Abdel-Aty 2004]. Although the mechanisms leading to accumulation of Gd-DTPA in myocardial tissue downstream of a total coronary occlusion are not fully understood, positive signal intensity due to gadolinium accumulation in infarcts has been demonstrated both with [Lima 1995] and without reperfusion [De Roos 1989] [Abdel-Aty 2004]. A strong quantitative relationship between the extent of myocardial infarction and hyperenhancement has been demonstrated [Kim 1999]. Late gadolinium enhanced (LGE) CMR is able to detect small volumes of focal injury (in the order of grams)[Nassenstein 2008, Ricciardi 2001] and identifies subendocardial scar not otherwise captured by regional contractile function and nuclear scintigraphy [Wagner 2003]. The accurate assessment of the transmurality of the scar as percentage of the wall thickness [Kim 2000] is crucial to properly identify viability and therefore reversible myocardial dysfunction [Kim 2000].

LGE applications also provide information on the extent of microvascular obstruction [Wu 1998] within the scar itself [Wu 1998]. This aspect will be discussed further.

1.2.4 Microvascular obstruction and post reperfusion myocardial hemorrhage

Microvascular obstruction occurs due to lack of patency of the microvessels (often despite restoration of epicardial artery patency). The angiographic phenomenon known as 'no-reflow' [Kloner 1974, Niccoli 2009, Van Gaal and Banning 2007] is thought to be the result of a complex interaction between inflammatory processes, local injury and distal embolization of atherothrombotic material, which is markedly accelerated by the increase in intravascular pressure due to reperfusion. Using LGE techniques, [Wu 1998] MO appears as a dark hypo enhanced core within the hyper enhanced infarcted area (Figure 1.4). This peculiar appearance is the result of a temporary inaccessibility of the core of the infarct to Gd-DTPA due to loss of function of the microvessels that are plugged with thrombus, cells and oedema. Timing of acquisition of CMR data is crucial as the contrast passively diffuses into areas of MO over time. It is still debated which technique is the optimal but there is consensus that late acquisitions may underestimate the area of MO [Mather 2009]. It is known that MO imaged 2 minutes post injection, is an adverse indicator of functional recovery and clinical outcome [Hombach 2005, Wu 1998]; importantly MO is a predictor of clinical outcomes independently from scar mass and LV function; therefore its assessment is crucial for a comprehensive assessment of the patient and his prognosis. Furthermore, these techniques may aid in the evaluation of reperfusion strategies, which are being

investigated in order to reduce the incidence of MO and improve remodelling of the ventricle [Atar 2009, Sardella 2009].

The phenomenon of the MO is strictly linked to the formation of haemorrhage. Reimer and Jennings showed a high prevalence of haemorrhage in histologic samples from the core of the infarcted myocardium [Reimer 1977]. The authors hypothesized that the causative factor is related to the ischemic injury to the vasculature with consequent loss of structural integrity of the microvessels and haemorrhage. The risk of haemorrhage is increased by late reperfusion, exacerbated in the context of thrombolysis. Recent developments suggest that CMR is able to distinguish the features of haemorrhage *vs.* microvascular obstruction in acute MI [Basso 2007, Ochiai 1999]. Figure 1.4 illustrates the pathological events at tissue level and the corresponding macroscopic CMR images.

The presence of a hypo intense zone on T2*W [Ochiai 1999] has been demonstrated to indicate the presence of myocardial haemorrhage on histology [O'regan 2009]. O'Regan *et al* [O'regan 2009] applied CMR sequences including T2W imaging for oedema, T2* mapping for haemorrhage and LGE, in 15 patients with STEMI who underwent primary PCI within the previous seven days. Results showed presence of haemorrhage (indicated by a T2* decay constant of less than 20 msec) associated with large infarcts and MO in 40% of the patients after reperfusion. Importantly, the presence of haemorrhage has been shown to correlate with a reduced area of myocardial salvage, reduced ejection fraction and to be the strongest independent predictor of adverse left ventricular remodelling compared to baseline LVEF, infarct size and area at risk [Mather 2011]. Similar findings have been demonstrated using T2 weighted CMR imaging [Eitel

2011] [Ganame 2009]. However, the clinical utility of T2W CMR imaging for haemorrhage is not yet established and its use cannot be recommended as yet.

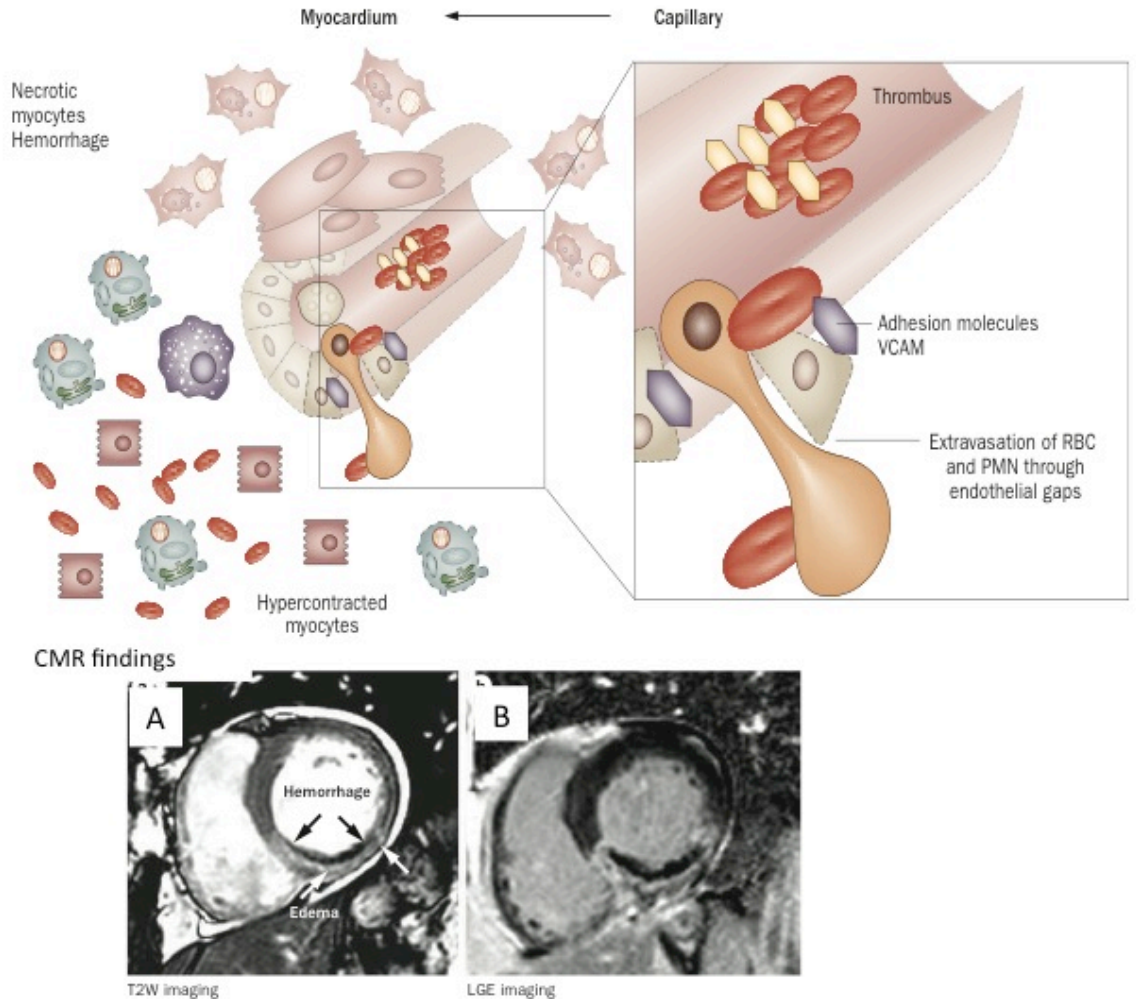


Figure 1.4. Complicated reperfused myocardial infarction. Following restoration of the patency of the vessel, a release of mediators of inflammation and oxidative stress causes damage of the endothelium with loss of function and structural integrity of the endothelial barrier. The combination of increased pressure and loss of structural integrity of the microvessels leads to increased interstitial oedema together with accumulation of polymorphonuclear leukocytes and platelets and extravasation of red blood cells (hemorrhage). These events lead to an obstruction of the microvessels. a | CMR T2W images show the presence of oedema (white arrows). Furthermore, a hypo intense area is consistent with presence of hemorrhage (black arrows), which determines a lack of surrounding perfusion resulting in little contrast penetration on LGE images. b | Microvascular obstruction is depicted by CMR after infusion of gadolinium as a dark core in the hyper enhanced area. Abbreviations: PMN, polymorphonuclear leukocyte; RBC, red blood cell; VCAM, vascular cell adhesion molecule. [Dall'armellina 2010]

1.3 Applications in Acute Coronary Syndromes

Thanks to the new imaging techniques discussed above, CMR applications in CAD including ACS are becoming numerous. In the next paragraphs I intend to discuss how CMR may be helpful in: (i) diagnosis of chest pain in emergency department (ED), (ii) risk stratification of patients with NSTE (non ST elevation)-ACS, (iii) assessment of salvage myocardium in STE (ST elevation)-ACS patients (iv) monitoring treatments effects and determining prognosis in STE-ACS patients.

1.3.1 Non ST elevation acute coronary syndromes

Diagnosis of non ST-elevation acute coronary syndrome in the emergency department

As the scope for CMR characterization of myocardium has increased, the potential application of CMR in ACS has become apparent. Kwong [Kwong 2003] first investigated the diagnostic performance of CMR (including rest perfusion, myocardial function and LGE) compared to clinical assessment based on TIMI risk score, ECG and biomarkers of myocardial injury, (i.e. Troponin and CK-MB) in 161 patients with low probability for CAD within 12 hours of presentation. Out of these, 25 were confirmed to have experienced NSTE-ACS (either unstable angina or infarct). CMR was the strongest predictor of ACS, with significantly higher sensitivity and specificity (84% and 85% respectively) compared to ECG and TIMI risk score.

Depiction of myocardial oedema by CMR T2W techniques [Canby 1987] [Abdel-Aty 2004] in addition to the standard established assessments (function, perfusion and LGE), raises significantly the diagnostic accuracy of CMR imaging at time of admission (82% versus 96%,) as demonstrated by Cury *et al*. [Cury 2008] in 62 patients with chest pain. Furthermore, CMR adenosine stress perfusion has been demonstrated to allow

stratification in patients presenting to ED with NSTE-ACS diagnosis, and predict the need for revascularization [Greenwood 2007]. Results showed that a comprehensive CMR approach (functional, perfusion at rest and after stress, LGE) is significantly more accurate than single CMR method and TIMI risk score (overall accuracy TIMI = 56%, CMR = 94%) to detect the presence of ACS.

1.3.2 ST elevation acute coronary syndromes

Assessment of salvaged myocardium: a potential way to monitor treatment effects

Clinically, salvaged myocardium in acute MI reflects restoration of flow to ischemic tissue aborting threatened infarction. Salvaged myocardium is assessed by CMR as the difference between oedema and scar. The extent of the area of oedema has been shown to be 16 ± 11% larger than the myocardial scar in STE-ACS patients post reperfusion [Friedrich 2008]. Clinically, salvaged myocardium after acute MI is defined by early restoration of flow and, in the long-term, by improvement in contractile function. The recovery of contractile function is inversely related to the transmural extent of LGE. [Kim 2000] Recent data suggest that recovery of wall motion abnormalities is also correlated to resolution of oedema as assessed by T2W imaging [Willerson 1977] [Aletras 2006, Garcia-Dorado 1993]. The assessment by CMR of the dynamic relation between myocardial reversible (area at risk /myocardial oedema) and irreversible damage (as assessed by LGE) is potentially useful to quantify the effects of cardioprotective treatments. The myocardial salvage index (% of salvaged myocardium within the area at risk calculated by (volume of area at risk-volume of scar) / vol area at risk) takes into account the main determinants of salvaged myocardium such as size of the perfusion bed

and the final infarct size. The latter one has been shown to be strictly dependent on the timing of reperfusion in patients with STEMI[Tarantini 2005] as CMR T2W data suggest an inverse correlation between salvaged myocardium and time of reperfusion longer than 90 mins [Francone 2009]. Importantly, STEMI patients who underwent primary PCI and received early treatment resulting in no or minimal scar (aborted MI) as assessed by CMR have a much better prognosis compared to patients with myocardial infarction (cardiac events rate at 6 months 1.7% versus 19.6%, $p<0.01$) [Eitel 2009]. Further investigation is being performed to understand the contribution of myocardial oedema to the impairment of microvascular reperfusion [Phrommintikul 2010] and the development of myocardial irreversible injury . These investigations are needed in order to fully understand which and how specific insights into myocardial status (such as inflammation, haemorrhage or wall stress) might provide information on final infarct size (and/or myocardial salvage). Also, salvaged myocardium has been demonstrated under certain conditions (STE-ACS) but it has not yet been verified in different population with CAD and different underlying pathophysiology (NSTE-ACS).

1.4 Clinical challenges for application of CMR in acute settings

The application of CMR in the acute setting presents significant challenges. Acute coronary syndromes (STE-ACS in particular) require rapid therapeutic intervention, while CMR protocols take time. The duration of a CMR exam for assessment of ACS may vary from 30-40 mins on average for a short standard protocol including time for patient preparation,[Cury 2008] acquisition of T2W, perfusion, SSFP and LGE images to 60-75 minutes for a more advanced protocol with additional stress perfusion in lower risk patients. Furthermore, CMR acquisitions are conducted during breath holding, a

condition that proves difficult to be fulfilled by acutely unwell patients. Also, CMR is contraindicated in claustrophobic patients and in patients with metal implants (including pacemakers, but not coronary stents). In patients with severe impaired kidney function (eGFR< 30 mls/min/1.73m^2), a condition that is relatively common in elderly patients with vascular disease, the use of gadolinium is problematic because it has recently found to have a rare association with the development of Nephrogenic Systemic Fibrosis (NSF), a systemic disease that can potentially result in death, especially in patients with severe kidney impairment[Nacif 2012]. However, these impediments need to be balanced against the detail and diagnostic precision provided by CMR, which provides diverse and complementary information of the heterogeneous consequences of ischemia, offering a comprehensive efficient and cost effective assessment in one single scan [Cury 2008].

1.5 The controversies and the need for new techniques to characterize myocardial tissue: T1 and T2 mapping

There are still many questions that need to be answered in order to improve efficacy of treatment in patients with ACS. The benefits of early intervention [Hasche 1995, Reimer 1977] are currently limited by ischemia-reperfusion injury [Piper 1998]. Complex pathophysiological changes are the cause of the partial inefficiency of reperfusion and they have not been yet entirely clarified. Current knowledge of CMR findings and their relation to the underlying pathophysiology during acute myocardial ischemia is based primarily on experimental research. The main limitation in reproducing / translating experimental knowledge into human model lies in the lack of reproducibility in patients due to the large number of clinical variables (such as time and mode of presentation, preconditioning angina, risk factors, presence of collaterals, effects of

treatments, etc.). This potential variability is even more pronounced in the acute setting due to the dynamic and evolving nature of myocardial ischemic consequences. Although oedema CMR imaging, in combination with LGE, is widely used to assess myocardial salvage, the underlying assumption that bright signal on T2W imaging reflects the area at risk and / or reversible injury is strongly debated [Wince and Kim 2010]. Previous pathological findings by Jennings et al.[Jennings 1985] claim substantial myocardial oedema only in the infarcted area with 5 to 10 fold less oedema in the myocardium reversibly injured [Whalen 1974]. Whether such a difference in myocardial oedema between infarcted and reversibly injured myocardium can be resolved by current CMR T2W techniques has not yet being demonstrated.

Finally, the imaging features of LGE are not simply due to inhomogeneity of the signal. Myocardial scar following infarction usually shows a core and a peri-infarct zone [Yan 2006] which are not easily distinguishable, especially in acute injury due to the presence of myocardial oedema. Therefore, delineation of the borders of the myocardial infarction is highly dependent on the segmentation algorithm and operator, and no optimal technique for a proper quantification is available as yet [Kwong and Farzaneh-Far 2011]. The same issues are valid for quantifying myocardial oedema and there is no clear consensus on the intensity threshold to be used in defining oedema or LGE [Wince 2010]. In fact, whilst 5SD and FWHM are believed to be the most reproducible thresholds in assessing LGE, 2SD is commonly used for assessing oedema. The use of different thresholds for LGE and or oedema is not recommended as the comparison between techniques would be inherently biased [Wince 2010].

New CMR techniques may help to: 1) better understand the pathophysiology of tissue injury and repair e.g. ischemia-reperfusion 2) assess new treatments to prevent/reduce the related myocardial injury. CMR imaging techniques including T1 / T2 / T2* mapping can potentially help identifying acute myocardial injury and increase sophistication of tissue characterization, but further investigation will be needed in order to understand their prognostic value. Techniques to image oedema are prone to artifacts and are not optimal for objective quantification of myocardial oedema [Giri 2009]. New developments (T1 and T2 mapping), which allow direct quantification of changes in myocardial signal intensity on a voxel by voxel level as a result of the change in composition of the myocardial tissue, have recently become available [Giri 2009, Messroghli 2004, Piechnik 2010]. Mapping techniques have only been used in a few studies applying different CMR sequences. Most data have been published on T1 mapping post gadolinium administration in order to assess fibrosis of the myocardium. Iles *et al.* [Iles 2008] showed a significant correlation between T1 values 15 minutes post contrast and collagen volume fraction on myocardial biopsies in 25 patients with heart failure. Messroghli *et al*.[Messroghli 2007] showed that T1 mapping in acute and chronic myocardial infarction increased T1values in acute infarcts before contrast administration. Experimental data on applications of T2 mapping in myocardial infarction demonstrate the ability of this new technique to assess myocardial oedema [Giri 2009] and longitudinal changes in signal intensity and to depict different tissue composition due to myocardial hemorrhage or microvascular obstruction [Ghugre 2011].

In summary these new techniques are very promising not only because they allow more objective quantification myocardial injury, but also more importantly because they

may give more insights into tissue remodeling processes happening in the very early hours post myocardial infarction.

1.6 Conclusions

There is a pressing clinical need to treat patients with ACS promptly and efficiently in order to improve their prognosis. It is commonly appreciated that the standard tools available in ED, while useful, do not optimally or comprehensively characterize ACS for either diagnosis or risk stratification. CMR provides a range of complementary techniques that are extremely useful in assessing both myocardial composition and function. Newer techniques are adding further utility for CMR in ACS. However, at present there are still limitations, which do not allow routine application of these techniques. Further investigations are also needed to prove whether CMR will add information essential to change treatments and outcomes. The role that CMR may play in the future will depend in part on developments that provide for safe monitoring of acutely unwell patients. If CMR fulfils it promise as a safe and accurate imaging technique it should provide pathophysiological insights in patients with ACS in the very first hours and therefore provide a platform for rational treatment selection in individual patients.

1.7 Study aims and Hypothesis

In Chapter 2, I aim to describe the methods used in this study including the patient population, the study protocol, the CMR protocol, and the post processing.

In Chapter 3, I aim to introduce and validate T2W oedema imaging in a protocol for acute imaging at 3T. In order to do so, the preferred technique of choice has been the bright blood single shot T2prep SSFP because it allows for free breathing acquisition and

therefore is more suitable for sick acute patients. I also aim to validate a reproducible method to analyse oedema images by choosing a correct signal intensity threshold.

In Chapter 4, I aim to standardise the optimal imaging time for oedema post ischemic injury. On the grounds of multiple studies published (including clinical trials) aiming to establish the efficacy of new treatments to reduce irreversible myocardial damage and using CMR to assess oedema during a variable time frame of 10 days post event, I reasoned that it was important to provide the optimal imaging window to identify reversible versus irreversible injury. Further, given the potentially important changes happening in the myocardium in the early hours post ischemia, we hypothesised that other CMR findings might be affected as well and therefore we combined LGE acquired early after the event and correlate it to the oedema findings and to the final infarct size at 6 months.

In Chapter 5, in light of the findings related to the optimal imaging time, we aimed to use oedema imaging in ACS (both STEMI and NSTEMI) to assess the functional and pathological significance of bystander disease.

In Chapter 6, given a novel technique T1 mapping (SHMOLLI),[Piechnik 2010] recently developed in our department to further characterise myocardial tissue damage, we aimed to assess the diagnostic performance of this techniques to depict myocardial injury in the early hours post an ischemic event. Further, we aimed to compare the SHMOLLI imaging findings to the standard conventional T2W oedema imaging and late gadolinium imaging used to assess acute ischemic injury. We hypothesised that T1 mapping is more accurate than T2W in depicting small amount of acute myocardial

injury and that T1 values increase in proportion to the amount of injury assessed by T2W and LGE.

Chapter 2: Methods

2.1 Patient population

This prospective study was undertaken in a single tertiary centre. The study protocol was approved by the local ethics committee and all patients gave written informed consent.

Between October 2008 and October 2011, patients presenting with first events identified as acute coronary syndrome (ACS) were eligible if the symptom onset had been < 12 hours prior to presentation to the emergency department. Two subgroups of patients were identified based on the following inclusion criteria:

According to the AHA international guidelines[Kushner 2009] patients were identified as having ST segment elevation MI (STEMI) if their ECG showed ST-segment elevation of at least 0.1 mV in ≥ 2 contiguous limb leads or at least 0.2 mV ≥ 2 contiguous precordial leads. Patients with myocarditis, previous MI, previous revascularization procedure (coronary artery bypass grafts [CABG] or PCI), severe heart valve disease, known cardiomyopathy or hemodynamic instability lasting longer than 12 hours following revascularization were not enrolled. Further exclusion criteria were contraindications to CMR, including implanted pacemakers, defibrillators, or other metallic implanted devices and claustrophobia.

According to the AHA international guidelines,[Anderson 2007] patients presenting with suspected cardiac chest pain or anginal equivalent and either abnormal serum troponin-I (TnI) level or ischemic ECG changes (such as transient or stable ST-segment deviation greater than 0.5 mm (0.05 mV) or T-wave inversion greater than or equal to 2 mm (0.2 mV) were identified as having Non ST-elevation MI (NSTEMI)/ACS.

Acute clinical management for both STEMI and NSTEMI patients was at the discretion of the responsible physician, with the intention to reflect contemporary practice and guidelines (including use of aspiration catheters; glycoprotein IIb IIIa receptor inhibitors and high-dose clopidogrel loading).

Blood sampling

Blood samples were collected for Troponin I at the time of admission and every 12 hours until discharge and during following visits up to 15 days post discharge. After collection, the blood samples were sent to the biochemistry department to be analysed. The Troponin I essay used was the ADVIA Centaur cTnI-Ultra assay with a 10% imprecision at 0.05 µg/l, with a 99th percentile URL of 0.06 µg/l.

2.2 Study protocol

Four separate 3Tesla CMR scans (using a TIM-Trio, Siemens Healthcare, Erlangen, Germany) were performed on each patient at the time points as described below.

In STEMI patients, CMR was performed following primary PCI at: 12 - 48 hours (24H); 5 - 7 days (1W); 14 - 17 days (2W); and 6 months (6M) (Figure 2.1 A)

In the NSTEMI patients, CMR was performed at 12 -48 hours post chest pain onset before coronary angiography; 12- 48 hours post coronary angiography; 5-7 days post coronary angiography and at 6 months. (Figure 2.1 B)

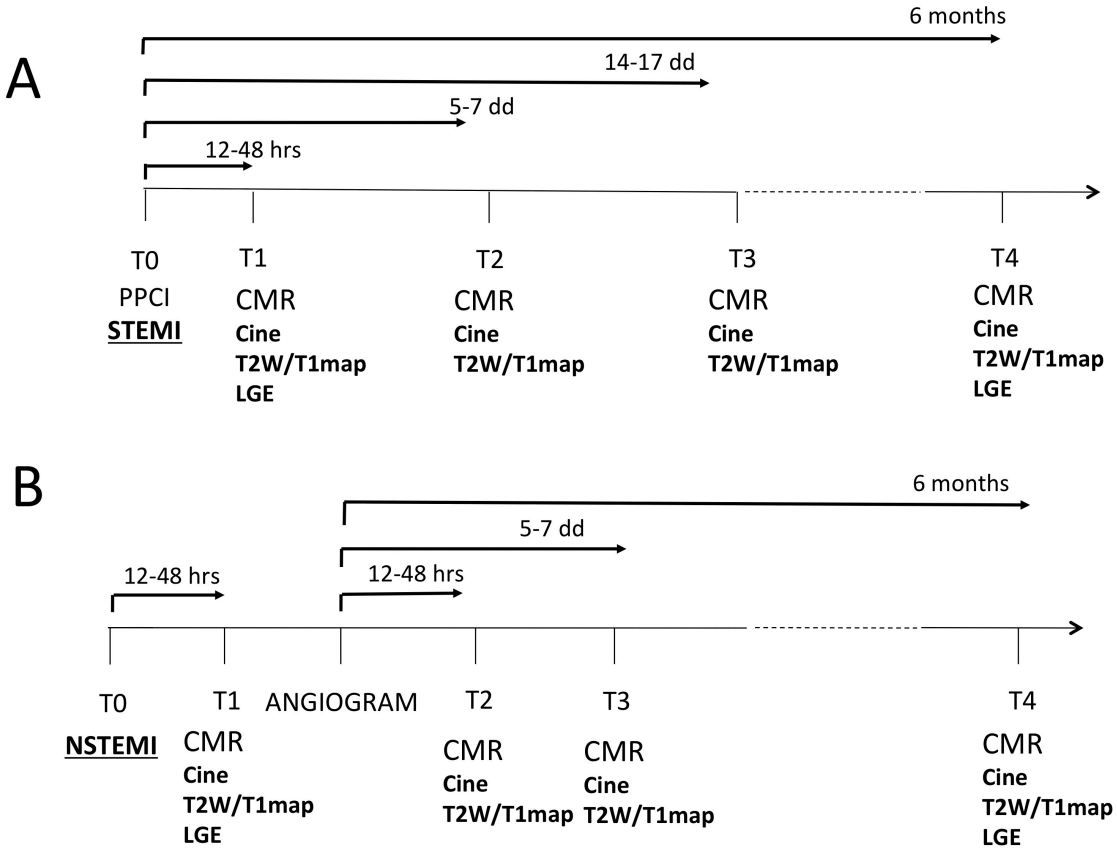


Figure 2.1 Study protocols for (A) STEMI and (B) NSTEMI. Imaging time points (TP) in relation to the acute MI and primary percutaneous coronary intervention (PPCI)/ angiogram and coronary intervention. For each TP, the CMR data acquired is given.

The first and last CMR scans assessed LV function, myocardial perfusion at rest, myocardial tissue characterization using oedema imaging, T1 mapping, LGE. The second and third scans included only functional imaging and tissue characterization imaging based on oedema/T1 mapping imaging (Figure 2.1).

Patients from CCU or ward were transferred to the CMR unit monitored by medical and nursing staff: during the CMR scan, hemodynamic parameters such as blood pressure and heart rate were continuously monitored.

2.3 CMR protocol

The CMR protocol was optimized to reduce the scan time to the minimal possible in consideration of the acute nature and potential clinical instability of the patient population.

An overview of the CMR protocol is reported below (Figure 2.2); details of acquisitions and sequences will be further discussed in dedicated paragraphs.

Identical short axis slices with full coverage of the left ventricle were acquired using different CMR sequences including: 1) T2 weighted (T2-prep) for myocardial *oedema* imaging 2) ShMOLLI T1 mapping for quantitative tissue characterization 3) regional and cardiac function using SSFP CMR sequence 5) LGE imaging (PSIR) for assessment of potentially irreversible myocardial injury and /or scar. LGE was acquired 10-20 minutes post infusion of Gadolinium

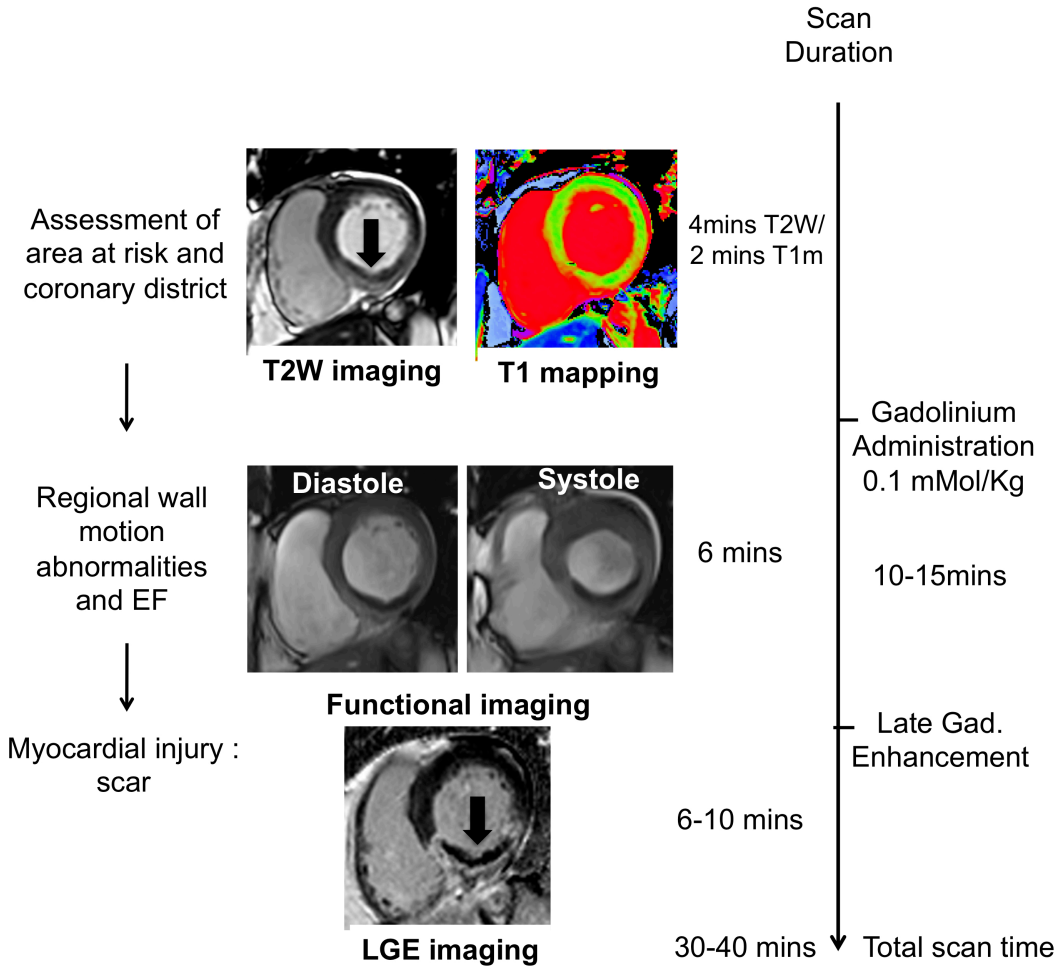


Figure 2.2 Cardiovascular magnetic resonance in ACS. An example of an acute imaging protocol applied in a case of acute inferior myocardial infarction is shown here. The execution of the CMR protocol begins with the acquisition of short-axis T2W oedema imaging, which reveals bright signal in the inferior wall (black arrows in top panel). Matching T1 mapping short axis images are acquired pre administration of gadolinium contrast agent. Within a minute post infusion of the contrast agent early gadolinium imaging can be also performed (not shown here). Functional short-axis images are acquired before the late gadolinium images. As shown in the figure, impairment of regional wall motion is present in the systolic frame at the level of the inferior wall. At the end, 10 to 20 minutes post gadolinium infusion, the presence of co-localized hyper enhancement is also evident on the LGE images (black arrows in bottom panel) in keeping with the other the imaging findings.

Piloting and image acquisition

In order to be able to post-process the images and compare the imaging findings by different CMR modalities, the acquisition of the images was performed using an identical 3D orientation in the field of view. In order to establish such orientation, we initially acquired low-resolution images to localise the heart ("localisers") followed by pilot images (Figure 2.3). Long axis functional images (horizontal long axis (HLA) and vertical long Axis, (VLA) were then planned.

Short axis slices of the heart were acquired parallel to the atrio-ventricular groove in 1 cm increments (slice thickness 8 mm, inter-slice gap 2 mm).

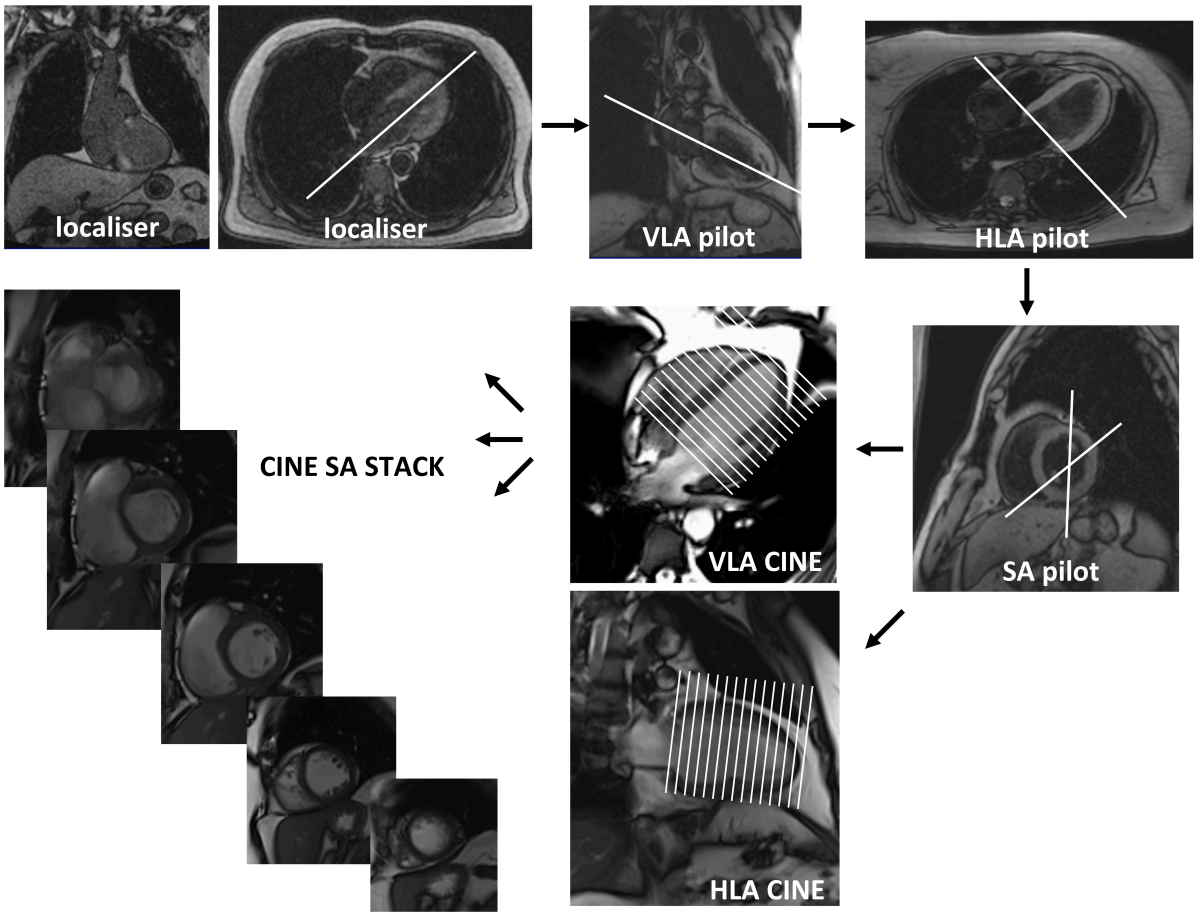


Figure 2.3 Strategy for obtaining short axis images in the same tridimensional orientation. The white lines on the localiser, long-axis and short axis pilots, and long axis cine indicate the slice positions for obtaining the subsequent views demarcated by the black arrows. (Abbreviations= HLA, horizontal long axis; VLA, vertical long axis; SA, short axis)

2.3.1 Functional imaging

After piloting, steady-state free precession (SSFP) cine images using retrospective gating (TE / TR = 1.4 / 3.2 ms; flip angle = 50°; pixel size: 1.6 x 1.6 mm; slice thickness: 8 mm) were acquired. The short axis slices were obtained during a breath-hold at the end of normal expiration to minimize the effects of respiratory motion.

2.3.2 T2Prep-SSFP

Oedema imaging was performed using a T2 prep-SSFP single shot sequence with coil signal intensity correction [Kellman 2007]. Single-shot imaging was chosen as it may be conducted during free breathing, which is desirable in acute patients who may not tolerate breath holding. A spine coil and a phased array 6-channel flexible surface coil were used. Short axis images covering the ventricle and matching slice position with cine images were acquired. Scan parameters were typically: voxel size 2.1 x 1.6 x 8.0 mm, FOV = 400 x 300mm, matrix 144 x 256, TR / TE = 325.38 / 1.14 msec, flip angle 60^{o}, T2 prep duration 60ms, GRAPPA = 2, 20 reference lines, measurements = 8, segments = 84, bandwidth= 977 Hz/Px.

If necessary, shimming and centre frequency adjustments were performed before T2W imaging to generate images free from off-resonance artefacts (example in Figure 2.4). T2 –prep_SSFP are also sensitive to "Gibbs or ringing artefact" (red arrow on Figure 2.4), which appears as a dark endocardial rim parallel to abrupt change in signal intensity in the object at this location. This specific artefact is due to insufficient sampling of high spatial frequency and it is therefore intrinsically linked to the image resolution. Post processing of T2W oedema imaging counted for the intrinsic limitation due to the "Gibbs artefact "as described in the paragraphs below.

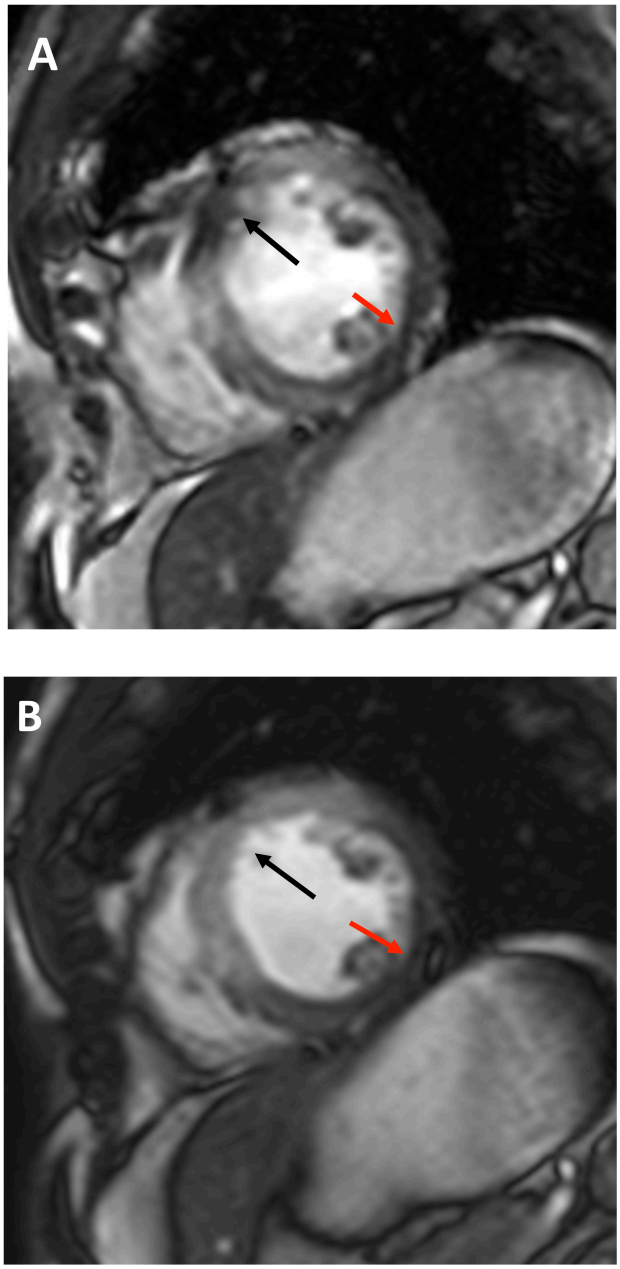


Figure 2.4. Improvement of image quality by shimming and frequency adjustment. On panel A, example of an off-resonance artefact (black arrow) and ringing artefact (red arrow). After performing shimming and frequency adjustment, the image quality has improved with no more artefacts visible.

2.3.3 T1-mapping

Following standard planning, at least 5 short-axis stack images starting from the base of the left ventricle were collected using the newly developed ShMOLLI sequence for T1- mapping [Piechnik 2010]. Images for specific TI were collected using SSFP readouts, typical parameters were: TR / TE = 206.42 / 1.07 msec, flip angle=35º, FOV= 340 x 255 mm, matrix = 192 x 192, interpolated voxel size = 0.9 x 0.9 x 8 mm, GRAPPA = 2, 24 reference lines, cardiac delay time TD = 500 msec; 206 msec acquisition time for single image, phase partial Fourier 6/8. ShMOLLI T1 maps were generated from 5-7 SSFP images with variable inversion preparation time as described previously [Piechnik 2010]. If necessary, shimming and centre frequency adjustments were performed before T1-mapping to generate images free from off-resonance artefacts.

2.3.4 Late gadolinium enhancement (LGE) imaging

Short axis images covering the ventricle and matching slice position with cine images were acquired using a T1-weighted segmented inversion-recovery GRE_PSIR sequence (typically: echo time 2.5ms, voxel size 1.8x1.4x8mm, FOV=360x270mm, matrix 256x152, TR / TE=650 / 2.5 msec, flip angle 20°, GRAPPA=2, 24 reference lines, segments=22, phases=1, concatenations=1, 4 shots per slice, bandwidth 201 Hz/Px) 10 - 20 minutes after the administration of a top-up intravenous bolus of 0.1 mmol/kg body weight of gadolinium contrast agent (Gadodiamide, Omniscan, GE Healthcare, Amersham, UK) at 6ml/s followed by a 15 ml saline flush (at 6ml/s). The inversion time was meticulously adjusted for optimal nulling of remote normal myocardium. In case of

questionable or unexpected LGE findings and to exclude off resonance artefacts, acquisition of image was repeated with phase encoding direction swapped.

2.4 Post processing

The post processing aimed to the analyses of the images in order to obtain the data described in Table 2.1.

Table 2.1. List of the data obtained analysing SA images acquired using different sequences

Sequence	Image orientation	Data
Functional images	SA	LV volumes, EF Regional wall motion scoring/ WMSI
Oedema imaging	SA	LV % damaged volume
T1 mapping	SA	T1 values of the myocardium/ LV % damaged volume
LGE	SA	LV % damaged volume
Oedema/LGE	SA matching slices	Salvaged myocardium

Image co-registration and post-processing analysis

Matching short axis slices acquired by cine, oedema, T1 mapping and LGE, were radially aligned to the position of the papillary muscles. CMR image sets acquired at different time points were analysed in random order by observers blinded to the origin of

the image. The segmentation of each slice included 6 equiangular segments with myocardial anatomical segmentation according to the American Heart Association 17 segment model (excluding segment 17, true apex) [Cerqueira 2002] (Figure 2.5).

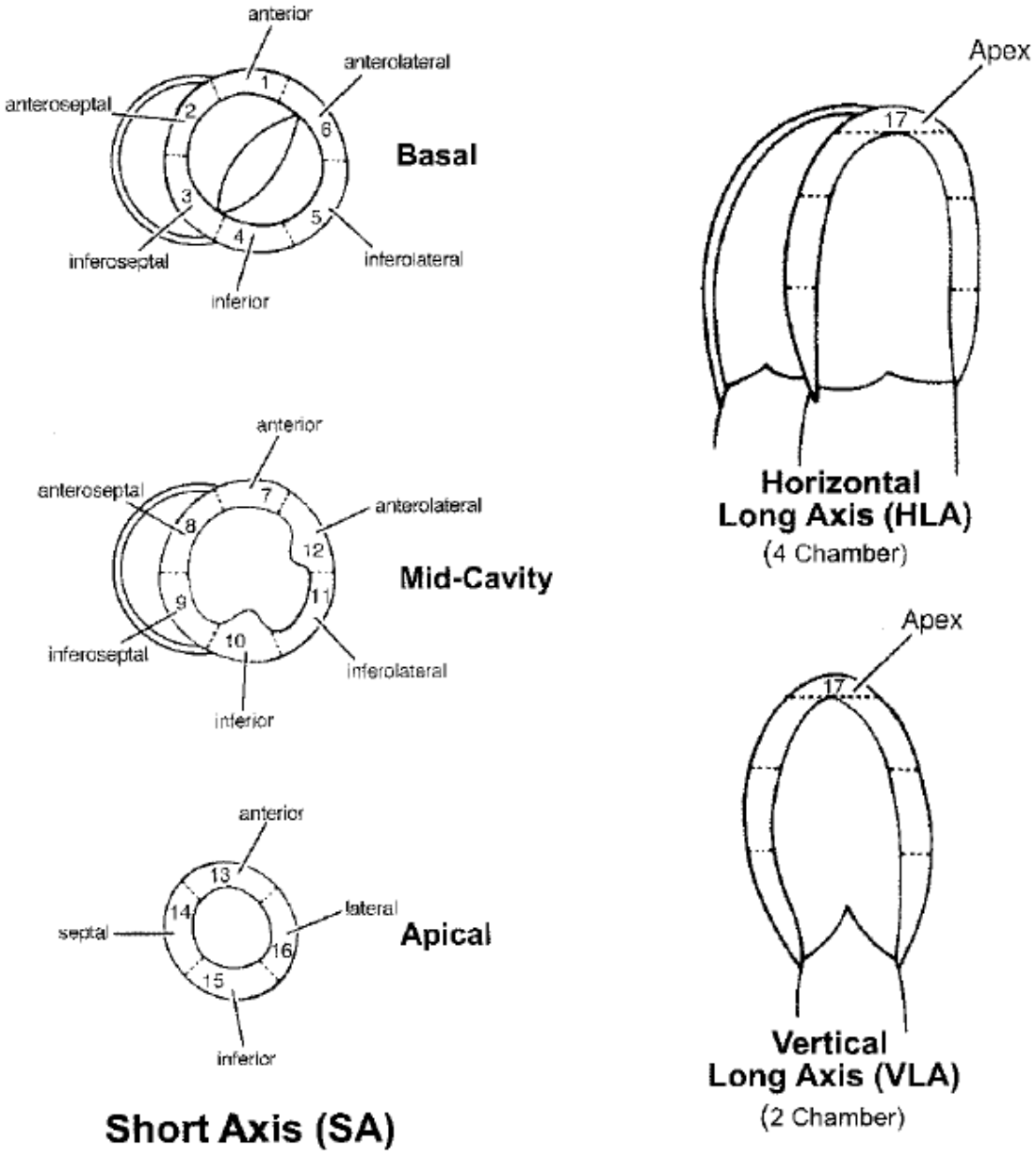


Figure 2.5: Standardized Myocardial 17 segment model (segment number given in each segment) and Nomenclature for Tomographic Imaging of the heart. Adapted from A Statement for Healthcare Professionals From the Cardiac Imaging Committee of the Council on Clinical Cardiology of the American Heart Association [Cerqueira 2002].

Quantification of LV volumes and damaged myocardium

Left ventricular volumes and ejection fractions were calculated from the short axis images using Argus software (Version 2002B, Siemens Medical Solutions) as previously described [Karamitsos 2007]. Injured fractions (injured myocardium volume / slice volume) in each short axis slice both for LGE and T2W images were quantified using computer assisted planimetry in MATLAB version 7.3.0.267 (Natick, USA) by a single experienced operator (ED). Basal slices including LV outflow tract and apical slices were not included in the analysis due to partial volume effects.

For objective quantification of oedema (assessed by T2W) or scar (assessed by LGE), a reference region of interest (ROI) was placed in remote myocardium. The signal intensity threshold indicating increased signal intensity on T2W (oedema)/LGE (scar) images, was imposed 2 standard deviations above the mean intensity of the reference ROI, as previously described [Berry]. Microvascular obstruction (MO) / haemorrhage was defined as the low intensity core within an area of LGE or T2W respectively. Both MO and haemorrhage were included in the measurement of the areas of infarction or oedema.

Inter and intra observer variability for LGE quantification were assessed on 10 patients by two independent observers (see table 2.2.)

Table 2.2. Reproducibility of LGE quantification (% of LV myocardium) assessed with Bland-Altman test on 10 patients.

%LV myocardium	Bias	SD	95% limits of agreement
Intra observer variability (N=10)	-3.3	2.8	- 8.7 - 2.2
Inter observer variability (N=10)	-0.7	9.5	-19.5 - 18.1

A second reader blinded to the results of the first and to the results of PCI and CMR imaging, analysed oedema images to assess inter observer variability on 20 randomly selected patients (Figure 2.6).

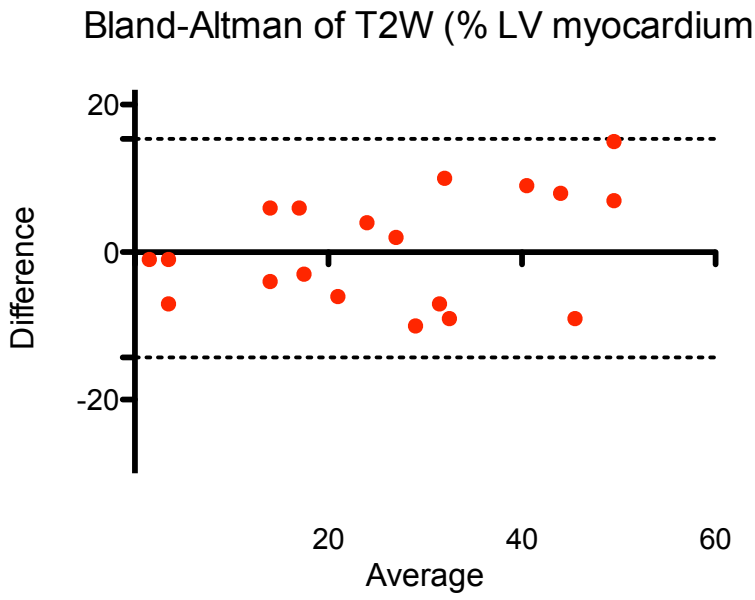


Figure 2.6: Bland-Altman chart illustrating the Inter observer variability for T2W continuous measurements of oedema (% LV myocardium) on 20 patients. Bias is 0.5 with a SD of 7.6, and 95% limits of agreements from -14.3 to 15.3

The index of myocardial salvage was calculated as difference in area between oedema and late gadolinium divided by the area of oedema. Our standardised methods for analysing and calculating LGE, along with reproducibility, have been reported previously [Hudsmith 2006, Porto 2006].

Semi-quantitative assessment of regional function, oedema and late gadolinium

Semi-quantitative assessments of wall motion abnormalities, myocardial oedema and LGE were undertaken by an experienced observer (E.D.) using Argus software (Version 2002B, Siemens Medical Solutions). For regional function, segments were graded: 1 = normal; 2 = hypokinetic; 3 = akinetic or 4 = dyskinetic. Change in regional contraction was defined as a difference of ≥ 1 functional grade between time points. Wall motion score index (WMSI) was defined as the sum of segmental scores divided by the number of segments scored, as previously published [Dall'armellina 2008].

The extent of LGE within each segment was estimated visually and categorized according to the percentage hyper enhanced area of each segment:[Kim 2000] 0 = no LGE; 1 = 1 - 25% LGE; 2 = 26 - 50% LGE; 3 = 51 - 75% LGE and 4 = > 75%. Similarly, the extent of oedema per segment was also assessed visually and categorized for each segment according to an equivalent scoring system. A second blinded reader scored the images for LGE / oedema and wall motion in 20 patients. The infarct size score (% Score) was also calculated based on the scoring system as previously shown[Choi 2001] (sum of all the scores throughout the LV (range 0 to 4) / total number of segments x 4).

T1 mapping analyses

All short axis images were manually contoured using an in-house software MC-ROI (IDL v.6.1, www.ittvis.com) to outline the endo- and epicardium. Each slice was segmented in 6 equiangular segments. Quantitative average T1 values were obtained for each of the 6 segments.

Chapter 3. Validation and reproducibility of T2W images analysis.

3.1 Introduction

While CMR late gadolinium enhancement (LGE) is the gold standard imaging technique to assess myocardial scar in chronic ischemic heart disease, [Kim 2000, Lima 1995] T2-weighted (T2W) CMR is a novel technique, which allows for depiction of myocardial oedema following an acute ischemic insult. Thanks to T2W CMR, it is now possible to differentiate between acute and chronic infarction and to assess reversibly injured myocardium [Abdel-Aty 2009, Abdel-Aty 2004]. Furthermore, the combination of T2W and LGE CMR imaging techniques has been used to derive the important prognostic factor of the "index of salvaged myocardium" (volume of oedema –volume of LGE/volume of oedema) [Friedrich 2008] and to assess the efficacy of treatments in clinical trials [Bøtker 2010, Francone 2009]. Despite these CMR techniques being widely used in clinical trials, there are still on-going contentions regarding 1) the optimal T2W CMR sequence to assess myocardial oedema 2) the post processing/analyses methods used to derive volumes of injured myocardium both on T2W and LGE images, 3) the clinical significance of the acute CMR imaging features.

In this chapter I will:

a) provide an overview on the CMR techniques available to depict myocardial oedema;
b) consider the current methods of analyses and in particular the related issues
c) focus on the validation of a reliable and reproducible method to analyse T2 W CMR images for quantification of myocardial oedema.

T2W sequences

The sequences available to assess myocardial oedema can be divided into two major categories: conventional black blood TSE based and the novel T2-prep SSFP bright blood.

The TSE based sequences have been available for a long time but their applicability has been limited by long breathold acquisitions (not suitable for sick patients), by the low contrast to noise ratio between normal and abnormal, by multiple artefacts, by the presence of a gradient of signal intensity on the image due to the sensitivity profile of the receive radiofrequency coil array and by the inability to implement it at magnetic fields other than 1.5T due to SAR limits. The artefacts are due to: 1) posterior wall motion with signal drop out which happens frequently especially at high heart rates 2) mistriggering and inappropriate sequence timing 3) false brightness at the level of the endocardium due to stagnant blood, especially in the apex and in the case of impaired ventricles. The more advanced STIR sequences with the use of the body coil only [Abdel-Aty 2004], represented a slight improvement in terms of image signal intensity gradient; however long scan times are still needed due the lack of parallel imaging and significant artefacts are still an issue. Novel bright blood techniques (T2 prep SSFP) have been recently demonstrated to overcome the limitations hampering conventional TSE based sequences including artefacts and those related to signal intensity gradient (see details below), and to allow for implementation at higher magnetic field (3T) as well [Kellman 2007]. T2 prep SSFP have also been demonstrated to be superior in detecting myocardial oedema in patients with acute coronary syndromes [Payne 2011].

The challenges of T2W analyses

The analyses of T2W oedema images is challenging for the following reasons: 1) current methods use a region of the myocardium remotely located to estimate normal signal intensity values of the myocardium 2) a signal intensity threshold of 2SD above the mean is used to depict injured myocardium: whether or not this threshold accurately reflects the underlying biological changes happening in the myocardium is matter of controversy. [Wince 2010]

In CMR image post processing, in order to assess changes in signal intensity of the myocardium, it is desirable to use tissues with the same magnetic properties to establish normal signal intensity as reference. While this might be the case for skeletal muscle and myocardium, the choice of a reference ROI externally to the heart is limited by the signal intensity gradient present on the images acquired with conventional TSE based sequences. Therefore, the methods to analyse T2W images published so far, are based on the assumption that the remote myocardium in acute ischemia is normal, and therefore an arbitrary threshold of mean + 2 standard deviations (SD) of the S.I. determined in the remote myocardium is commonly used [Berry 2010, Friedrich 2008]. However, using "remote myocardium" as reference of normal myocardial tissue is a contradiction in terms because although "remote", it is still part of the same injured heart/myocardium and because of the inability to exclude global myocardial involvement [Lee 2012]. Therefore the use of a reference ROI in the remote myocardium could potentially lead to false negative findings.

A technical insight into the T2-prep single shot sequence

Single shot T2-prep SSFP has been demonstrated to improve detection of myocardial oedema at 1.5 T by Kellman et al.[Kellman 2007].

The combination of two novel technical aspects make this sequence superior:

1) The single shot imaging protocol (with T2-prep SSFP readout) allows for acquisition of multiple images during free breathing. This is important for 2 main reasons: 1) for acute patients who may not tolerate breath-holding 2) as part of the image reconstruction routine, the different images are co-registered and averaged ("motion corrected"); the motion correction/averaging can be utilized to provide significant increase in signal-to-noise ratio and contrast-to-noise ratio and eliminated breathing artefacts or artefacts due to arrhythmias.

2) The T2prep SSFP sequence includes also the acquisition of a proton density map to precisely compensate signal heterogeneities originated from surface coil sensitivity variation in the region of interest (normalised images). Kellman et al. [Kellman 2007] validated the sequence at 1.5T and showed a uniformity of the signal intensity throughout the myocardium in normal volunteers with a signal loss of the posterior wall of the LV compared to the septal wall of 0.6% ± 4.2% compared to 23 % ± 14 % using a TSE sequence.

3.2 Aims

The aim of this chapter is to validate a reproducible method of analysing oedema imaging by: 1) verifying the uniformity of signal intensity in the myocardium at 3T when using the T2-prep SSFP; 2) assuring that by using a threshold of 2SD above the mean

remote signal intensity (based on previously published methods), our method of analysis is robust enough to overcome the potential issue related to the presence of a potential S.I. gradient. For this purpose, I conducted a single experiment on a phantom as proof of principle, I acquired T2 prep SSFP images of the myocardium in three volunteers (and repeated the scan twice to assess reproducibility between scans), and finally I analysed images in an initial subgroup of patients with acute MI.

3.3 Methods

For our research CMR study, the sequence T2-prep SSFP has been imported from 1.5T to our 3T scanner.

The phantom and subjects were meticulously placed in the isocentre of the scanner to ensure reproducibility. A T2 prep-SSFP single-shot sequence with coil signal intensity correction was used with the same settings as indicated in the Methods section. A spine coil and a phased-array 6-channel flexible surface coil were used.

Phantom experiments were conducted using a sphere (diameter = 22 cm) filled with water. The artificially generated ECG scanner trigger was used.

Three normal volunteers were recruited and scanned using T2 prep SSFP CMR. The set up was the same as indicated in the Methods chapter. A mid short axis slice of the left ventricle was acquired. To assess reproducibility between scans, subjects were scanned twice in the same day.

For acute MI patients, CMR scans were conducted as described in the imaging protocol in the Methods chapter.

The entire short axis slices both in normal volunteers and patients were acquired in the same 3D spatial orientation.

Image analysis

Phantom data were analysed using purpose-written software in idl 8.0 (itt, Boulder, US). Profiles in x- and y-direction through the isocentre of the phantom of the magnitude and the normalized images were divided by the respective mean-value (obtained in a central region of interest) and multiplied by 100 to express signal variations in %.

In normal volunteers, short axis slices were manually post processed as described below. Myocardium was delineated by drawing epicardium and endocardium contours.

To assess the uniformity of the signal intensity in skeletal muscle and left ventricular myocardial wall, and the dependence on the orientation in the scanner, 4 manually drawn ROI were placed in the anterior and posterior skeletal muscles; the signal intensities of the left ventricular myocardium were also assessed by using a 6 equiangular segment model per slice with LV-RV anterior junction as reference.

In patients, in order to determine the change in signal intensity (S.I.) between affected bright regions and adjacent / remote regions, four different regions of interest (ROI) were manually identified based on the presence of positive LGE in the corresponding acquisitions: starting form the affected oedematous region, the first adjacent ROI was identified anticlockwise (Adjacent ROI 1), followed by the remote one and the second adjacent ROI (Adjacent ROI 2) (Figure 3.1). Furthermore, to assess the change in signal intensity in relation to the anatomical location of the oedematous region we grouped the patients depending on the regionality of the oedema.

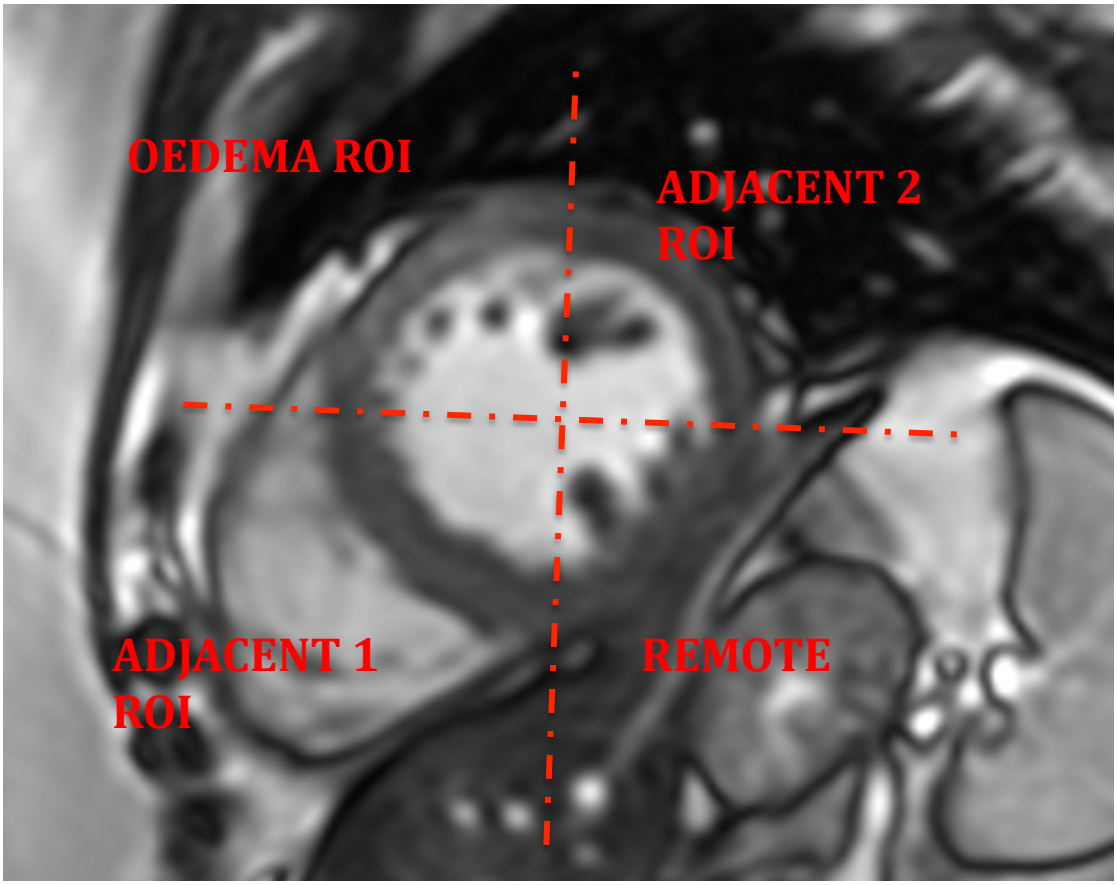


Figure 3.1. Assessment of change in signal intensity (S.I.) between affected bright myocardium and adjacent or remote unaffected myocardium. The oedematous myocardium (here indicated as OEDEMA ROI) was manually identified by drawing an ROI. The adjacent myocardium was identified as 1 or 2 depending on the anatomical position (either anticlockwise =1 or clockwise =2). The remote myocardium was the most distant from the oedema ROI.

To quantify the degree of variation in signal intensities, coefficients of variation (C.V.) were calculated as ratio of the standard deviation to the mean.

Continuous variables are expressed as mean ± standard deviation (mean ± SD). To assess differences in signal intensities, logistic regression model with a repeated – measures variable for the patient to adjust for the non-independence of the data, was used.

3.4 Results

Assessment of signal homogeneity on T2prep-SSFP images at 3T: phantom work

In order to assess for presence/absence of gradient on T2 prep SSFP images at 3T, I started by conducting a single experiment on a homogeneous liquid filled sphere (as described in the methods paragraph above).

Figure 3.2 shows the output images resulting from the application of the T2prep SSFP sequence. Two different images were produced: uncorrected (magnitude – panel a) and corrected for coil sensitivity (normalized – panel b) through the isocentre of the sphere. The bottom row shows the corresponding signal variation in percent along the x- (panel c) and y-direction (panel d) of the phantom. It can be seen that the signal decreases in y-direction relative to the isocentre to 60% for the magnitude, and to 85-90% for the normalized profile. The changes in x-direction were more pronounced with decreases down to <40% for the magnitude, and to <80% for the normalized profile, respectively. This suggests that signal changes due to patho-physiological processes in the heart have to exceed 20% in order to be reliably quantifiable.

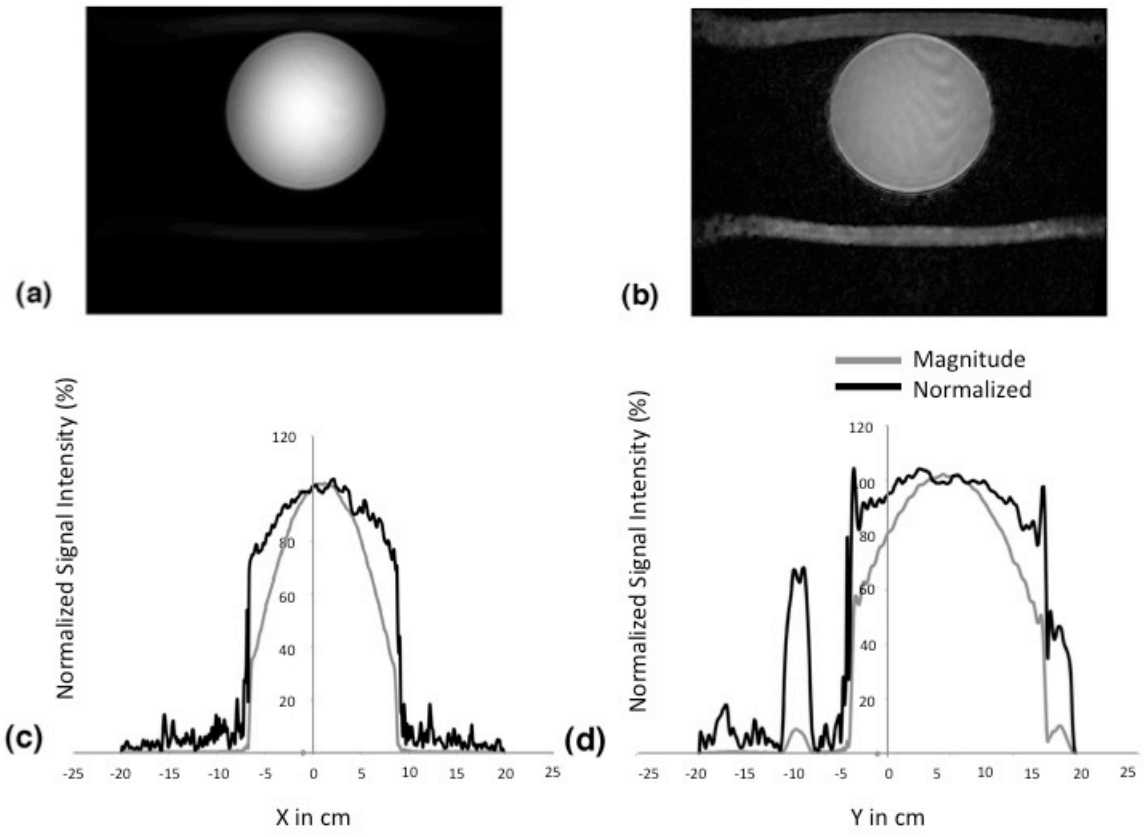


Figure 3.2 Phantom experiments to investigate the signal homogeneity of T2-prep SSFP sequence at 3T. Panels a and b: axial images across homogeneous phantom without (a) and with (b) correction for coil-sensitivity. Panel c and d: corresponding profiles across the isocentre in x (c) and y (d) direction. The grey trace corresponds to the uncorrected image ("magnitude") while the black trace corresponds to the corrected image from panel b ("normalized"). The coil sensitivity correction results in considerably improved homogeneity across the field of view.

Assessment of signal homogeneity on T2prep-SSFP images at 3T: work on volunteers

To determine the presence of oedema in the myocardium of patients with acute ischemia, it would be desirable to use as normal reference, tissue with magnetic properties similar to the myocardium but external to the heart. Skeletal muscle could be the normal control but the potential presence of a gradient would affect the reproducibility of the method, given the spatial remoteness from the myocardium. In order to assess how the difference in SI identified on the phantom, affects the distribution of SI in the entire image including skeletal muscle and the myocardium itself, we assessed signal intensities in different ROIs (12 in total, 4 per each volunteer) placed in the skeletal muscle (Figure 3.3).

A representative example is shown in Figure 3.3 demonstrating of the signal intensity gradient present in each volunteer: the maximum difference in mean signal intensity between anterior and posterior skeletal muscle was 66 a.u.

.

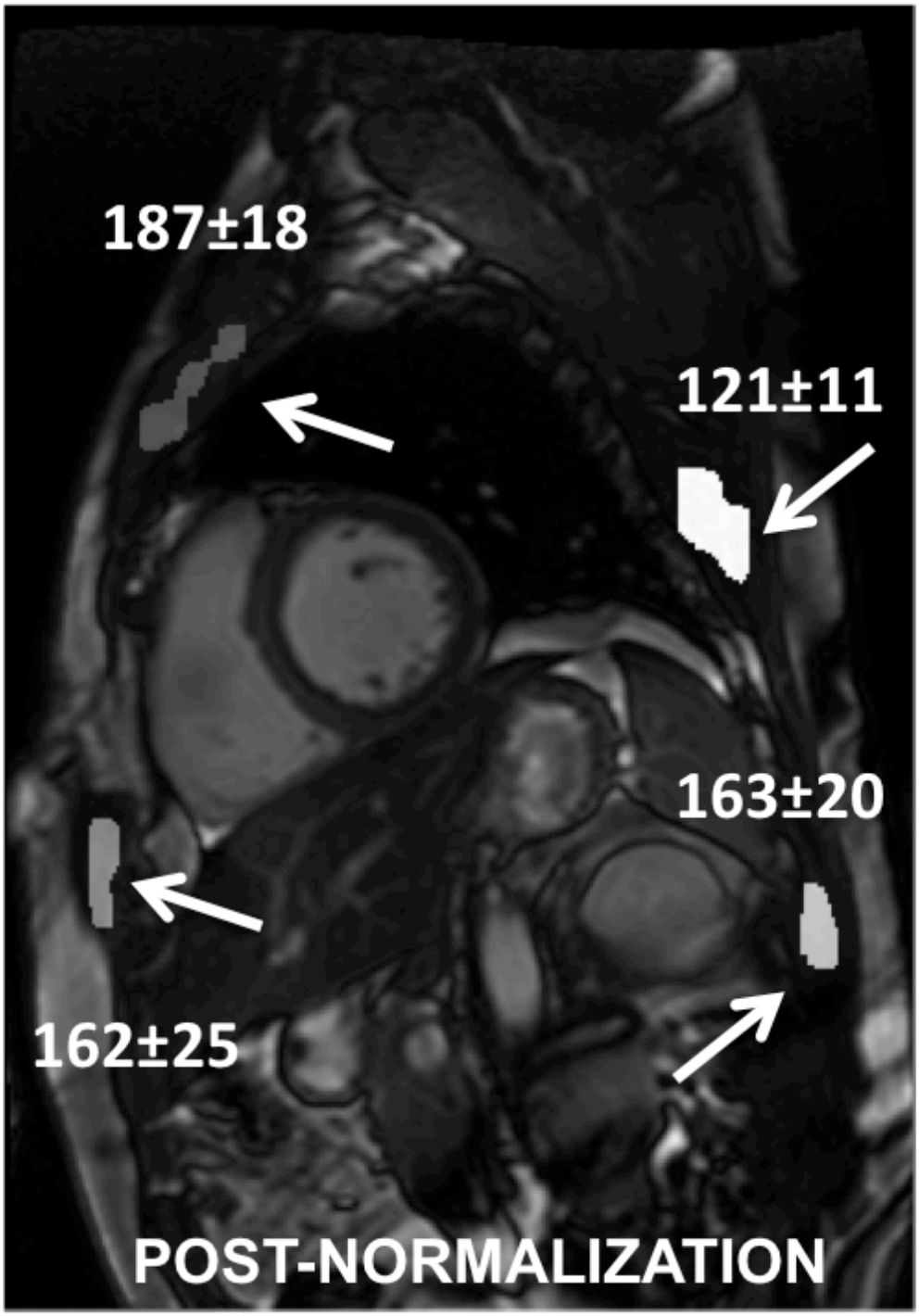


Figure 3.3. Example of signal intensity gradient in a short axis image of a volunteer. The 4 ROIs in skeletal muscle are shown (white arrows) together with the corresponding mean ± SD.

The signal intensities in each segment of the myocardium in 3 normal volunteers (each of them scanned twice) are presented in Figure 3.4, Panel A. A significant variation in signal intensities between myocardial segments depending on the spatial location was found: the anterior wall showed the lowest value of signal intensity while the highest values were found in the septum (60 ± 11 a.u. vs 97 ± 10 a.u. respectively, n = 3, $P < 0.01$) corresponding to a drop in signal between the two segments of 38 ± 10%. The overall mean signal intensity over the entire LV was 76 ± 15 a.u. for scan 1 and 72 ± 13 a.u. for scan 2, corresponding to a coefficient of variation (C.V.) of 19% and 18% respectively. We therefore can conclude that the variability of the mean signal intensity over the entire heart of normal volunteers did not exceed the variation in signal intensity of 20% shown by our phantom work. Furthermore, given the inhomogeneity of the overall signal within the normal myocardium, we expected the largest signal intensity difference required to distinguish bright oedematous from normal / remote myocardium to be up to 40%. We therefore proceeded to examine the magnitude of the signal intensity change in oedema to verify that a 40 % difference in signal enables sensitivity to myocardial oedema identification using T2 prep SSFP imaging.

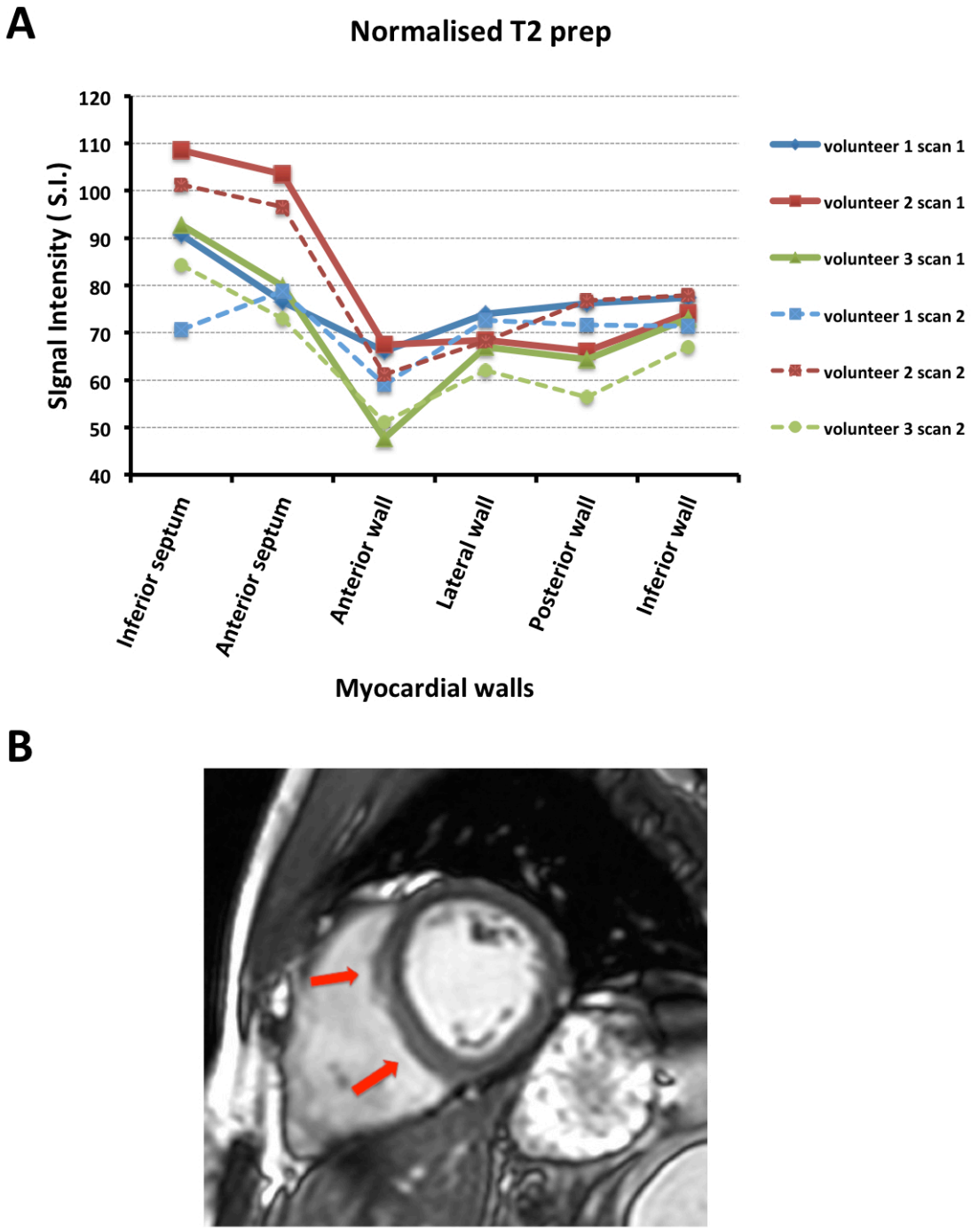


Figure 3.4: Assessment of myocardial signal intensity (SI) variation in normal volunteers using a 6 equiangular segment model. Panel (A) Signal intensities of the myocardial walls in 3 volunteers in 2 different scans. I.S.=Inferior septum, A.S.= anterior septum, A.W.= anterior wall, L.W.= lateral wall, PL.W. = Posterolateral wall, I.W.= inferior wall. Panel (B). Example of a T2prep SSFP short axis image acquired in a volunteer. The red arrows indicate an area of increased signal intensity at the level of the septum in keeping with an artefact.

Analyses of T2 W oedema in patients: verification that the change in signal intensity between oedema and remote is greater than the existing signal intensity gradient.

Images from the first 13 patients enrolled in the study were analysed: these included 8 NSTEMI and 5 STEMI patients. The mean (± SD) signal intensities of the adjacent and remote myocardial ROIs in relation to the oedematous ROI, are shown in Table 3.1 (Please see paragraphs above for identification of regions). The signal intensities in the regions identified as bright (oedema) were significantly higher compared to S.I. in the adjacent and remote ROIs. Figure 3.5 shows the signal intensities on a patient-by-patient basis.

Table 3.1. Signal intensities in areas of oedema versus adjacent and remote myocardium in patients with acute myocardial infarction (both STEMI and NSTEMI)

S.I.	ROI4 adjacent	ROI3 remote	ROI2 adjacent	ROI oedema	P - value	Post HOC
Mean ± SD (ALL)	71 ± 12	68 ± 7	71 ± 9	100 ± 20	<0.01	Oedema vs. ROI4 = 0.01 ROI 3 = 0.02 ROI2 = 0.000

The difference in signal intensities between bright oedematous ROIs and adjacent contiguous ROIs was on average 29 ± 19 a.u., corresponding to an increase of 47 ± 25% above the remote SI and 43 ± 28 % above the SI of the adjacent ROI. ($P < 0.001$) (Figure 3.5). Based on these results the overall difference between oedema and remote

myocardium exceeded the up to 40% change in signal intensity measured in normal volunteers.

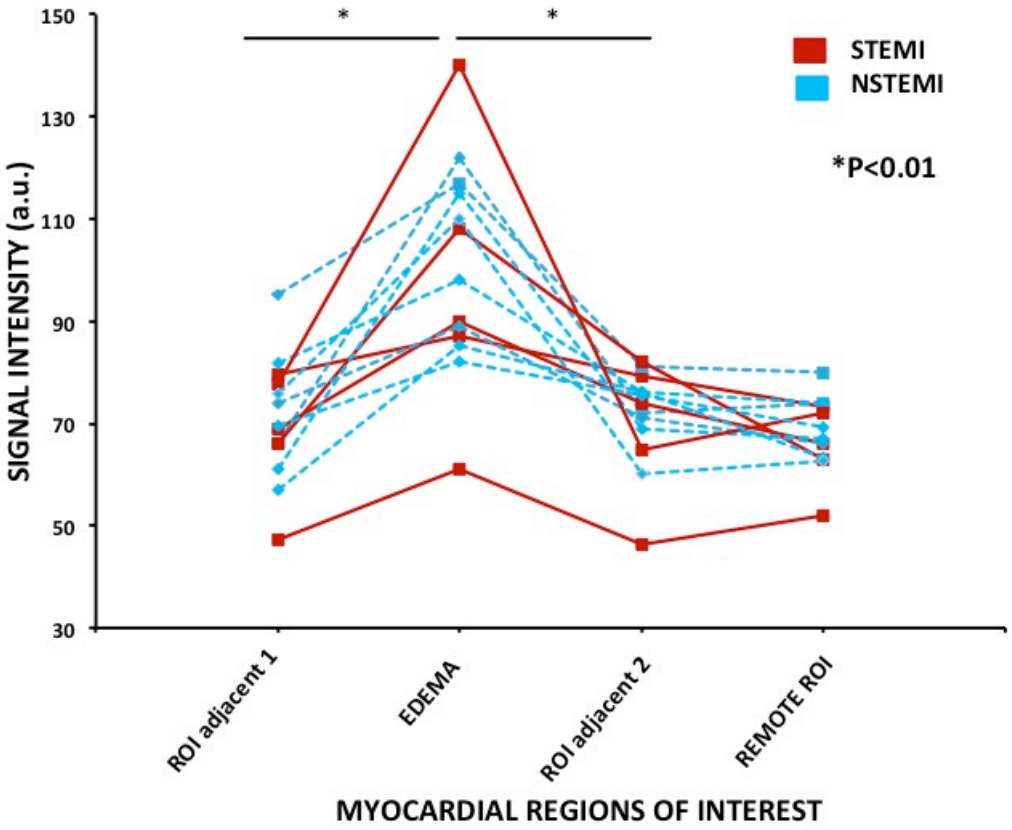


Figure 3.5: Signal intensities of T2-prep SSFP images of the myocardium in STEMI and NSTEMI patients. Signal intensities were measured in 4 different regions of the myocardium including the zone identified as bright (oedema), a remote region, and regions adjacent to the oedema (1 positioned clockwise and 1 anticlockwise of the oedema area). The signal intensity in the adjacent regions area shown significantly lower than the area with oedema.

Given the significant variation in myocardial signal intensities found in volunteers depending on the anatomical location (i.e. anterior wall showed the lowest value of signal intensity while the highest values were found in the septum), we sought to assess further whether the position in the heart (anterior versus inferior rather than lateral versus septal) would affect the difference in signal intensity between oedema and remote areas and underestimate the damage volume. As shown in Table 3.2, we grouped the 13 patients by location of the affected region and assessed in each of them the percentage difference in SI between the area of oedema (highlighted in grey in Table 3.2) and regions of remotely located myocardium (DELTA SI% = S.I. in the oedema- S.I. remote/S.I. remote). The DELTA SI % varied between 17% and 94% depending on the location of the oedematous ROI (lateral versus inferior respectively) versus the remote ROI. In case of the remote ROI positioned in the septum the difference in signal intensity to the oedema located in the lateral wall was within the variability of the normal myocardium. This may represent a limitation because it may lead to underestimation of the volume of injured myocardium. Importantly, the DELTA SI % was positive in all cases indicating that oedematous regions consistently exhibited more signal than the remote ROI. Finally, we demonstrated that the S.I. variability of myocardium within the remote ROI (C.V.= 12%) was significantly less than the variability across the entire heart (i.e. less than 20%,) as shown in Table 3.2.

Table 3.2. Signal intensities in affected and non-affected areas of the myocardium in patients grouped by location of the injured myocardium in the heart. Signal intensities of the oedematous regions are highlighted in grey.

Damaged myocardium		ROI Septum	ROI Inferior wall	ROI Lateral wall	ROI Anterior wall	DELTA SI (%) (oedema-remote/remote)
		Adjacent1	**Remote**	**Adjacent2**	**Oedema**	
GROUP 1: oedema in the anterior wall	**NSTEMI1**	95 ± 13	80 ± 14	81 ± 10	117 ± 7	46%
	NSTEMI3	74 ± 7	66 ± 3	71 ± 4	89 ± 4	34%
	STEMI3	80 ± 5	73 ± 6	79 ± 12	87 ± 8	18%
	STEMI4	69 ± 6	66 ± 6	74 ± 15	90 ± 9	36%
	Mean ± SD	**79 ± 11**	**71 ± 7**	**76 ± 5**	**95 ±14**	
		Oedema	**Adjacent1**	**Remote**	**Adjacent2**	
GROUP 2: oedema in the septum	**NSTEMI2**	122 ± 9	66 ± 8	74 ± 8	72 ± 12	64%
	NSTEMI4	115 ± 15	61 ± 12	67 ± 5	69 ± 8	71%
	NSTEMI5	98 ± 7	82 ± 7	74 ± 9	76 ± 9	32%
	NSTEMI7	110 ± 12	76 ± 7	63 ± 10	60 ± 7	74%
	Mean ± SD	**111 ± 10**	**71 ± 9**	**69 ± 5**	**69 ± 7**	
		Adjacent2	**Oedema**	**Adjacent1**	**Remote**	
GROUP 3 oedema in the inferior wall	**NSTEMI6**	76 ± 3	85 ± 6	57 ± 6	63 ± 6	35%
	STEMI1	65 ± 6	140 ± 15	78 ± 16	72 ± 13	94%
	STEMI5	82 ± 10	108 ± 10	66 ± 6	63 ± 8	71%
	Mean ± SD	**74 ± 9**	**111 ± 28**	**67 ± 10**	**66 ± 5**	
		Remote	**Adjacent1**	**Oedema**	**Adjacent2**	
GROUP 4 oedema in the lateral wall	**STEMI2**	52 ± 6	46 ± 5	61 ± 7	47 ± 7	17%
	NSTEMI8	69 ± 8	75 ± 7	82 ± 15	69 ± 11	19%
	Mean ± SD	**60 ± 12**	**60 ± 20**	**71 ± 15**	**58 ± 15**	

3.5 Discussion

The established methods to analyse oedema images acquired using T2-prep at 1.5T are usually conducted using an arbitrary chosen threshold of 2SD above the mean of the remote S.I. The CMR T2-prep technique has not been used at higher magnetic fields (as 3T) and therefore potential issues related to inherent artefacts or image signal intensity gradient could hamper the image post-processing.

Based on our findings, we demonstrated that:

1) There is a signal intensity gradient across the entire image affecting skeletal muscle, which therefore cannot be used as reference ROI.
2) Based on our phantom work, because of the signal intensity gradient, a change in SI has to exceed 20% difference in order to be reliably quantifiable.
3) An overall variability (coefficient of variation) in signal intensity of 20% is expected within the LV myocardium in normal volunteers. However, the dispersion of signal intensity depends on the location of the indexed myocardium with the septum showing up to ~ 40% higher values than the anterior wall.
4) In most of the patients, the difference in signal intensity between the oedematous region and the remote myocardium is about 40% or greater, which is well above the overall variability of the normal myocardium (C.V.= 20%) and exceeds the inhomogeneity due to the image gradient.
5) In case of myocardial injury in the lateral wall, due to the inhomogeneity of the signal intensity and the high signal intensity in the remote normal myocardium, the myocardial injury could be underestimated.

These findings allow us to establish criteria to analyse T2-prep SPSS images in a precise and reproducible way (please see Page 56 for reproducibility data on continuous T2W measurements)

The CMR techniques used in the past to assess myocardial oedema showed issues related to the presence of a signal intensity gradient. We demonstrated a variation in signal intensity on images acquired at 3T using T2 prep SSFP of 15-18%. This may represent a limitation in cases of small myocardial injury with only a small increase in signal intensity of the indexed injured tissue. However based on our findings only a minority of cases showed a difference in signal intensity lower than 20% with the majority exceeding 40%.

Furthermore, in order to quantify myocardial oedema, we empirically chose a threshold of 2 SD above the remote mean signal intensity in agreement with previously published data. We demonstrate the S.I. variability of myocardium within the remote ROI to be less than the variability across the entire heart (i.e. less than 20%, Table 3.2).

The threshold based image analyses method is frequently a matter of discussion for both oedema and LGE images.[Wince 2010] Oedema imaging techniques such as STIR use a reference ROI positioned in the skeletal muscle. The advantage in using this approach is that it overcomes the issue of potential remote or global inflammation, affecting others areas of myocardium other than the culprit. Unfortunately the presence of significant artefacts decreases the accuracy of the technique. Furthermore, it is not known whether the use of arbitrary thresholds (2SD up to 5 SD) reliably reflects pathophysiological changes happening in the myocardium post acute ischemia. The work published by Kim et al.[Kim 2000] validating the use of LGE to predict functional

improvement in patients with myocardial infarction, used a threshold of 2SD. Recently published data used different thresholds to analyse LGE and/or oedema images (5SD versus 2SD respectively): [Eitel 2009] this approach has raised concerns because of the inherent likelihood of increasing the area of oedema by increasing the sensitivity of the oedema imaging analyses. The use of the same threshold for both LGE and oedema images analyses is therefore desirable. Based on the significant difference between remote and injured myocardium across patients, a threshold of 2 SD above the mean remote S.I. will therefore provide sufficient sensitivity and specificity to accurately quantify myocardial oedema in most of the cases. Our results showed that in case of patients with lateral infarction, the volume of injury might be underestimated due to inhomogeneity of SI. However, patients presenting with lateral infarcts are less frequent and poorly characterised by ECG [Berry 1989, Huey 1988, Stribling 2011] and therefore I expected only a relatively small group of patients to be recruited in my cohort.

3.6 Conclusions

In conclusion, we have identified potential limitations inherent to the T2 prep SSFP sequence used at 3T in normal volunteers. We have demonstrated that in patients with ACS the increase in signal intensity in the injured area as identified on the LGE images, exceeds the inhomogeneity of normal myocardium. This allowed us to establish a method for analysing oedema images using a signal intensity threshold the mean of the SI of the remote myocardium ± 2SD. This threshold ensures good specificity while sacrificing little sensitivity in respect to lesions in the lateral wall, leading to systematic underestimation of the myocardial injury.

Chapter 4: Dynamic changes of oedema and late gadolinium enhancement after ST elevation acute myocardial infarction and their relationship to functional recovery and salvage index

4.1 Introduction

Cardiac magnetic resonance (CMR) is established as a key non-invasive modality for the evaluation of patients with stable coronary disease. It is the gold standard technique for the assessment of function (cine CMR) and the quantification of scarred myocardium in patients with previous myocardial infarction (MI) (late gadolinium enhancement, [LGE]) [Kim 2000].

Recently, the development of T2-weighted (T2W) oedema-sensitive sequences has enabled the identification of acutely ischemic myocardium, which is of particular interest in the evaluation of myocardial status in acute MI [Abdel-Aty 2009, Aletras 2006, Cury 2008, Kellman 2007]. By comparing the area 'at risk', determined by T2W imaging, and the final infarct size, obtained with LGE CMR imaging, myocardial salvage following treatment can be derived, and expressed as proportion of myocardial volume initially presumed at risk [Berry , Friedrich 2008]. A number of clinical trials have used this measure, assessed in the acute setting, as a primary endpoint [Francone 2009, Larose , Ortiz-Pèrez 2010].

However, to capitalize fully on these quantitative CMR techniques requires clear understanding of the dynamic features of each in the context of the rapidly changing pathological conditions that pertain in the myocardium after acute ischemic injury and reperfusion [Buja 2005]. Under these circumstances, there are profound changes in perfusion pressure; small vessel patency and permeability; pH; tissue water content and

cellular composition [Buja]. Over time, there is desorption of oedema, resolution of inflammation and replacement of irreversibly injured myocytes with fibrous tissue [Kim 1999]. In the acute setting, although it is known that CMR oedema imaging may identify both infarct and myocardium at risk and LGE overestimates the infarct zone, acute LGE is still considered a robust prognostic factor; though whether it necessarily always reflects irreversible injury is still debated [De Roos 1988, Klein 2007, Saeed 1999].

Accordingly, we designed a detailed early time course CMR evaluation in patients within 48h of technically successful percutaneous coronary intervention (PCI) for acute MI. We quantified (1) myocardial oedema at 4-time points post MI (12-48 hours; 5-7 days; 14-17 days and 6 months) and (2) characteristics of LGE early (12-48 hours) and late (6 months) after ischemic injury. We relate each of these parameters to temporally matched measurements of myocardial function at both global and segmental levels.

4.2. Aims

Our aims were to establish the longitudinal changes of myocardial oedema by CMR and to determine the extent to which oedema and LGE, obtained in the acute phase, predicted recovery of global and regional LV function at six months. Clarification of these acute dynamic changes of oedema and LGE is crucial to the correct interpretation of CMR data in the acute setting and has important implications for the design, and the calculation of sample size, of clinical trials with myocardial salvage as endpoint.

4.3 Methods

Thirty patients with first ST segment elevation MI (STEMI) and onset of symptoms < 12 hours before PCI were included (see Methods chapter for inclusion and exclusion criteria).

Four separate 3Tesla CMR scans were performed on each patient at the following time points post-PCI: 12 - 48 hours (24H); 5 - 7 days (1W); 14 - 17 days (2W); and 6 months (6M). The first and last CMR scans assessed LV function, oedema, and LGE. The second and third scans acquired function and oedema imaging only (Figure 4.1).

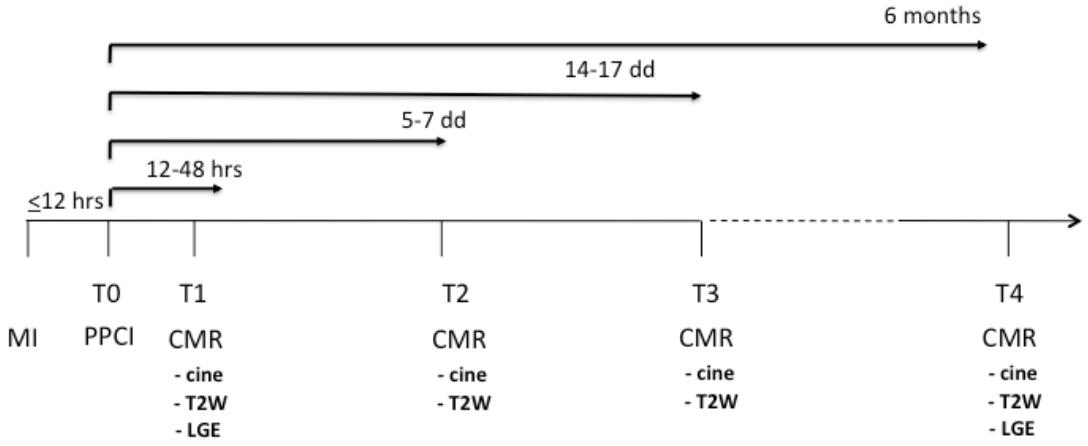


Figure 4.1. Study protocol. Imaging time points (TP) in relation to the acute myocardial infarction (MI) and primary percutaneous coronary intervention (PPCI). For each TP, the CMR data acquired is given. CMR = cardiovascular magnetic resonance; LGE = late gadolinium enhancement.

Post-processing analysis

Post-processing analyses included:

1) Quantification of LV volumes and wall motion
2) Quantification of oedema or LGE. The post processing for objective quantification of edema (on T2W images) and scar (on LGE images) was the same. Following manual delineation of epicardium and endocardium, a reference region of interest (ROI) was placed in remote myocardium of each LV slice. The signal intensity threshold indicating increased signal intensity on T2W (oedema) and /or LGE (scar) images, was imposed 2 standard deviations above the mean intensity of the reference ROI, as previously described [Berry]. The % of injured LV myocardium was derived as sum of the damage fraction per each slice.

Statistical Analyses

Values of continuous variables are expressed as mean (± SD). In order to investigate differences at multiple time points in LV volumes, EF, WMSI, myocardial volume of oedema and LGE assessed by CMR, ANOVA analyses with adjustment for repeated measurements were performed. The Bonferroni procedure, where the overall Type I error (0.05) is distributed across multiple hypothesis tests, was used for post-hoc comparisons. For categorical variables, Wilcoxon signed-rank test was used to compare regional wall motion abnormalities with segmental scoring of oedema and late gadolinium. A chi-squared test and a logistic regression model with a repeated-measures variable for the patient (to adjust for the non-independence of the data) were used to assess the relationship between the transmural extent of myocardial injury i.e. oedema / LGE and improvement in regional function. The relationship between the improvement

in wall motion along 6 months and the clinical and CMR characteristics were evaluated using linear regression analyses. Bland-Altman test for continuous T2W measurements and Cohen's Kappa coefficient for T2W, LGE and wall motion abnormalities categorical measurements were performed to evaluate inter-observer variability for oedema assessment and for transmurality grading and wall motion scoring respectively.

All statistical tests were two-tailed, and all P values of less than 0.05 were considered statistically significant.

4.4 Results

Patient characteristics are given in Table 4.1. All patients presented with ST segment elevation on the ECG and were treated by primary PCI (except for 2 who were transferred from a different hospital and received thrombolysis and rescue PCI). All PCI took place within 12 hours of chest pain onset, with the mean time from onset of pain to balloon treatment 253 ± 150 minutes.

Table 4.1. Patient characteristics.

Variable	Value (%) or mean ± SD (except where indicated)
Age (yrs.)	56 ± 9
Sex (M: F) (N)	26:4
Ethnicity (Caucasian: Asian) (N)	29:1
BMI	29 ± 6
Risk Factors [No (%)]	
Smoking	16 (53)
Hypertension	11 (37)
Diabetes	3 (10)
Family history	9 (30)
Hyperlipidaemia	11 (37)
Troponin I (12 hours post PCI) (mg / mL)	40 ± 16
Pain to balloon time (mins)	253 ± 150
Door to balloon Time (mins)[median (interquartiles)]	44 (30; 62)
Culprit coronary artery [No (%)]	
LAD	15 (50)
LCx	2 (6)
RCA	13 (43)
Number of vessels diseased [No (%)]	
1	20 (67)
2	6 (20)
3	4 (13)
TIMI FLOW pre PCI [No (%)]	0.6 ± 1
0	21 (70)
1	3 (10)

2	4 (13)
3	2 (6)
TIMI FLOW post PCI [No (%)]	2.5 ± 0.6
0	0
1	2 (6)
2	10 (33)
3	18 (60)
Medications during PCI [No (%)]	
GP IIb / IIIa inhibitor	23 (76)
Clopidogrel	30 (100)
Heparin	28 (90)
Aspirin	30 (100)
Concomitant medications on admission [No (%)]	
Beta-blockers	1 (3)
Ace-inhibitors	6 (20)
Statins	4 (13)
Medications post infarct [No (%)]	
Beta-blockers	28 (93)
Ace-inhibitors	30 (100)
Statins	30 (100)
Aspirin	30 (100)
Diuretic	3 (10)
Nitrates	8 (27)

Of 33 patients enrolled, 2 could not complete the first CMR examination due to claustrophobia, 1 patient was excluded due to urgent re-intervention, 2 did not undergo third scan due to technical difficulties or because of patient refusal (Figure 4.2).

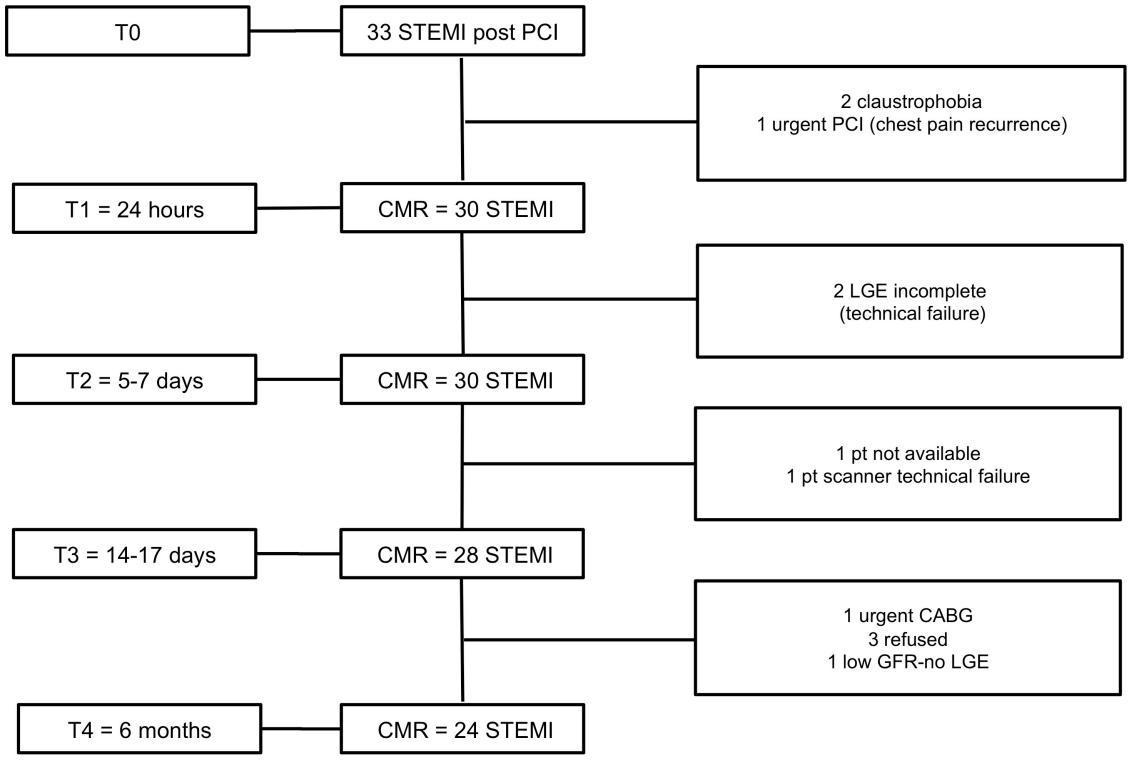


Figure 4.2. Patient flow. Disposition of patients with STEMI recruited to this study, indicating numbers at each follow-up CMR examination up to six x months and reasons for loss from study.

CMR findings

The first CMR took place at 29 ± 10 hours from the PCI (24H), the second (1W) at 6 ± 1.4 days post PCI, the third (2W) at 16 ± 2.7 days post PCI and the fourth (6M) at 6.2 ± 1 months post PCI. The total number of successful scans was 112 (30 at 24H and 1W, 28 at 2W and 24 at 6M) and all were suitable for analysis. In segmental analyses, 8 segments at 24H and 12 at 2W showed off resonance artefacts in T2W images and were excluded from analyses at all TP (Table 4.2).

Both Bland-Altman (bias = 0.2 ± 7.56%) for continuous T2W measurements (See T2W imaging Inter-observer differences) and Cohen's Kappa coefficient (kappa = 0.8) for T2W, LGE and wall motion abnormalities categorical measurements indicated excellent levels of agreement for inter-observer variability assessments.

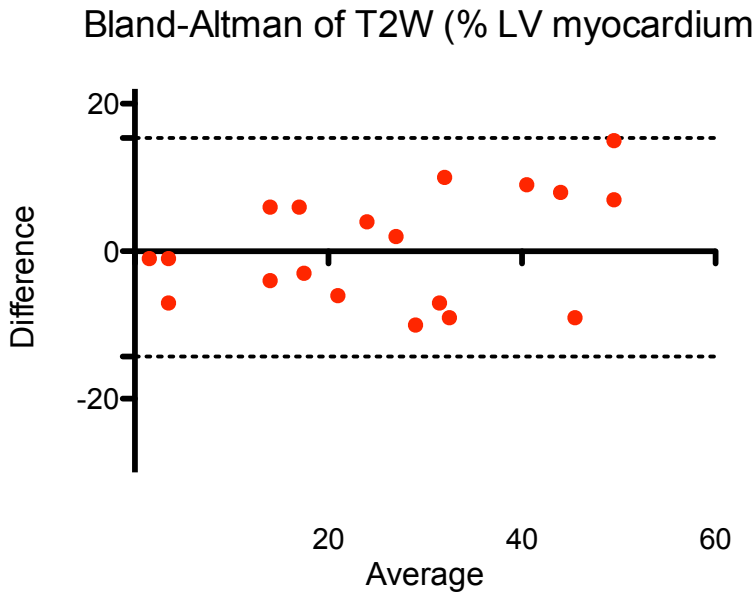


Figure 4.3 T2W imaging Inter-observer differences. Bland-Altman chart illustrating the Inter observer variability for T2W continuous measurements of oedema (% LV myocardium) on 20 patients.

Time course assessment of global left ventricular function and myocardial oedema

All patients had positive findings for myocardial injury assessed by T2W imaging at 24H except one. In this particular case, the lesion as assessed by LGE and oedema, was confined to the apical segment only. The apical slices were excluded to avoid partial volume artefacts.

The mean volume of oedema was stable over the first week (37 ± 16% of the LV myocardium at 24H and 39 ± 17 % at 1W) with a reduction by 2W (24 ± 13%; $P < 0.01$) and near resolution (7 ± 10%; $P < 0.001$) by 6M (Figure 4.4).

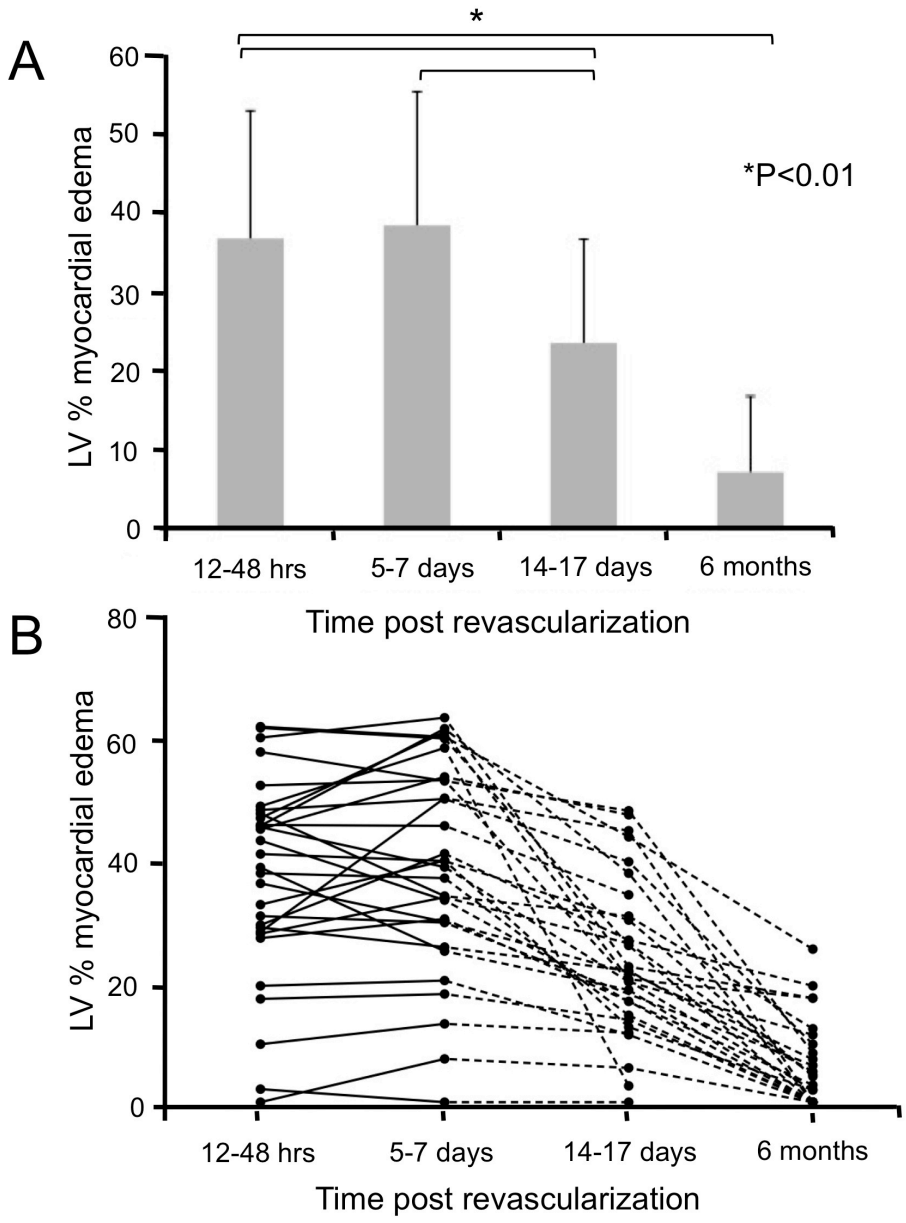


Figure 4.4. Time course of oedema. **A.** Mean percentage of LV volume positive for myocardial oedema at each time point. The volume of oedema remained stable in the first week post event with a significant decrease at 15 -17 days with near resolution by 6 months. **B.** The time course of oedema and resolution is given for each patient. There was a large range of LV % volume of oedema (0 to 60%). This analysis on an individual level confirms the constancy of oedema measured in the first 5-7 days, that is suggested in Panel A, with marked variation thereafter. Using the objective thresholding methods described in the text, a small number of patients had a substantial volume of apparent residual oedema at 6 months.

The ejection fraction (EF) was well conserved (53 ± 9 %) at 24H and not significantly different at 6 months (59 ± 6 %; P = n.s.) (Table 4.2).

Table 4.2. CMR findings.

	24 hours (n=30)	5-7 days (n=30)	14-17 days (n=28)	6 months (n=23)	p-value	Post-HOC
EF (%)	53 ± 9	55 ± 10	54 ± 8	59 ± 6	0.9	1.0
EDV (mL)	144 ± 25	153 ± 33	156 ± 37	158 ± 22	0.2	1.0 (24H vs 1W, 24H vs 2W, 24H vs 6M) 0.1 (24H vs 2W) 0.3 (24H, vs 6M)
ESV (mL)	68 ± 22	72 ± 30	73 ± 27	57 ± 24	0.6	1.0 (24H vs 1W, 2W, 6M)
SV	76 ± 15	82 ± 14	82 ± 16	88 ± 17	0.3	1.0 (24H vs 1W, 24H vs 2W) 0.7(24H, vs 6M)
WMSI	1.52 ± 0.3	1.4 ± 0.3	1.35 ± 0.3	1.36 ± 0.3	<0.001	<0.01 (24H vs 1W, 24Hvs 2W, 24H vs 6M)
OEDEMA (LV%)	37 ± 16	39 ± 17	24 ± 13	6 ± 9	<0.001	0.001 (24H vs 2W) 0.001 (1W vs 2W) 0.001 (24H,2,3 vs 6M)
LGE (LV%)	27 ± 15			21 ± 11	0.002	0.002

Time course assessment of oedema and LGE on a segmental level: relations to wall motion (24H-2W)

At 24H, 151 out of 428 (35 %) segments were positive for myocardial oedema; 133 / 428 (31%) showed LGE, and 139 / 428 (32%) segments showed abnormal function (Table 4.3).

Table 4.3. List of segments included In CMR analyses at each time point.

	Segments oedema + n (%)	Segments LGE + n (%)	Segments WMA + n (%)	Total segments analysed per each modality
Time point 1	151 (35%)	133 (31%)	139 (32%)	428
Time point 2	157 (37%)	N/A	107 (25%)	428
Time point 3	152 (36%)	N/A	95 (22%)	428
Time point 4	25 (6%)	100 (29%)	94 (23%)	336

Segments with evidence of injury assessed by T2W or LGE imaging and those with wall motion abnormalities were co-localized (location agreement, Kappa = 0.77; $P < 0.001$) with 120 / 133 (90%) showing all of oedema, LGE and wall motion abnormalities. Similarly, of 277 segments with no oedema, 257 (93%) showed normal wall motion, while of those with no LGE, 264 (89%) showed no myocardial oedema either. Only 31 / 428 (7%) of segments were positive for oedema in the absence of LGE. (Figure 4.5)

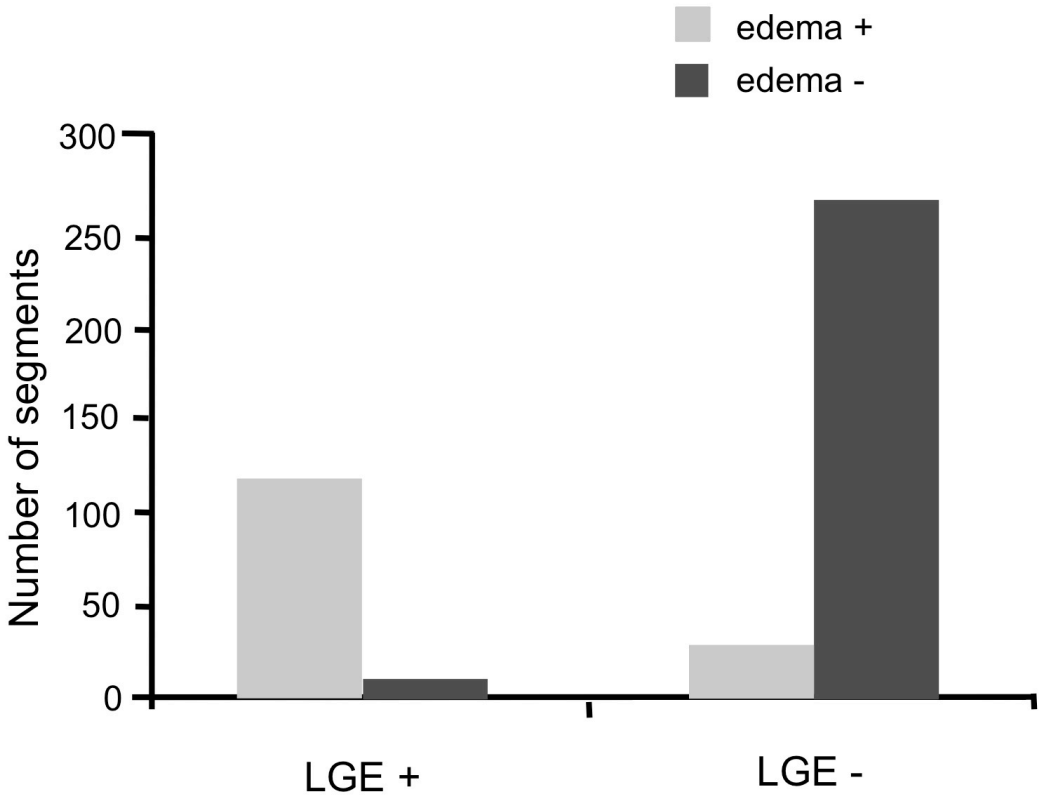


Figure 4.5. Segments with acute myocardial injury as identified either by presence of late gadolinium (LGE) and/or oedema in patients with STEMI.

In order to assess whether or not the extent of the acute myocardial injury was associated with regional dysfunction, we examined the relationship between within-segment injury (% segment affected by oedema or LGE) and the presence or absence of wall motion impairment in that segment. At 24H, the proportion of segments with wall motion impairment increased in relation to the extent of both myocardial oedema ($P < 0.01$; Figure 4.5A) and LGE ($P < 0.01$; Figure 4.6 B). Of the injured segments (those having either oedema or positive for LGE), 75 (17%) had improved motion in the first 2 weeks. This was associated with an improvement in WMSI (from 1.52 ± 0.3 at 24H hrs to 1.3 ± 0.3 at 2W, $P < 0.01$) (Table 2).

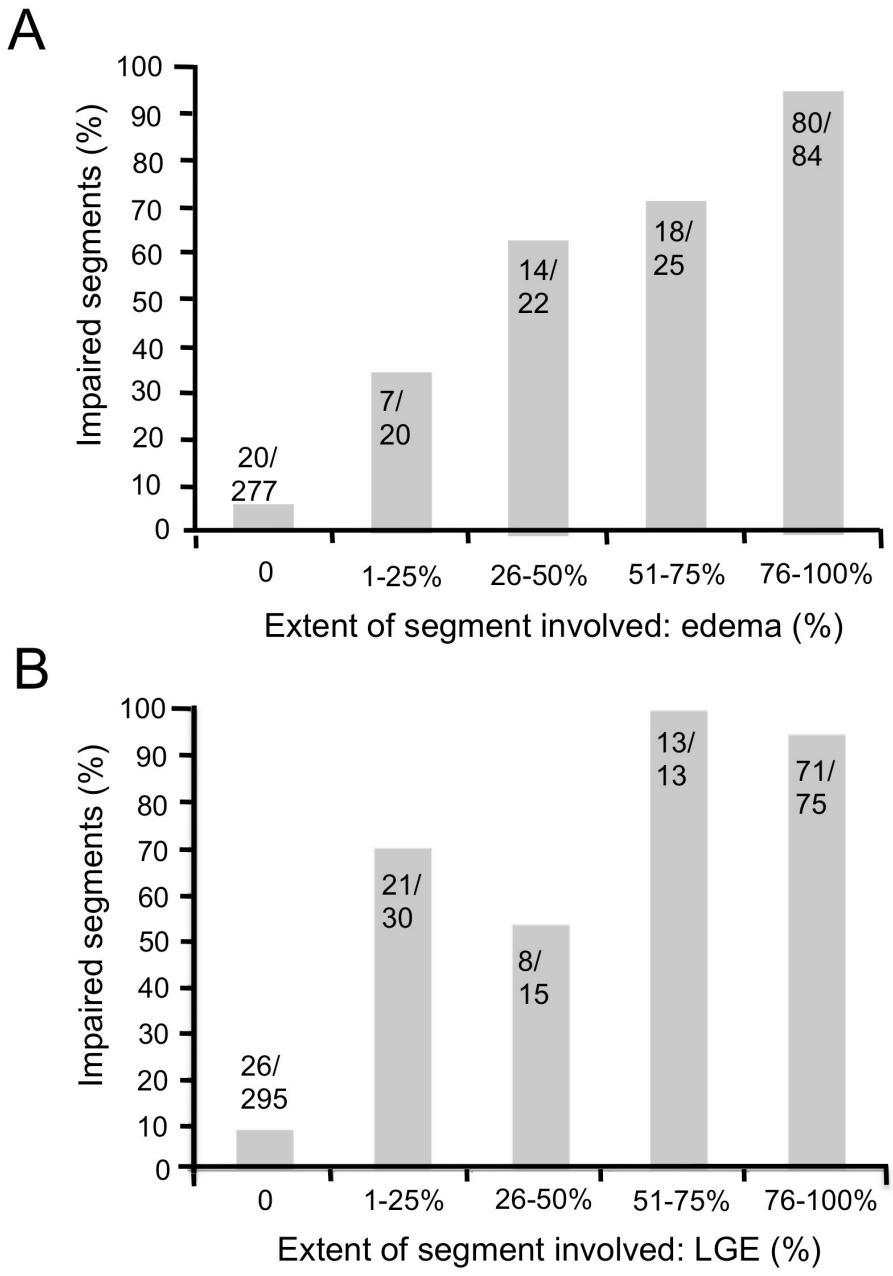


Figure 4.6. Impaired segments (% affected) as a function of the extent of segment positive for (A) oedema and (B) LGE at 24H. Segments with acute myocardial injury as identified either by presence of late gadolinium (LGE) and/or oedema. For both oedema and LGE, the probability of segmental dysfunction increased with the fraction of segment affected. For unaffected segments, as expected, a large majority showed normal function.

LGE volume reduction over 6 months

The volume of LGE decreased significantly between the first time point (27 ± 15% of LV myocardial volume) and the last time point at 6M (22 ± 12%, P = 0.002) (Figure 4.7A).

Furthermore, on a patient by patient basis, there was considerable variation in the extent of reduction in LGE. The reduction in LGE from acute to 6M was up to 68%, with 46% of patients showing some reduction in LGE at 6 months. LGE was also reduced when analysed at segmental level. Out of the 336 segments analysed at 6M, 108 had been positive for LGE at 24H of which 54 (50%) showed resolution of LGE at 6M (representative examples are shown in Figure 4.8).

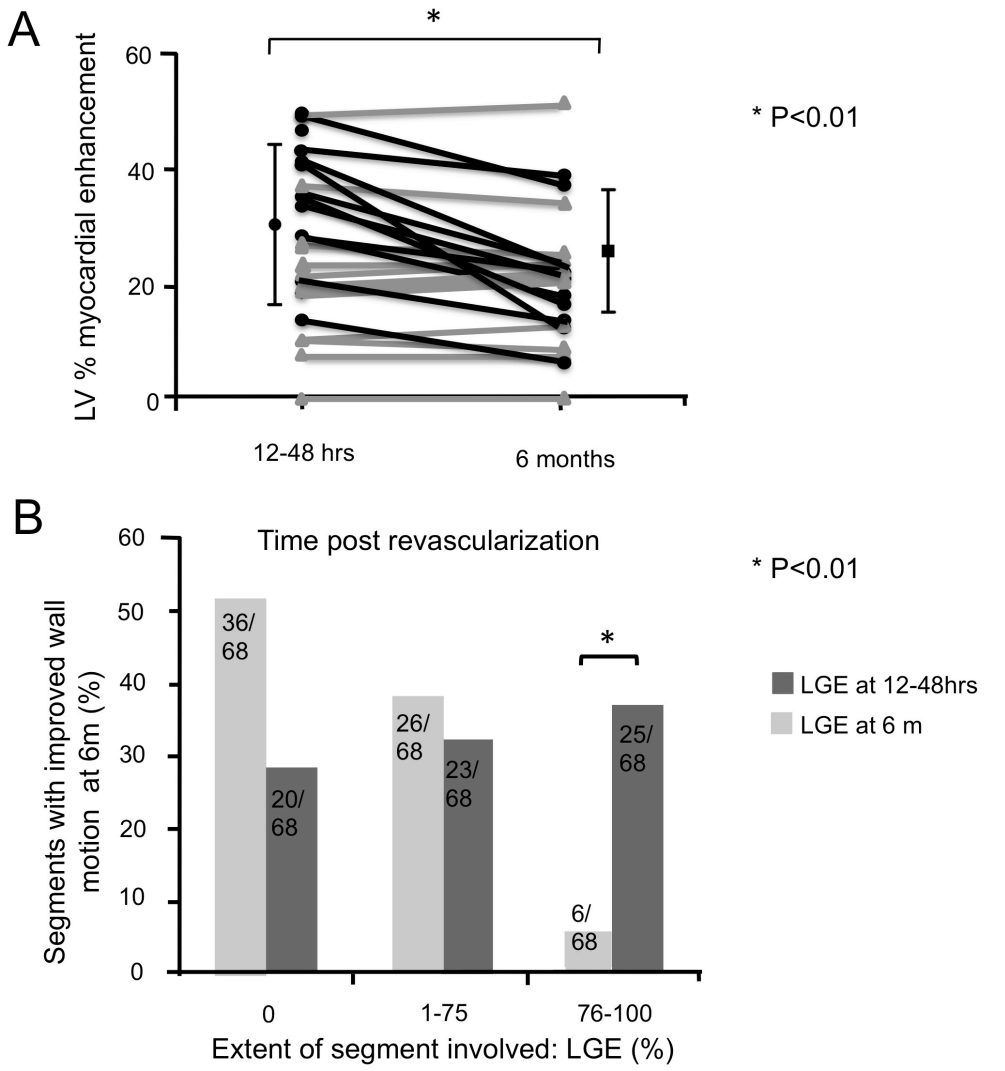


Figure 4.7. (A) Myocardial LGE early (12-48hrs) *vs.* late (6 months) and (B) wall motion improvement abnormalities. A. The myocardial volume (mean % ± SD) positive for LGE, decreased significantly from 12 - 48 hrs to 6 months. The change in extent of LGE is also shown for each patient. Patients with unchanged LGE at 6 months are shown in gray while those with decreased LGE in black. Eleven patients out of 23 (46%) who underwent CMR at 6 months time, showed a reduction in LGE volume (of 38 ± 14%). In the remaining 13 patients, no reduction in size of the LGE volume was identified (23% ± 14% *vs.* 23% ± 14% respectively). **B.** Segments with improved function at six months (n = 68) broken down by extent of LGE within that segment LGE (none; 1-75% = partial thickness and 76-100% = full thickness) at both 24H and 6M. Across categories, the extent of LGE, measured at 12 - 48 hours (dark bars) was a poor predictor of functional recovery. Significantly, even segments showing full thickness LGE were associated with functional recovery. By contrast, LGE extent at 6 months (light bars) was strongly inversely correlated with improved function in that segment.

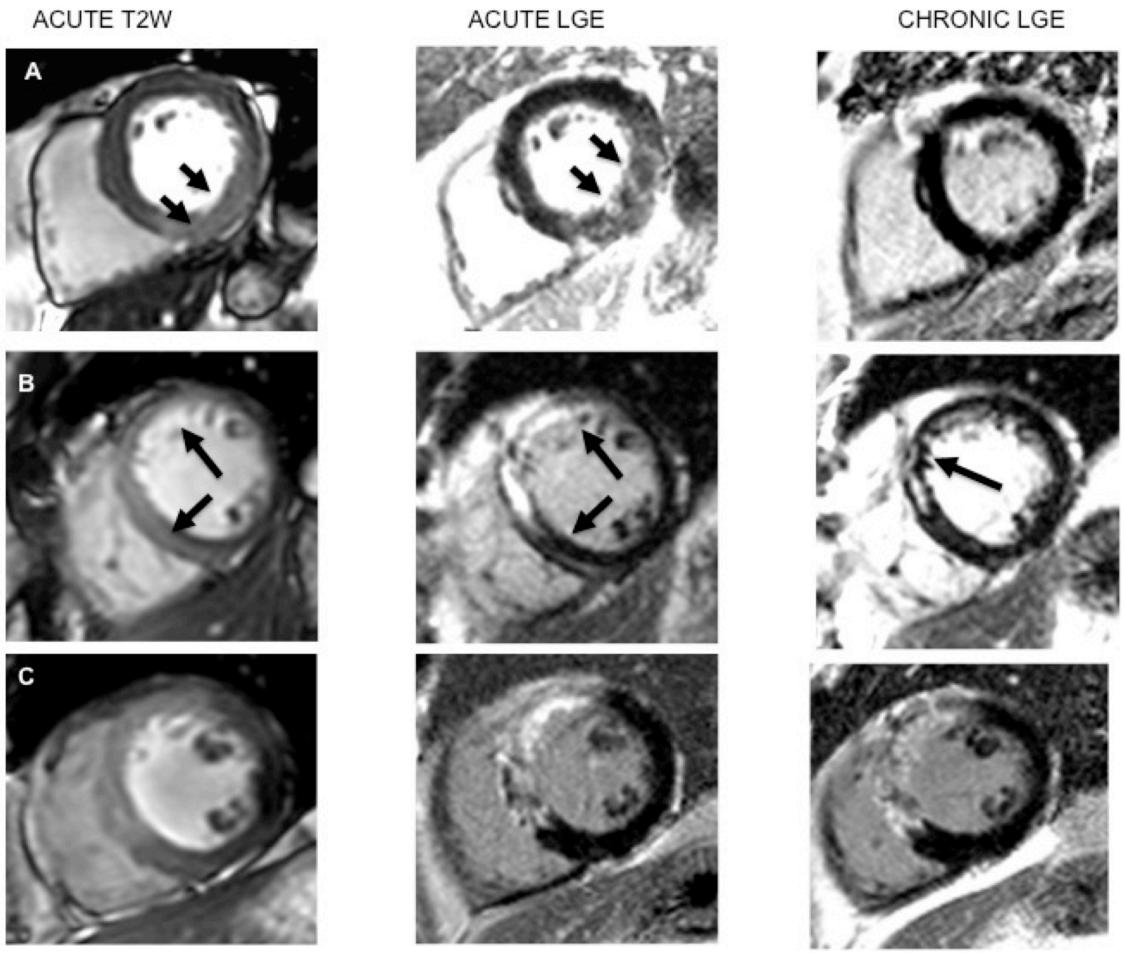


Figure 4.8. Representative CMR images. Oedema images (left column), acute LGE images (centre), chronic LGE (right column) are displayed. Three separate patients (rows A to C) representing alternative patterns of acute *vs.* chronic CMR features are shown. **A.** Oedema is present in inferior wall; the appearance of LGE is unambiguous as high signal zone that corresponds to the area of oedema, but there is no LGE present at 6 months. **B.** T2W image, on the left, shows oedema in the anterior wall; the acute LGE shows compact enhancement, which is reduced in size by 6 months. **C.** The oedema imaging confirms acute injury. In this example LGE present early persists without significant alteration to the 6 month time point.

Recovery of function accompanies resolution of LGE

We next examined whether resolution of LGE could be associated with recovery of function in affected segments. Out of 336 segments analysed at 6M, 79 had shown abnormal function at 24H of which 68 (86%) showed recovery of function at 6M.

Importantly, of those segments that showed an improvement in LGE at 6 months 35 / 54 (65%) also showed an improvement in wall motion ($P < 0.0001$) indicating that LGE at 24H did not necessarily signify irreversible myocardial injury.

Conversely, only 8% (6/68) of segments with persistent transmural LGE at 6M had improved function ($P < 0.01$) (Figure 4.6 B). Furthermore, on multivariate analysis the only CMR measure that was predictive of functional recovery was the infarct size determined by LGE CMR (% LV_{score}) at 6M ($P = 0.015$). The importance of CMR assessment of infarct size at 6 months is further emphasized by the strong correlation between the infarct size (% LV_{score}) assessed at 6 months and troponin I, assessed at 48 hrs ($r = 0.9$; $P < 0.01$); while the equivalent relationship with LGE measured at 24H was relatively weak ($r = 0.7$, $P < 0.01$; Figure 4.9).

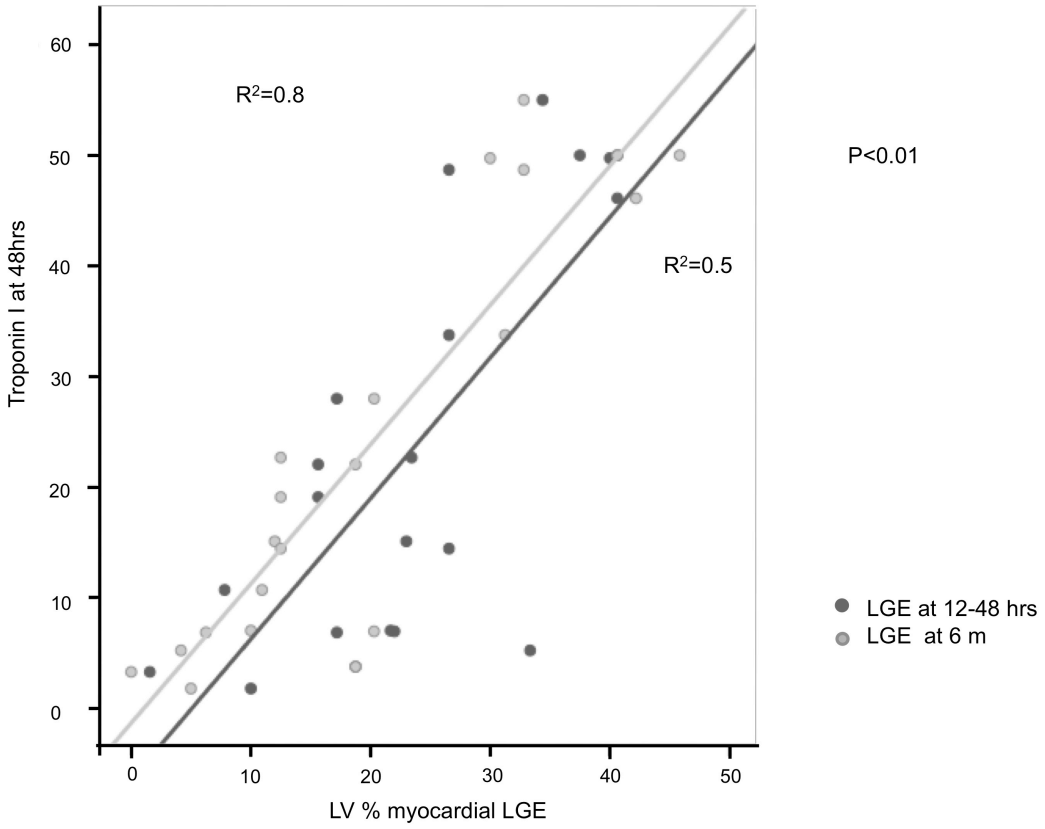


Figure 4.9. Relationship between the extent of late gadolinium (LGE) and the Troponin I at 48 hrs. The correlation between the LV % of LGE (% LV_{score}) assessed at 6 months and troponin I assessed at 48 hrs (R^2 = 0.8; P < 0.01) is shown in comparison to the equivalent relationship with LGE measured at 12 - 48 hours (R^2 = 0.5, P < 0.01).

Effects of timing of LGE measurement on the calculation of salvage index

Calculation of myocardial salvage [index] depends both on (a) the acutely determined area at risk (T2W image) and (b) the final infarct size (LGE). Given the variation in LGE described above, we calculated the effect of its assessment early (24H) *vs.* late (6M) on the estimation of salvage. Depending on the imaging time for LGE, the salvaged myocardium index was substantially different: 26 ± 21% at 24H *vs.* 42 ± 23% at 6M (P = 0.02). Thus, LGE timing critically determines the calculated salvage index.

4.5 Discussion

Optimal application and accurate interpretation of CMR in acute myocardial ischemia require that the nature and patterns of change of CMR features are fully defined. We report the first detailed time course study that examines early changes in myocardial function, oedema and LGE in patients treated with primary PCI for STEMI, and which relates these early features to late measures of infarct size and functional recovery at global and segmental levels.

The principal findings are that: (1) oedema was present in virtually all cases; the volume of oedema remained unchanged over the first week but decreased significantly by 15 days. (2) A large majority of segments that were positive for oedema also showed evidence of LGE, assessed at 24H. (3) In 46% of the patients, LGE present on early scans had diminished in size by 6 months and, in some cases, dramatically. (4) Acute LGE was a weak predictor of functional recovery compared to chronic LGE, as even segments with transmural LGE at 24H, showed an improvement in contractility at 6 months. (5) The reduction in LGE at the later time had a profound effect on the calculation of salvage

index, which varied by up to ~ 60%, depending on the time point used. These findings have important implications for the timing and interpretation of CMR after acute STEMI, including in the estimation of viable *vs.* infarcted tissue and on the design and implementation of clinical trials that use salvage index as an end point.

Acute myocardial ischemia-reperfusion is a dynamic process, involving a complex cascade of intracellular and interstitial changes that affect: oxygenation and pH in the myocardium; intravascular pressure, small vessel permeability and patency; tissue water content, inflammatory cell infiltration and local haemorrhage [Van Gaal 2007]. These changes potentially alter both the inherent MR characteristics of the tissue and the delivery, distribution and removal of exogenous contrast agents, compared to the stable setting [Lima 1995]. Specifically, the kinetics of gadolinium distribution and precise tissue specificity in acute infarction are not fully understood [De Roos 1988, Klein 2007, Saeed 1999] and the potential for accumulation of LGE even in viable myocardium has not been excluded.

Myocardial oedema

Both intracellular oedema due to decoupling of water molecules from proteins [Kuntz 1969] and/or tissue accumulation of water leads to a prolongation of T2 [Friedrich 2010] that appears as transmural bright signal on T2W images [Karolle 1991]. In dogs, myocardial oedema has been demonstrated after 30 minutes ischemia [Abdel-Aty 2009]. Previous reports have identified persistence of oedema signal for at least 12 days post infarction [Friedrich 2008, Kellman 2007], but the timing of maximal myocardial oedema and its early evolution had not been defined. This information is important in order to establish the optimal imaging window for the assessment of salvaged myocardium [Berry

, Friedrich 2008] and for estimation of prognosis [Larose 2010, Raman]. We demonstrate that oedema is maximal and constant during the first week post MI, reducing thereafter. Therefore, the window for retrospective quantification of myocardium 'at risk' is up to 7 days, with a risk of underestimation after that time.

Late gadolinium enhancement

Late gadolinium enhancement occurs following myocardial infarction. In the context of established MI and scar formation, the area of myocardial fibrosis is very closely linked to the extent and distribution of LGE [Kim 1999, Kim 2000]. Furthermore, the extent of LGE can be used to predict recovery of myocardial function after revascularization,[Kim 2000, Selvanayagam 2004] with the transmural segmental extent of LGE / scar inversely correlating with the probability of functional recovery. Reduction in LGE has been previously reported from the acute phase to a chronic stage, and attributed to "shrinking of the scar", together with compensatory hypertrophy of adjacent myocardium [Ichikawa 2005, Ingkanisorn 2004].

Although LGE occurs in context of acute MI, this cannot reflect tissue fibrosis, which takes several weeks to develop. In a dog model, Fieno *et al* showed that fibrosis increased 11-fold between 3 and 60 days after permanent coronary artery occlusion [Fieno 2004]. Conversely, in a model of acute MI, LGE can be positive within 1 hour of injury [Schulz-Menger 2003]. Given the variant tissue composition between acute and chronic states, it cannot be assumed that the presence of LGE necessarily always implies irreversible injury. We found that the overall volume of LGE decreased by 22% between the first time point and six months and, that on a patient by patient basis, there was considerable variation in the extent of reduction in LGE. Importantly, of those

myocardial segments showing reduction in LGE at 6 months, 68% also showed an improvement in wall motion ($P < 0.0001$). Using a technique based on differential signal intensity threshold analysis, Yan *et al* identified an peri-infarct 'border zone' on the periphery of the LGE area [Yan 2006]. However, recovery confined to a putative 'border zone' is unlikely to account for the observations in the current study, since 51% of segments showing improved function had transmural (or near-transmural) LGE extent when imaged < 48 hours after primary PCI. These findings indicate that LGE within this time frame does not necessarily reflect irreversible injury. Our findings do not identify the tissue correlate of LGE at early time points, but do stress the important possibility of resolution, even of transmural LGE, *in association with recovery of myocardial function in that area*.

LGE and recovery of function

The ability of LGE obtained in the acute setting to predict later functional recovery is contentious [Beek 2003, Choi 2001, Gerber 2002, Rogers 1999]. Choi *et al* found that improvement in segmental contractile function between < 7 days post infarct and 8-12 weeks later was inversely related to the transmural extent of infarction on the first scan [Choi 2001]. That work differs from the current study in several important respects. Most importantly, the second CMR scan did not include assessment of LGE, making it impossible to know if LGE had changed between scans. While early assessment of LGE will, on average, indicate injured tissues, our work demonstrates that LGE early after an event does not always reflect irreversibly injured, non-viable tissue, and even transmural LGE early after acute ischemia can be associated with recovery of function in that segment. In keeping with these findings, Beek *et al* reported that 25 % of

segments with transmural hyperenhancement 7 ± 3 days post MI had the potential for functional improvement after 13 weeks [Beek 2003].

Our findings of resolving LGE are further consistent with a recent clinical study showing that LGE diminishes within one week of acute MI [Engblom 2009]. The authors speculated that reduction in LGE might have reflected initial LGE in *reversibly* injured myocardium. By incorporating oedema imaging, to demonstrate the extent of the ischemia zone, and combining this with (a) early and late phase LGE and (b) functional assessment at a segmental level, the current study demonstrates conclusively that this is indeed the case — and that early LGE does not always lead to late scar. Our findings cannot determine mechanisms of 'shrinkage' of the LGE area or whether there is hypertrophy of adjacent viable myocardium in the long term [Holmes 1994, Rehwald 2002], which may contribute to recovery of function at a later stage.

Salvage index

The difference between volume of myocardium at risk and of that eventually infarcted gives a measure of myocardial salvage that can be indexed to the area at risk to provide the salvage index [Friedrich 2008]. In clinical trials, this indexed measure should reduce the inter-patient variability associated with measures of absolute infarct size, with a consequent reduction in sample size[Klocke] needed to assess therapies intended to reduce infarct size [Larose 2010].

Our data suggest that, given the tendency to reduction in LGE over time, studies incorporating imaging time points as early as 12 hours [Larose] will markedly overestimate the area of irreversible injury in some patients. Based on our findings the magnitude of the underestimate of salvage that could be introduced in assessment < 48

hours post MI (*vs.* 6 months) is 38 % ± 14%, with important implications for trial design and implementation.

4.6 Limitations

Our data suggests almost complete resolution of oedema at 6 months. However, in a small number of cases persistently increased T2 signal intensity was identified at 6 months. From experimental studies, resolution of myocardial oedema occurs within 2 months of acute MI [Reimer and Jennings 1979]. While accumulation of lipid may occur in the very early phases post acute MI [Bilheimer 1978], this would not contribute significantly to T2 relaxation properties. A further possibility may relate to the threshold for oedema quantification. While efforts were made to impose a recognized and objective segmentation protocol, it is possible that an alternative segmentation strategy or the measurement of absolute myocardial relaxivity values may provide additional benefit. The use of new CMR techniques as T2 mapping should provide a better understanding of tissue composition both in acute stage and chromic stage; however further research will be needed to validate these techniques. The patients in this study were subject to an intensive sequence of MR scans, including 3 CMR scans within 15 days of acute MI. For reasons of safety, gadolinium was not given at each time point, but reserved for the first and last. For this reason, we were unable to define the precise time course of resolution of LGE. Although LGE resolution was associated with improved myocardial segmental function, we did not undertake any additional evaluation of myocardial viability, specifically no comparative study using positron emission tomography (PET), nor, in this clinical study, were histological samples available to define precisely the tissue correlates during each MR time point. Finally, preliminary analyses looking at: 1) clinical

characteristics to define discrete groups of patients with or without in LGE, 2) correlations between changes in image parameters and clinical characteristics, did not reveal significant results. This is most likely due to the small sample size and it requires further investigation.

4.7 Conclusions

Oedema of the myocardium occurs in almost all cases of STEMI and primary PCI. It is maximal and constant over the first week post MI, providing a stable window for the retrospective evaluation of area at risk. By contrast, LGE, while present early in acute MI, recedes over time and acutely detected LGE does not necessarily equate with irreversible injury. These findings have important implications for the interpretation of CMR early after acute MI and the design of clinical research studies using CMR-derived infarction or salvage index as endpoint.

Chapter 5: 3T CMR depict myocardial injury downstream remote coronary plaques in patients presenting with acute myocardial infarction

5.1 Introduction

Acute coronary syndromes are most often caused by the thrombotic complications of atherosclerotic plaque rupture or erosion [Naghavi 2003]. Transient or sustained ischemia of downstream myocardium may progress to tissue necrosis, where ischemia is prolonged. Plaque disruption and coronary thrombosis reflect interaction between events in the plaque and elements in circulating blood. However, the precise factors determining the timing and location of acute events have not been precisely defined. While local, plaque-associated events such as proteolytic degradation of the fibrous cap; cellular inflammation and intraplaque haemorrhage are all likely contributors, systemic factors, such as catecholamine release; blood pressure variation; platelet activation and systemic inflammation may also contribute [Dall'armellina 2010, Goldstein 2000, Naghavi 2003].The concept that systemic factors contribute is supported by the finding that anatomically remote 'complex plaques' are present in the 'non-culprit' coronary arteries of patients presenting with acute myocardial infarction [Goldstein 2000]. As defined by intraluminal filling defect; plaque ulceration; hazy contour, plaque irregularity or impaired flow, almost 40 % of patients with ACS showed evidence of one or more complex plaques at coronary loci remote from the culprit plaque [Goldstein 2000]. Patients with remote lesions had higher rates of recurrent acute coronary syndromes; repeated angioplasty and coronary artery bypass surgery than those without. However it is not known whether the remote lesions actually *cause* recurrent events at the level of the myocardium, that is to say, whether features of 'plaque complexity' in a given non-culprit

artery are associated with current or future acute ischemic injury in that territory. This is important since the capability to detect such lesions and knowledge of their significance may provide a rationale for treatment to ameliorate risk.

Recently developed cardiac magnetic resonance (CMR) techniques allow this question to be addressed [Dall'armellina 2010]. T2-weighted CMR imaging can identify oedema due to acute myocardial ischemia, even where this is insufficient to cause tissue necrosis [Abdel-Aty 2004, Arai 2008]. Importantly, the oedema is apparent by CMR for at least 7 days after the ischemic insult, allowing the volume and anatomical distribution of myocardium 'at risk' to be identified and quantified retrospectively [Dall'armellina 2011]. The complementary CMR technique of late gadolinium enhancement (LGE) can be used to determine the final infarct size and has been applied to determine location and quantity of even small quantities of injured tissue, for example in the context of high-risk percutaneous coronary intervention (PCI) [Selvanayagam 2005].

Accordingly, we designed a study in which patients with acute coronary syndromes, treated by PCI, underwent (i) invasive X-Ray coronary arteriography and (ii) CMR scanning at two separate time points. The first CMR (within 48 hours) was performed to determine territories 'at risk' and the second, at 6 months, to determine the clinical significance adjudged by (a) infarct size (LGE) and (b) segmental myocardial function.

5.2. Aims

The study aimed to address: (1) the prevalence of multiple 'complex plaques' in STEMI and NSTEMI in a contemporary population; (2) whether there was evidence of

acute ischemia (oedema) in multiple coronary territories, as predicted by the location of those coronary lesions and (3) whether there is CMR evidence of new myocardial infarction assessed later by LGE in territories subtended by the non-culprit artery 'complex plaques'.

5.3 Methods

Patient population

This prospective study was undertaken in a single tertiary centre. The study protocol was approved by the local ethics committee and all patients gave written informed consent. Fifty patients (25 STEMI and 25 NSTEMI) were included (refer to methods chapter for detailed description of inclusion and exclusion criteria). Patients with possible myocarditis at presentation were excluded; furthermore if any CMR findings were indicative of cardiomyopathy or myocarditis the patients were also excluded.

Acute clinical management was at the discretion of the responsible physician, with the intention to reflect contemporary practice and guidelines (including use of aspiration catheters; glycoprotein IIb IIIa receptor inhibitors and high-dose clopidogrel loading). Blood samples were collected for Troponin I at the time of admission and every 12 hours post PCI.

CMR

Two separate CMR scans were performed on each patient at the following time points: 12 - 48 hours (24H) from the onset of symptoms and 6 months (6M). The STEMI patients underwent primary PCI before CMR.

CMR examinations were performed on a 3 Tesla MR scanner (Trio, Siemens Healthcare, Erlangen, Germany). The CMR protocol included assessment of LV function

(using SSFP), oedema (using T2prep SSFP), and LGE (using a T1 weighted segmented inversion-recovery GRE_PSIR) (refer to Methods chapter for specifications).

Image co-registration and post-processing analysis

Cine, oedema and LGE images were acquired parallel to the AV groove and were radially aligned to the position of the papillary muscles. CMR image sets acquired at different time points were analysed in random order by observers blinded to the origin of the image.

Quantification of LV volumes and damaged myocardium

Post-processing analyses included:

1) Quantification of LV volumes
2) Quantification of oedema or LGE damaged fractions

(Refer to Methods chapter for further specifications)

Angiographic analyses

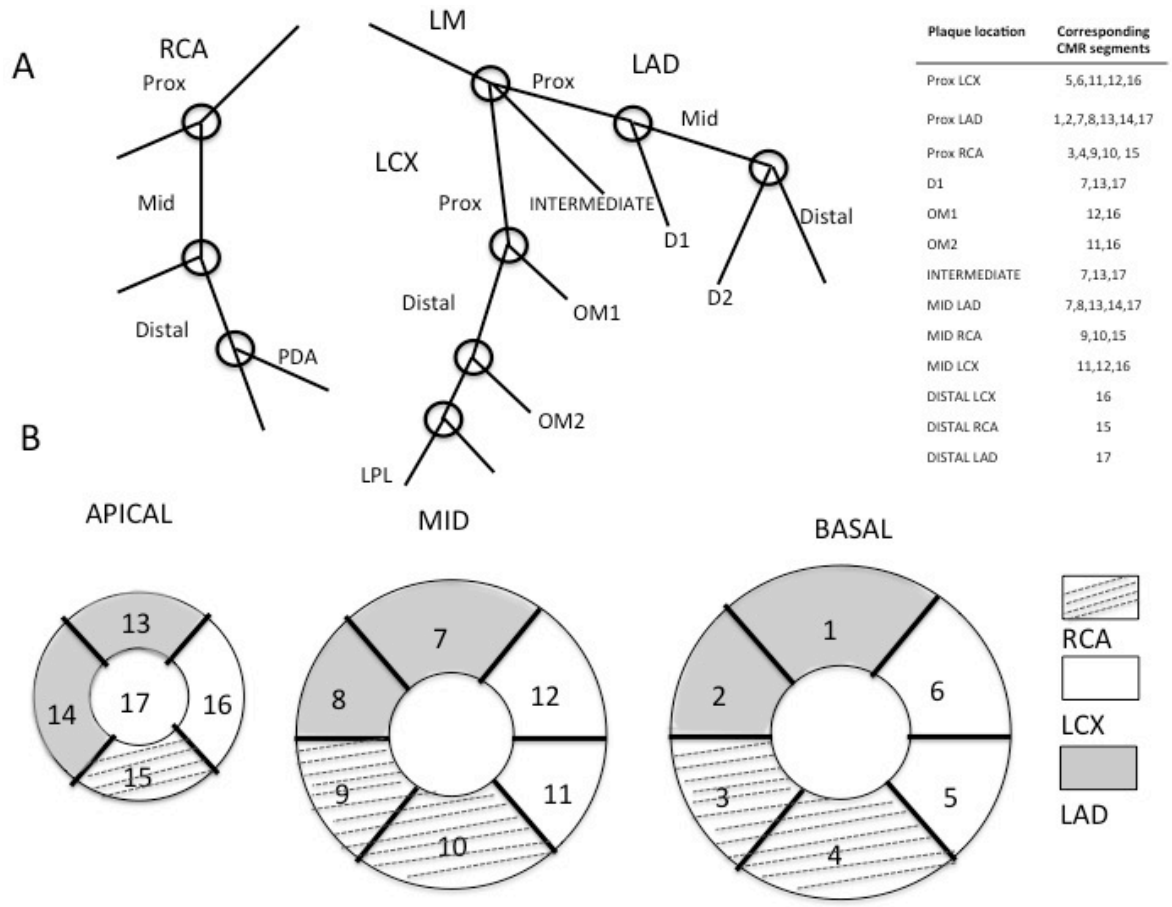
All baseline angiograms were analysed by two independent observers (training level ST 5 and 7) by means of pre- specified methods, without knowledge of the CMR findings, or subsequent events. The identification of the culprit lesion was guided by the surface ECG. Coronary angiograms were analysed for presence of 1) anatomically remote plaques; 2) '*complex plaques'*. Coronary lesions were defined as significant with a stenosis estimated > 50% as previously described, [Goldstein 2000]. Coronary stenosis were measured by quantitative analysis of the QCA- (Medcom-McKesson horizon cardiology, Israel - version 12.2 - area and diameter) using the guide catheter for calibration and automated border recognition of the contrast-enhanced lumen to measure

the QCA stats - stenosis/area. To allow for accurate QCA measurements, the angiograms were acquired using a Siemens axiom artis arm, in single plane and the images were obtained at 15 frames/second with a field of view of 20 cm in the presence of a solid flat plate (i.e. no need for grids to be used with image acquisition)

For each patient, the coronary arterial tree was reviewed systematically to identify anatomically remote complex plaques. An anatomically remote plaque was defined as (1) one in a different artery from the artery containing the infarct-related plaque; (2) in the same artery as that containing the infarct-related plaque, but in a different branch; or (3) in the same artery and branch as the infarct-related plaque, but at least 5 cm from the infarct- related plaque, with an intervening segment of disease-free vessel. Complex coronary plaques were identified according to previously used criteria: (1) an intraluminal filling defect consistent with thrombus, defined as abrupt vessel cut-off with persistence of contrast, or an intraluminal filling defect in a patent vessel, within or adjacent to a stenotic region, with surrounding homogeneous contrast opacification; (2) plaque ulceration, defined by the presence of contrast and hazy contour beyond the vessel lumen; (3) plaque irregularity, defined by irregular margins or overhanging edges and (4) impaired flow. Lesions were considered “complex” if they caused at least 50 percent stenosis and had two or more of these morphologic features.[Goldstein 2000] As in previous studies, the angiograms were analysed by two independent angiographers (blinded to the PCI stenting procedure), the results were compared, and when there was disagreement, a final decision was made by consensus.

Matching the angiographic analyses to the MRI analyses

In order to match MRI findings to angiographic findings, we designed our own matching scheme described here. The downstream segments of myocardium vulnerable to injury pertaining to either the culprit or non-culprit vessel were identified based on the AHA 17-segment model (Figure 5.1).



Plaque location	Corresponding CMR segments
Prox LCX	5,6,11,12,16
Prox LAD	1,2,7,8,13,14,17
Prox RCA	3,4,9,10, 15
D1	7,13,17
OM1	12,16
OM2	11,16
INTERMEDIATE	7,13,17
MID LAD	7,8,13,14,17
MID RCA	9,10,15
MID LCX	11,12,16
DISTAL LCX	16
DISTAL RCA	15
DISTAL LAD	17

Figure 5.1. Matching angiographic and CMR segmentation analyses. The 16-segments coronary artery scheme (A) and the myocardial 17 segments model of the American Heart association (B) are here shown. Based on the plaque position, we matched the two schemes and we have extracted the correlations between various segments downstream the indexed plaque but also between segments and certain areas (left, right, proximal, distal) of the coronary tree. The legend at the top right shows some of the most representative correlations between anatomical location of the plaque in the vessel and the corresponding segments downstream of the indexed plaque.

All segments of the myocardium pertinent to the coronary territory, were classified in a binary fashion as “downstream segments” or not, depending on the relationship to the lesion location in the coronary artery. We match coronary segments and myocardial segments on individual basis accounting for anatomical variation of main side branches and for dominance. In particular, in ambiguous cases of distal stenosis or anatomical variable of small branches or multiple lesions, the segments of the myocardium potentially damaged downstream were nominated upon expert consensus [4 interventionalists consultants of the unit (Prof. RC, Prof AB, Dr. CF, Dr. BP,)].Cases of codominace or cases in which the arterial supply could not be discriminate between two coronaries or between culprit and non culprit, were identified and analyzed separately: specifically in case of ambiguity, CMR injured segments were assumed as pertaining to the culprit vessel. The results were then matched to the CMR segmentation by forced nomination of arterial supply to myocardial segments based on individual anatomy.

To account for anatomical imprecision of the delineation of arterial supply across CMR defined segments, we identified where injury in nominally distinct segments was adjacent to and contiguous with the indexed injured segment. In this way, only the truly remote segments were included in these analyses (Figure 5.2).

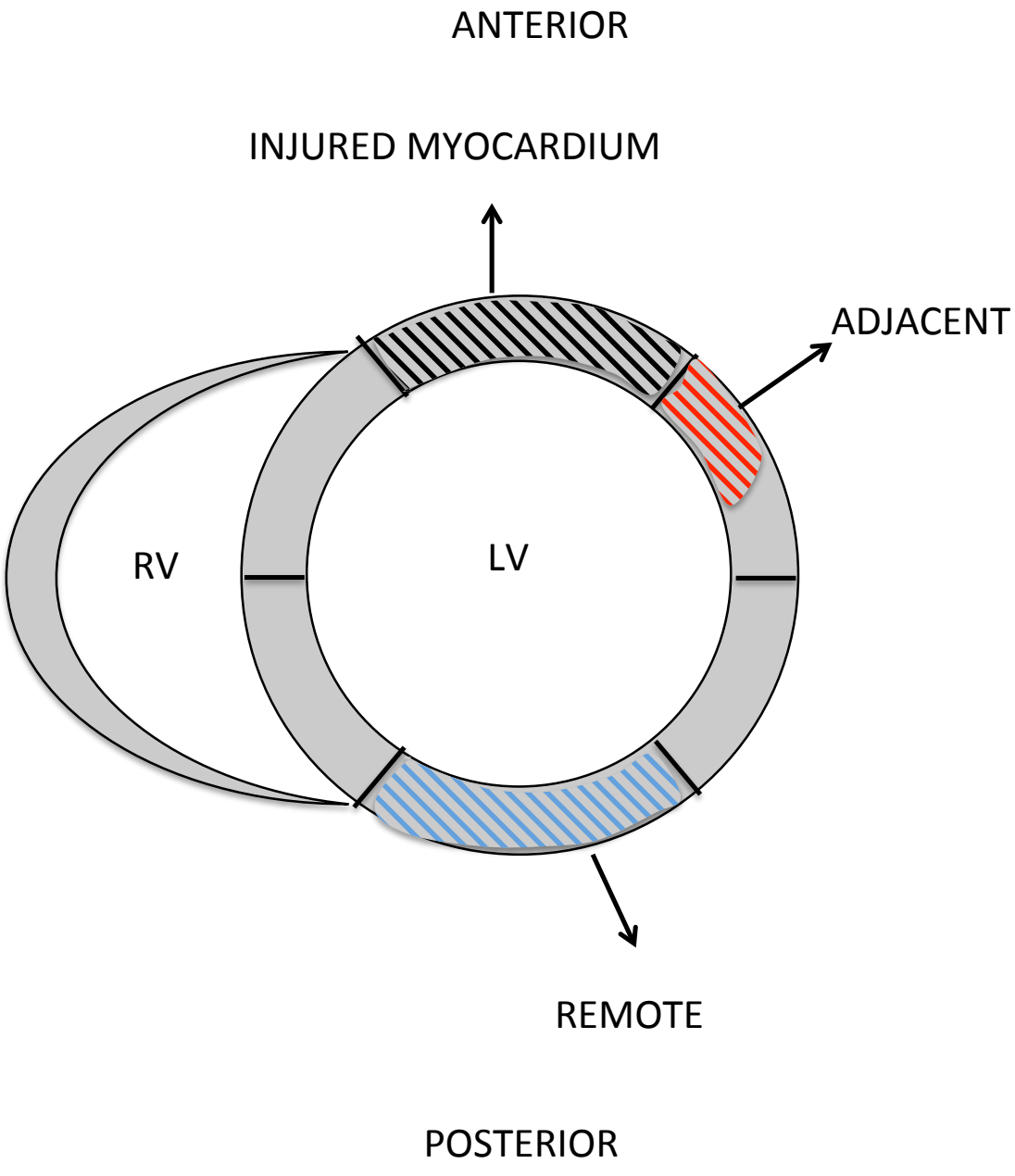


Figure 5.2. Representation of segments remote and adjacent to injured segments. The scheme shows injury in the anterior wall (black lines). The injured segment adjacent to the injured myocardium is shown in red (red lines) while the remote in blue (blue lines).

Statistical analyses

Values of continuous variables are expressed as mean (± SD). To investigate differences in LV volumes, ejection fraction, myocardial volume of oedema, and LGE assessed by CMR, between STEMI and NSTEMI, independent two-sample t-test was used. For categorical variables, a χ^2 test was used to assess differences in number of segments between groups. Cohen k coefficient for categorical measurements of culprit and non-culprit vessels was performed to evaluate inter-observer variability for culprit and non-culprit vessel identification. All statistical tests were 2-tailed, and all probability values of <0.05 were considered statistically significant.

5.4 Results

Study population

Patient characteristics are presented in Table 5.1. All patients were treated with dual antiplatelet agent and intravenous heparin: all STEMI patients underwent primary PCI within 12 hours from the onset of chest pain and prior to CMR with a mean time from onset of pain to balloon of 3.5 ± 2.5 hours. The 25 NSTEMI patients underwent coronary angiogram on average 33 ± 20 hours from onset of chest pain; out of these, 2 showed no coronary lesions and 1 showed diffuse disease and therefore did not receive invasive treatment (Table 5.2).

Table 5.1. Patients' characteristics

Patient characteristics	All N = 50	STEMI N=25	NSTEMI N=25	P-value
Age	**56 ± 8**	54 ± 8	57 ± 8	**0.2**
Sex (F:M)	**4: 46**	1 : 24	3:22	**0.6**
BMI	28 ± 4	27 ± 3	28 ± 5	**0.4**
Risk Factors [No (%)]				
Smoking	**19 (38)**	8 (32)	11 (44)	**0.4**
Hyperlipidemia	**20 (40)**	8 (32)	12 (40)	**0.4**
Diabetes	**5 (10)**	0	5 (20)	**0.05**
Hypertension	**21 (42)**	9 (36)	12 (48)	**0.6**
Family history	**25 (50)**	10 (40)	15 (60)	**0.2**
Presenting characteristics				
Troponin I (12 hours post admission) (mg / mL)	25 ± 22	42 ± 15	10 ± 16	**<0.01**
Median (IQR) Time from onset of symptoms to procedure (hrs.)	**10 (2.5,27)**	2.6 (2,3.7)	28 (21,28)	**0.0001**
Drug therapy n (%)				
Aspirin	50 (100)	25 (100)	25 (100)	**1**
Glycoprotein IIb IIIa inhibitor	28 (56%)	25 (100)	3 (12)	**<0.001**
Clopidogrel	50 (100)	25 (100)	25 (100)	**1**
β-Blockers	50 (100)	25 (100)	25 (100)	**1**
Heparin	50 (100)	25 (100)	25 (100)	**1**
Events in the first 12 months				
Staged PCI	6	2	4	
CABG	2	1	1	
Admission for angina	2	1	1	
Arrhythmias/ICD	1	1	0	

All patients underwent CMR in the acute phase (28 ± 11 hrs); the CMR was then repeated at 6 months in 23 STEMI and 18 NSTEMI. The 2 STEMI patients who failed 6 months follow-up did so for medical reasons (1 urgent coronary re-intervention and 1 surgery for aneurysm of the aorta); 7 NSTEMI patient did not undergo 6 months follow up: four due to medical reasons (2 staged PCI, 1 coronary artery by-pass (CABG) surgery, 1 impaired kidney function) and 3 declined.

Angiographic findings

The angiographic findings at the time of PCI are presented in Table 5.2. All the nominated culprit vessels by the two observers had been treated acutely. All STEMI patients underwent primary PCI. Of the NSTEMI patients 2 showed no focal angiographic coronary lesion and were treated medically and 1 showed diffuse disease and was treated with coronary artery bypass grafting (CABG). The remaining patients (23) underwent PCI. The Cohen kappa coefficient for categorical assessments of culprit vessel (k=0.892) and non- culprit vessel (k=0.816) indicated excellent levels of agreement for inter-observer variability assessments.

The incidence of multivessel disease (independently of the severity of the stenosis) in NSTEMI patients was significantly higher compared to the STEMI (18 vs. 9 pts., P=0.02) with a significantly higher number of non-culprit plaques on a patient-by-patient basis in NSTEMI compared to STEMI (1.6 ± 1.5 vs. 0.6 ± 1 respectively, P=0.01). No "complex plaques" as defined by previously defined criteria were identified.

As a result of the angiographic analyses, a total of 163 segments (97 in STEMI and 66 in NSTEMI, P=0.02) were identified as potentially vulnerable to an ischemic insult downstream of the lesions in the culprit vessels and 120 segments downstream of

lesions in any non culprit vessel (40 in the STEMI group and 80 in the NSTEMI group, $P<0.01$)

Table 5.2. Angiographic findings

	Tot	STEMI	NSTEMI	P-value
N of pts.	50	25	25	
CULPRIT nominated/treated		25/25	23/21	
CULPRIT LAD	18/16	10/10	8/6	**0.24**
CULPRIT RCA	21/21	13/13	8/8	**0.5**
CULPRIT LCX	9/9	2/2	7/7	**0.07**
Absence of culprit	2	0	2	
N of pts. with non- culprit disease (§)	27	9	18	**0.02**
N of pts. with 50% non culprit lesions	16	5	11	**0.13**
N of pts. with 1 non culprit vessel	15	7	8	
N of pts. with 2 non culprit vessels	3	0	3	
N of pts. with 3 non culprit vessels	7	2	5	
N of pts. with 4 non culprit vessels	2	1	1	
N of pts. with 5 non culprit vessels	1	0	1	
Total N of non culprit lesions	54	16	38	
N non culprit lesions/pt.	1.1 ± 1.4	0.6 ± 1	1.6 ± 1.5	**0.01**
QCA% diameter of lesions (mean ± SD)	50±15	48±16	50±15	
Non culprit lesions 50% QCA diameter	23	6	17	
Thrombus	0	0	0	
Ulcerated plaque	2	1	1	
Irregularity	5	1	4	
TIMI FLOW non culprit	2.88 ±0.6	3	2.76 ± 0.8	**0.16**

- Non-culprit lesions severity defined by QCA diameter [§] Plaques of any QCA diameter

CMR findings

All patients were in sinus rhythm during the CMR scan. While all the STEMI patients showed both oedema and LGE, 4 of the NSTEMI showed only oedema and no LGE at 24 hrs and 1 showed no oedema or LGE. The LV damaged fraction (LV %) assessed by oedema and/or LGE at 24 hrs was significantly larger in the STEMI patients compared to NSTEMI (Table 5.3). At 6 months although there was some improvement in LGE in both groups, the trend towards worse CMR parameters in STEMI persisted.

Table 5.3. CMR findings

	All	STEMI	NSTEMI	P-value
LV % Oedema 24 hrs	42 ± 14	46 ± 13	31 ± 12	0.0001
LV % LGE 24 hrs	29 ± 15	37 ± 13	16 ± 10	0.0001
EF % 24 hrs	55 ± 20	54 ± 29	61 ± 9	0.3
EDV 24 hrs	152 ± 37	153 ± 42	143 ± 28	0.3
ESV 24 hrs	76 ± 32	86 ± 30	59 ± 22	0.001
SV 24 hrs	77 ± 17	70 ± 16	85 ± 16	0.002
	N=41	**N=23**	**N=18**	
LV % LGE 6m	20 ± 12	26 ± 11	13 ± 10	0.6
EF % 6m	63 ± 13	58 ± 15	69 ± 5	0.01
EDV 6m	151 ± 38	161 ± 41	137 ± 31	0.06
ESV 6m	59 ± 39	72 ± 46	42 ± 13	0.02
SV 6m	92 ± 20	90 ± 20	95 ± 20	0.4

Matching CMR and angiography: segmental analyses

A total of 706 segments (342 in the STEMI and 364 in the NSTEMI) at the earlier time point were analysed; of these 216 (30%) were positive for oedema and 195 (27%) for LGE.

In order to exclude segments, that were affected by oedema or LGE because of their continuity with the indexed coronary territory, we excluded the segments identified as "adjacent" (133 positive for oedema and 76 for LGE). Using this method the angiogram predicted 288 affected segments compared with 216 actually identified using CMR criteria ($P<0.01$).

Of the 168 segments identified as potentially injured downstream a culprit vessel on the angiogram, 138 (83%) were positive for oedema on acute CMR and only 18 % (22/120) of the segments downstream of a lesion in a non culprit vessel (Table 5.4). As shown in Figure 5.3, the segments positive for oedema/LGE downstream of a non-culprit plaque pertained virtually all to NSTEMI patients.

The degree of stenosis of the plaques in non-culprit vessels with corresponding myocardial injury downstream was 71% ± 26% (range 41-100%).

Table 5.4. Distribution of segments positive for oedema on acute CMR and segments downstream the vessels on the angiogram.

ACUTE	STEMI			NSTEMI			TOT
	CULPRIT*	NON CULPRIT*	OTHER*	CULPRIT*	NON CULPRIT*	OTHER*	
OEDEMA +	96	1	16	42	21	39	215
OEDEMA -	2	24	123	28	47	133	357
ADJACENT (on CMR)		15	65		12	42	134
TOT	98	40	204	70	80	214	706

*CULPRIT indicates segments downstream of a culprit coronary lesion; NON CULPRIT= segments downstream of a non-culprit coronary lesion; OTHER= segments neither downstream a culprit nor a non-culprit coronary vessel.

Table 5.5. Distribution of segments positive for LGE on acute CMR and segments downstream the vessels on the angiogram.

ACUTE	STEMI			NSTEMI			TOT
	CULPRIT*	NON CULPRIT*	OTHER*	CULPRIT*	NON-CULPRIT*	OTHER*	
LGE +	90	1	23	35	22	27	197
LGE -	8	27	140	32	51	174	432
ADJACENT (on CMR)		12	41	3	7	13	76
TOT	98	40	204	70	80	214	706

*CULPRIT indicates segments downstream of a culprit coronary lesion; NON CULPRIT= segments downstream of a non-culprit coronary lesion; OTHER= segments neither downstream a culprit nor a non-culprit coronary vessel.

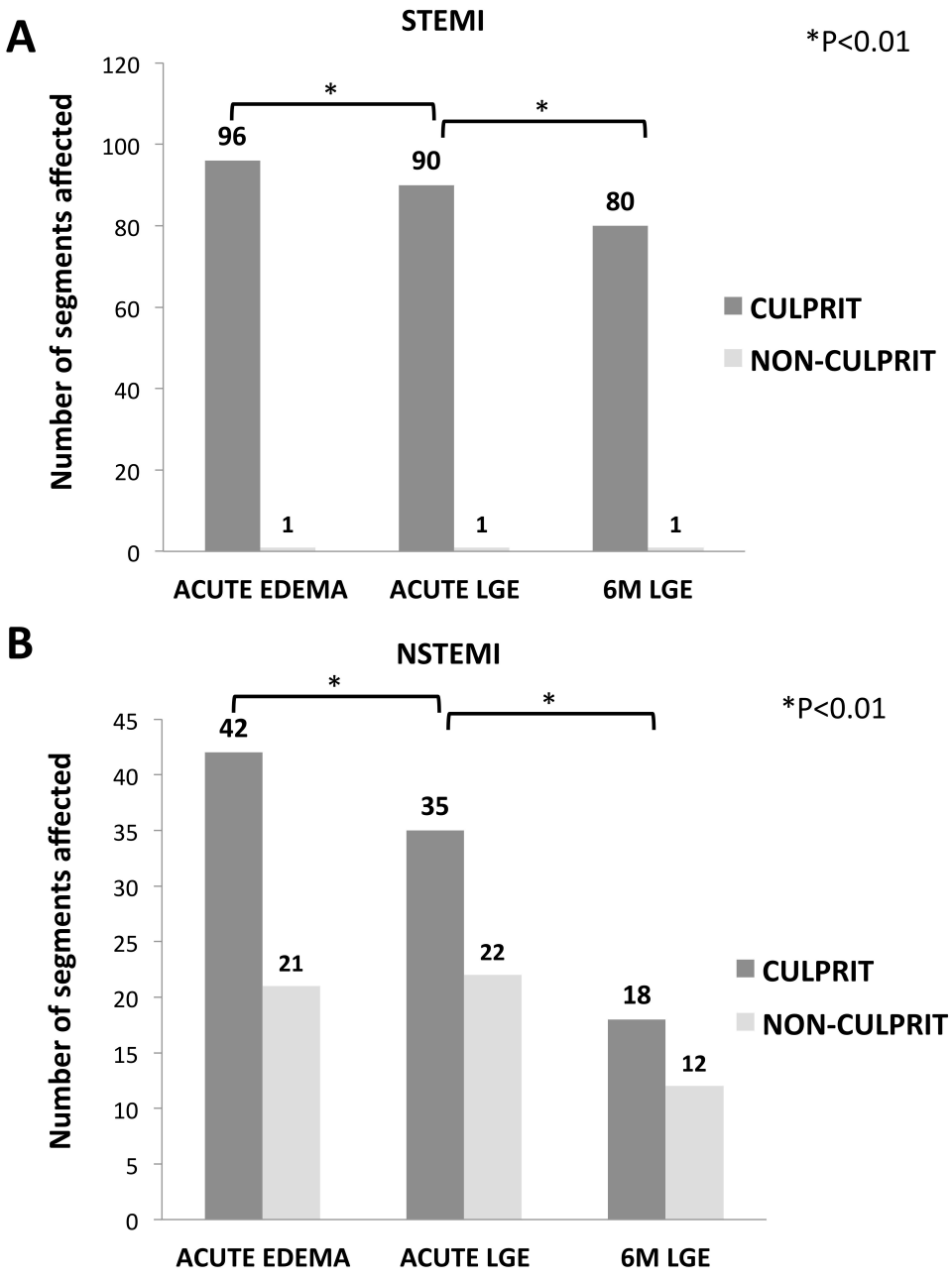


Figure 5.3. Segments affected (by oedema and LGE on CMR) downstream the culprit and non culprit vessel in STEMI (Panel A) and NSTEMI (Panel B). In STEMI patients (Panel A), acute myocardial injury either by CMR oedema or LGE was depicted downstream the culprit vessel while virtually no injury was shown downstream non-culprit stenosis. The number of segments positive for oedema was significantly larger than the number of segments positive for LGE. In the NSTEMI patients (Panel B), CMR showed acute oedema or LGE downstream both culprit and non-culprit vessels. While, the territory positive for oedema downstream the culprit was significantly larger than LGE, the area downstream the non-culprit by oedema was equivalent to the one LGE positive. (Adjacent segments have been excluded from these analyses).

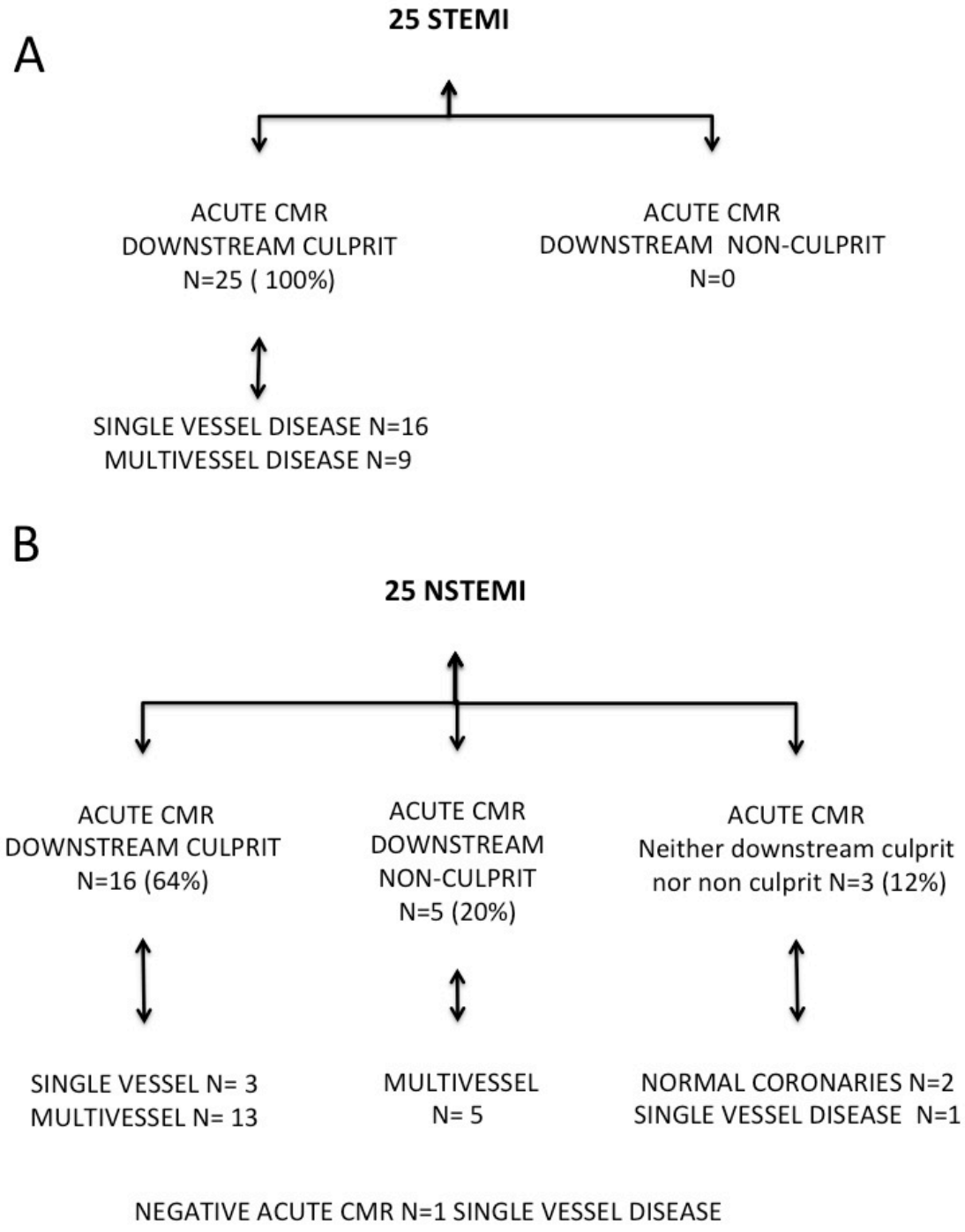


Figure 5.4 Angiographic and corresponding acute CMR findings in STEMI (Panel A) and NSTEMI patients (Panel B). As showed in Panel A, most of the STEMI patients had single vessel disease at the angiogram. The CMR showed positive findings downstream in the culprit vessel territory in all patients. Most of the NSTEMI patients had multivessel disease: in 28% of these CMR showed positive acute findings downstream from a non –culprit plaque (Panel B).

Matching CMR and angiography: analyses on a patient-by-patient basis

As shown in Figure 5.4, in STEMI patients myocardial injury by CMR (oedema or LGE) was identified downstream the culprit vessels only. In contrast 20% of NSTEMI patients, had significant non-culprit related areas of injury defined by CMR (Figure 5.5 and 5.6) (only one of these patients had positive CMR findings in both culprit and non culprit territories) (Figure 5.9). The clinical and angiographic presentation is reported in Table 5.6.

In three patients, acute CMR depicted mycoardial oedema in 16 segments not associated with any plaque (culprit or non culprit) : one patinet had single vessle disease (Figure.5.7) and 2 cases had no angiographic focal coronary diseae (Figure 5.8). in these NSTEMi the presence of atrial septal defect was excluded by echocardiography.

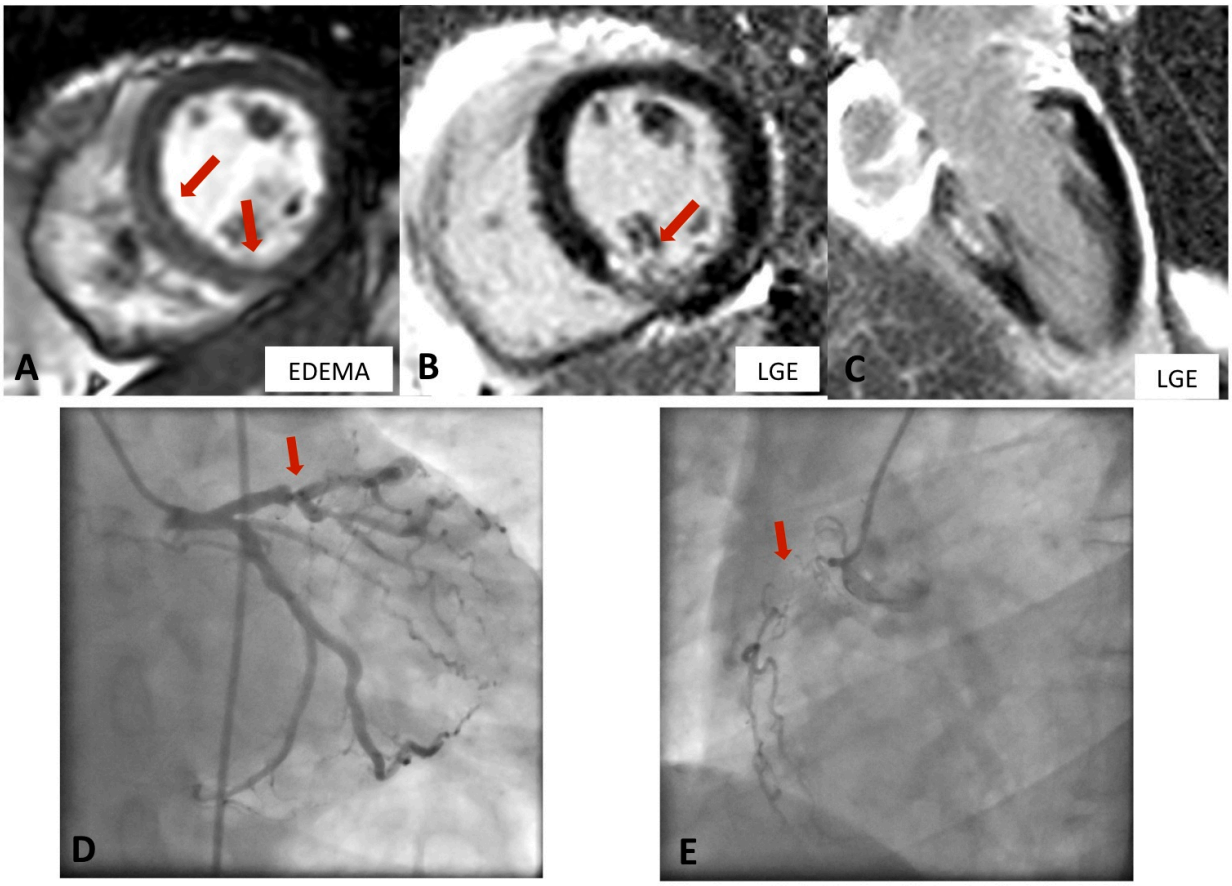


Figure 5.5. Representative example of a patient with multivessel disease and acute injury by CMR in a territory downstream a vessel different from the one identified as culprit. On panels A, B and C, CMR images of acute oedema and LGE show acute myocardial injury in the inferior septum and inferior wall pertaining to the RCA. On the angiogram (Panels D and E) the RCA was occluded and the vessel identified as culprit and treated was the left anterior descending (LAD).

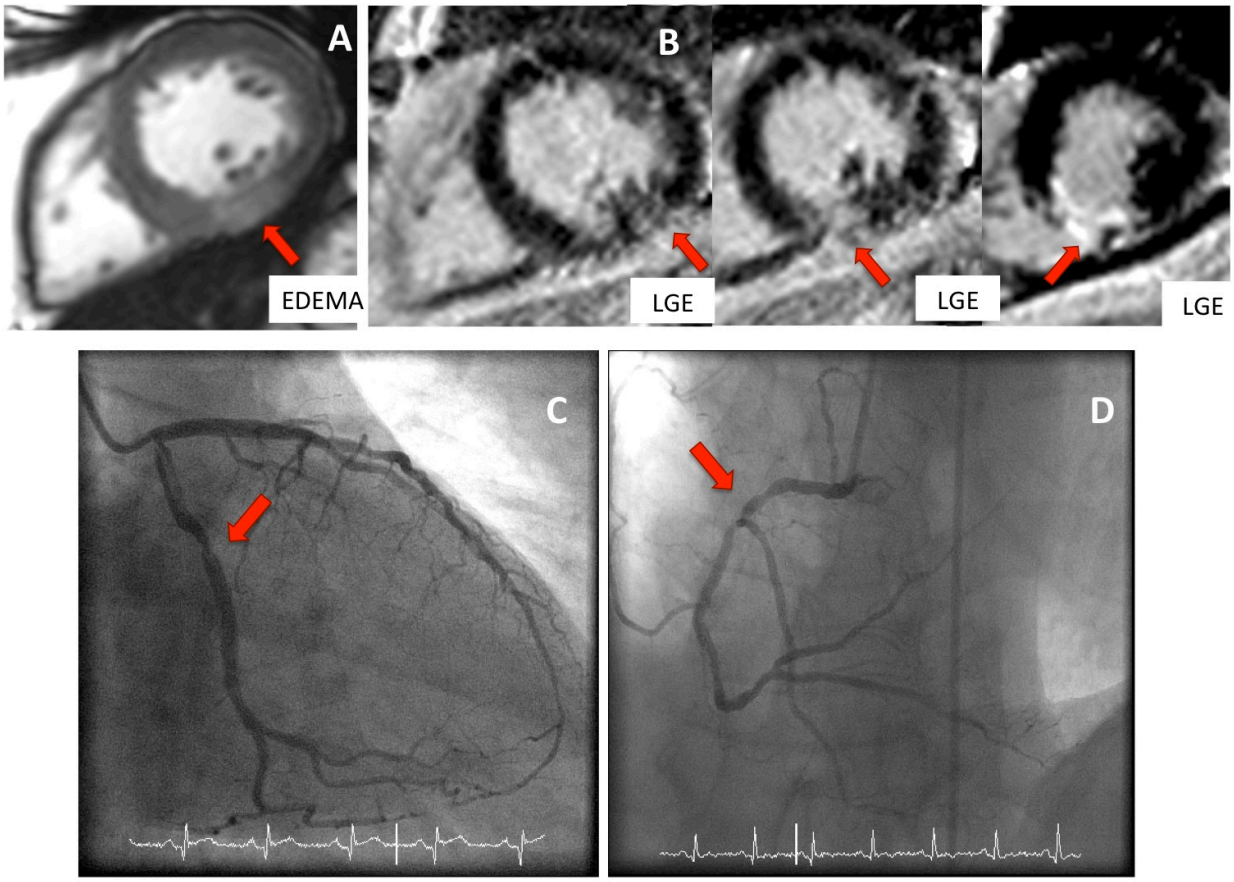


Figure 5.6. Representative case of a NSTEMI patient with multi-vessel disease and positive CMR downstream the non-culprit. As shown in Panel A and B, both oedema and acute LGE CMR show acute myocardial damage in the inferior wall downstream the right coronary artery (RCA). The angiogram (Panels C and D) revealed a significant stenosis at the level of the mid circumflex (Panel A) identified as the culprit plaque and two plaques of 48% and 31% stenosis in the proximal and mid RCA (Panel D).

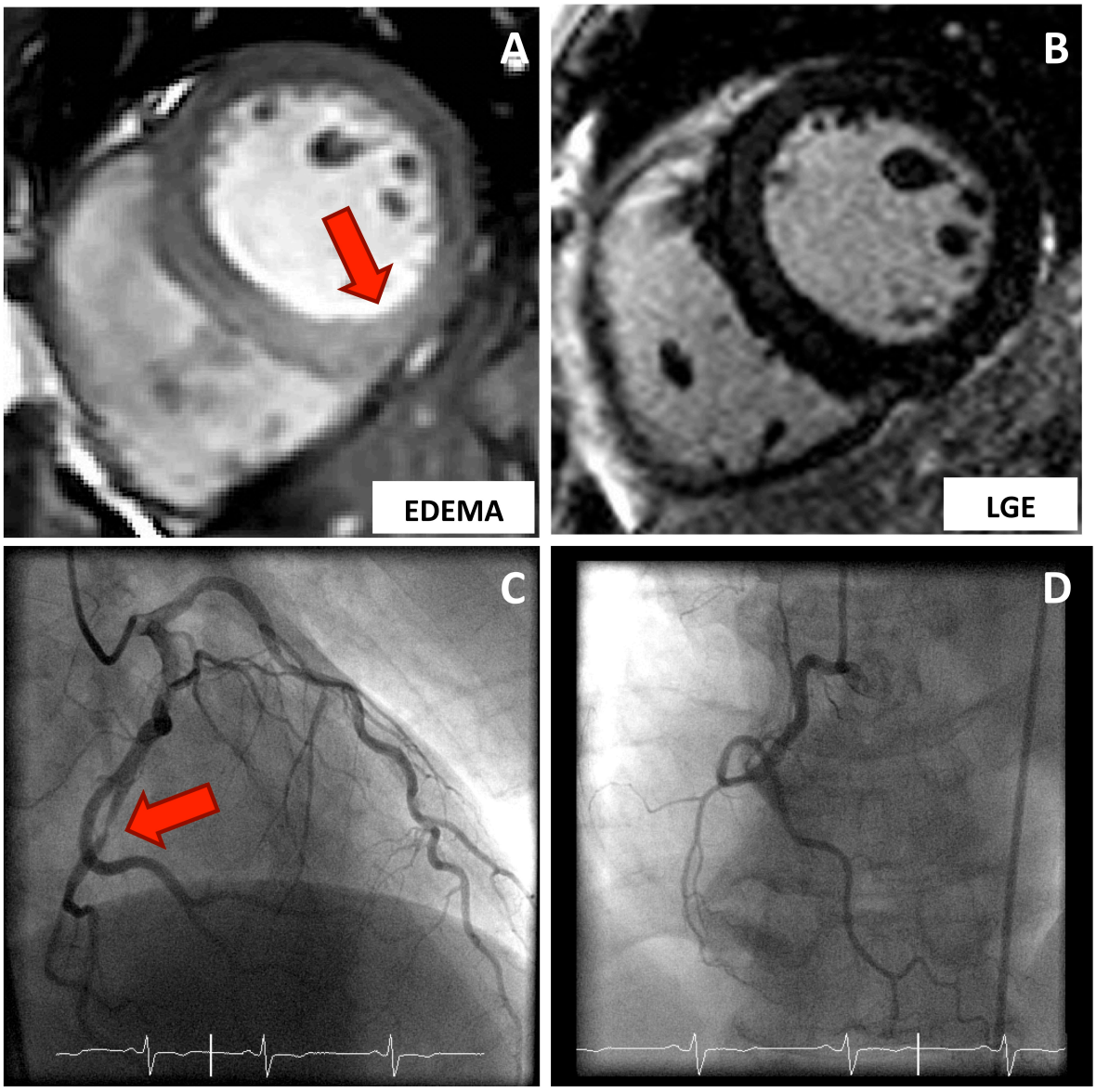


Figure 5.7 Representative examples of acute myocardial injury by CMR in regions other than downstream the culprit or non-culprit vessels. T2W CMR (Panel A) depicted oedema in the inferior wall (red arrow) while the LGE imaging (Panel B) is negative. The angiogram shows single vessel disease with the culprit plaque located in the distal LCx (red arrow on Panel C)

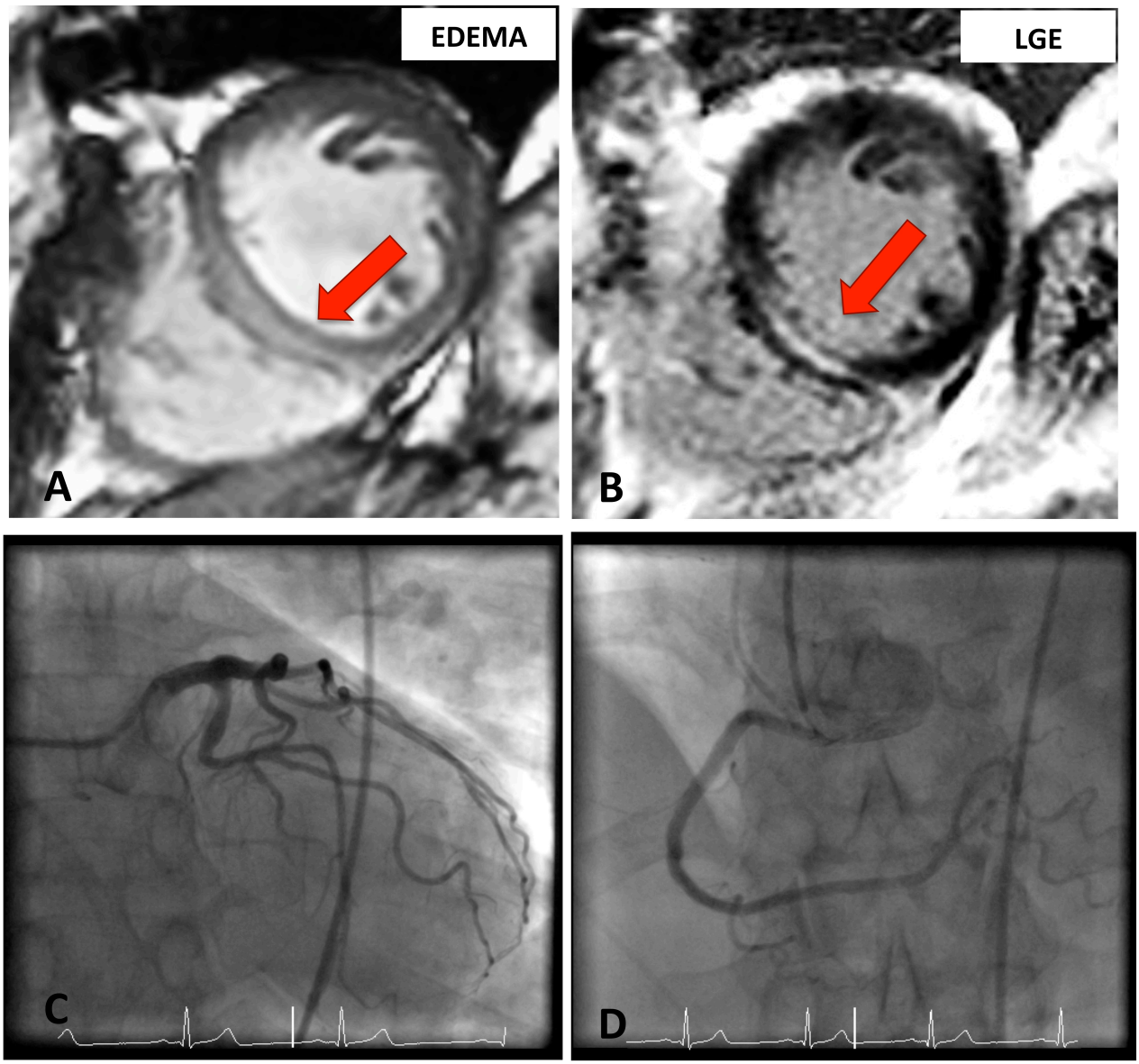


Figure 5.8. Representative examples of acute myocardial injury by CMR in a patients with normal coronaries Both oedema (Panel A) and LGE imaging (Panel B) reveal acute injury in the inferior septum. However the angiogram (Panel C and D) showed normal coronaries.

Table 5.6. Patients with lack of correspondence between CMR findings and angiographic findings

Patient	Tn I	ECG changes	CMR	ANGIO		
			Oedema and/or LGE	Culprit/ Stented	Non culprit (QCA diameter %)	Vessel responsible for myocardial damage (REAL CULPRIT)
NSTEMI 1	4.2	SR, ST depression in V3, V4, V5, I, II, aVL	Inferior and lateral walls	LCX/ LCX	Mid LAD (47%), Distal and prox RCA (61%)	RCA
NSTEMI 2	0.4	SR Biphasic T waves in V1 /V2, Q wave in III	Inferior septum	LAD/ LAD	Prox RCA (100%) Mid Lcx (47%)	RCA
NSTEMI 3	6.1	SR, Q wave in III and aVF (During procedure minor inferior ST elevation)	Inferior wall	LCX/ LCX	Ostial Lcx (47%), Prox and mid RCA (48%) Mid LAD (52%)	RCA
NSTEMI 4	0.7	SR, LVH, ST depression in V5, V6.	Inferior wall	OM1/ OM1	Mid LAD (56%) Prox RCA (65%) Mid/distal (65%)	RCA
NSTEMI 5	2.1	SR, Dynamic anterior T wave changes, Q wave in III	Inferior wall and inferior septum	LAD-D1/ LAD-D1	RCA (100%)	RCA

Matching CMR and angiography: findings at 6 months

The final number of patients undergoing CMR at 6 months was 23 for STEMI and 18 for NSTEMI. While CMR T2 W imaging did not reveal any persistent or new positive findings for oedema at 6 months, after excluding the adjacent segments, LGE depicted 136 segments affected, corresponding to 69% of the segments acutely injured by LGE. There were no new areas of LGE at 6 months. Out of the 136 segments at 6 m, 98 were downstream the culprit vessel and 13 downstream the non-culprit.

In those patients with misdiagnosed culprit, the LV damaged fraction by LGE at 6 months was 8% ± 10% and no significant difference in EF was found compared to the rest of the patients.

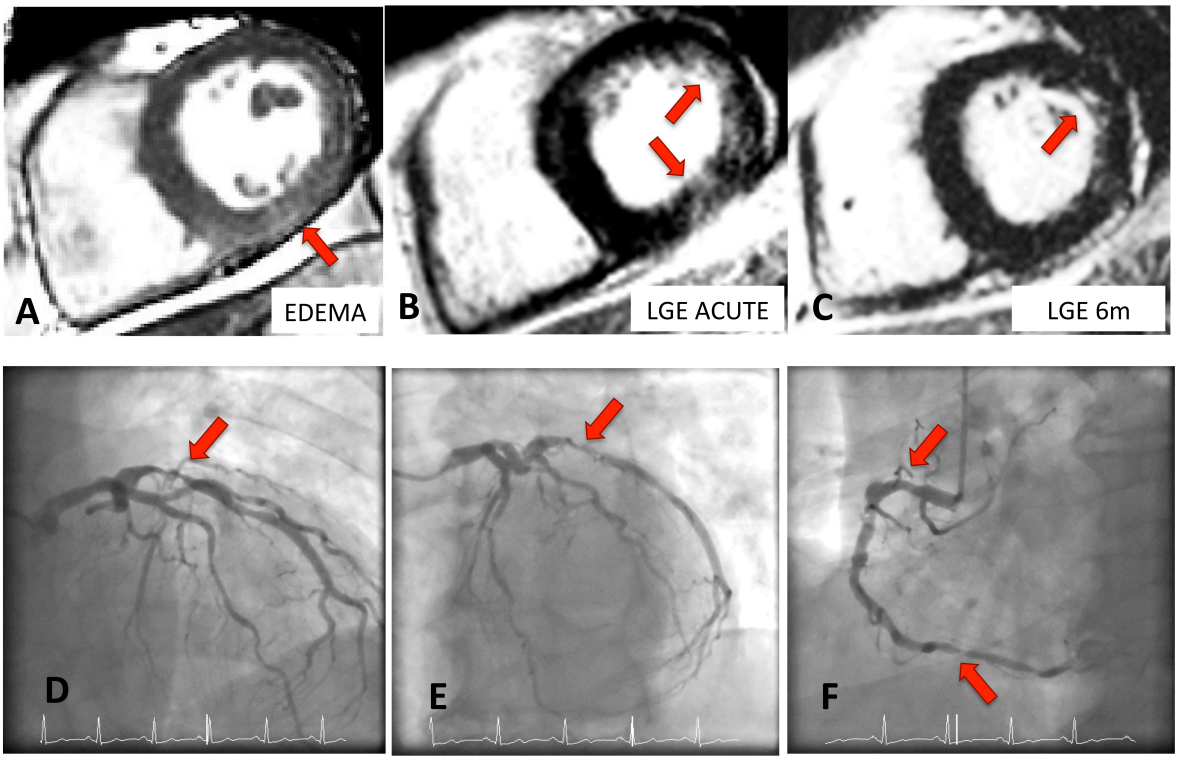


Figure 5.9. A case of multivessel disease patient with positive acute oedema and LGE by CMR, both in the inferior and lateral (Panels A and B). At 6 months the LGE shows minor persistent positive findings in the lateral territory (Panel C). On the angiogram (Panels D to F) the circumflex was identified as culprit vessel and treated, while the LAD (mid) and the RCA (proximal and distal) were identified as non-culprit.

5.5 Discussion

Patients with ACS are known to be at increased risk of recurrent major adverse coronary events (MACE) and repeated procedures despite optimal medical therapy. One cause of the worse prognosis in NSTEMI patients with multivessel disease may be the presence of remote complex plaques. However the pathophysiological meaning of these lesions is unknown and therefore the modality and the timing of intervention are still open issues. In order to better define the pathophysiological consequences in relation to multivessel disease, in this study we report on the existing correlation between the acute angiographic coronary findings and the corresponding findings of myocardial injury by CMR both in acute and at 6 months.

Our main findings are: 1) single vessel disease is the most frequent diagnosis in STEMI patients: we found a good correspondence between the culprit (treated) vessel and the myocardial territory injured downstream; this supports the current medical/interventionalist practice in STEMI patients; 2) multivessel disease was twice as frequent in the NSTEMI patients (72%) than in the STEMI ones. No complex plaque was identified. 3) Importantly in 20% of the NSTEMI patients, there was a discrepancy between the identified (and stented) culprit vessel on ECG / angiography and the myocardial injury downstream as assessed by CMR suggesting an inability to correctly identify the culprit vessel in a minority of cases 4) No new myocardial damage/injury was depicted by CMR at 6 months in patients with multivessel disease. These findings have important implications because they allow critical review of current clinical practice and the invasive approach especially in relation to the identification of the culprit lesion in cases with multivessel disease. To the best of our knowledge this is the first study in

which acute CMR (T2W and LGE) has been used to identify myocardial injury downstream culprit versus non-culprit lesions. Previously studies have reported on CMR assessment of myocardial injury in NSTEMI patients[Raman 2010, Verhaert 2011, Xu 2011]. In a publication by Raman et al on the prognostic values of acute CMR oedema imaging in 100 NSTEMI patients,[Raman 2010] the presence of myocardial oedema was mostly correlated with the presence of 70% coronary stenosis. However no specification was made regarding the correspondence of the myocardial injury to the culprit vessel and no follow up scan was performed.

In accordance to previously published data,[Goldstein 2000] 64% of our STEMI patients were identified as single vessel disease. Importantly the treated vessel was the one responsible for myocardial injury as assessed by CMR. This is also in keeping with recently published data that demonstrated a strong correlation between areas at risk assessed by the angiographic jeopardy score[Graham 2001] and CMR T2W oedema imaging in STEMI patients [Ortiz-Perez 2007]. The correct identification of the culprit vessel in STEMI is probably favoured by the "acute characteristics" of the plaques, which is often superimposed by thrombus [Kotani 2003, Montalescot 2007].

In our NSTEMI cohort, the data suggest that there is greater prevalence of multivessel disease and that the identification of the culprit plaque may be erroneous in a significant proportion of cases. This indicates that the decision to treat guided by the ECG and angiographic assessment only are not sufficient.

As previously shown, the ECG cannot be considered a robust way to assess myocardial viability. On-going ischemia or infarcts can be missed by silent ECG in a substantial proportion of patients[Kannel and Abbott 1984]. In these patients with silent

ECG and yet small infarcts, prognosis is worse. [Kim 2009] Conversely, the presence of Q waves on the ECG is not always indicative of a transmural myocardial infarction and therefore decision not to treat should not be made on the basis of the ECG alone [Moon 2004].

In relation to the angiographic assessment and based on our results, the issue of the correct identification of the culprit lesion unfolds into two different aspects: a) the failure to correctly assess mild-moderate looking plaques versus complex plaques and b) the invasive approach when one of the vessels is found occluded. Previously published data have shown that angiography fails to demonstrate a complex culprit plaque in one third of the patients[Kerensky 2002] and that even mild looking plaques may cause recurrence of events due to specific features such as a thin cap or a large burden which can be appreciated only by invasive imaging such as IVUS [Stone 2011]. The relative high-grade stenosis at the site of the missed culprit lesions in this study (71% ± 26%) (range 41-100%) might suggest that the current criteria to define unstable and complex plaques by presence of ulceration, thrombus, haziness and filling defect[Goldstein 2000] may benefit from revision because they are probably too stringent. Conversely, few of our NSTEMI patients had an occluded vessel which was identified as chronically occluded and therefore with no indication to treat. While this is common practice supported by previous evidence,[Hochman 2011] our results would suggest that an occluded coronary artery might actually be the cause of an acute event and that no assumption of long standing disease should be made without further investigation of the myocardium. The clinical trials to assess the optimal treatment in NSTEMI based on the outcome,[Hochman 2011] included patients 3 to 7 days after the event, while patients

with angina or inducible ischemia were excluded. However in these studies no imaging/ revascularization procedure was performed. In our study, the imaging time was performed acutely (24 hours post event). The use of an imaging technique like CMR to characterize the myocardium could help in stratifying the NSTEMI patients and guide and improve the invasive treatment.

Finally our findings did not reveal any new myocardial injury at 6 months in territories pertaining to moderate plaque stenosis (50% ± 9%). Although the prognosis in patients with multivessel disease is known to be impaired, it hasn't been shown whether or not this is due to an actual myocardial injury caused by non-culprit plaques. Although we cannot answer this question with certainty, our findings suggest an aggressive secondary medical prevention rather than an invasive approach could be considered in those patients with no evidence of LGE in myocardium downstream of non-culprit vessels, which are moderately stenotic.

5.6 Limitations

This study was not powered to investigate the effects of the CMR findings described on clinical outcomes. We excluded patients with previous myocardial ischemic events and also patients with indication for staged PCI or CABG as these further procedures may have confounded subsequent imaging findings. We therefore cannot comment on the relevance of the reported findings to those patient groups. Also our analyses of culprit versus non-culprit were based on angiographic analyses by experienced interventional cardiologists. Advanced coronary imaging techniques (IVUS or OCT) were not used to enhance angiographic assessment in this study. Furthermore, although we match coronary segments and myocardial segments on individual basis

accounting for anatomical variability, this method could still lead to some degree of error, as previously demonstrated by Setser et al.[Setser 2005]: hybrid technologies to match the coronary supply to the damaged myocardial injury should be considered for future studies. Finally, in the NSTEMI group, 35% of the patients were lost at follow up; further studies on much larger populations will be needed to support our initial findings in a small population and to support the clinical prognostic relevance of our findings but this goes beyond the scope of this chapter.

5.7 Conclusions

In patients undergoing PCI for NSTEMI, angiographic assessment alone fails to identify the culprit cause of myocardial injury in a significant proportion of patients. As a consequence, this small study showed inappropriate stenting of non-culprit lesions raising the possibility of potential clinical consequences due to the culprit vessel left unstented. Early T2-weighted CMR has the potential to improve accurate identification of the culprit and to guide optimal PCI in this patients group. Further prospective evaluation will be needed to confirm clinical efficiency.

Chapter 6: Cardiovascular magnetic resonance by non contrast T1 mapping allows assessment of severity of injury in acute myocardial infarction

6.1 Introduction

Cardiovascular magnetic resonance (CMR) with late gadolinium enhancement (LGE) is the current gold standard for assessing myocardial scar in chronic coronary artery disease (CAD), [Choi 2001, Lima 1995] while T2-weighted (T2W) CMR is the accepted method for detecting oedema in acute ischemic injury [Aletras 2006]. Myocardial oedema can be detected by T2W-CMR as early as 30 minutes after the onset of ischemia, and in the absence of LGE, is thought to represent reversible myocardial injury [Abdel-Aty 2009, Aletras 2006]. LGE and T2W-CMR are used as complementary techniques, to provide a comprehensive assessment of irreversible and reversible injury in acute myocardial infarction (MI) and to derive important prognostic indices such as salvageable area-at-risk and scar burden [Friedrich 2008]. The clinical significance of LGE as a precise measure of myocardial irreversible injury has recently been challenged. Firstly, in the early hours post ischemia, dynamic changes of LGE were shown within the ischemic myocardium, together with a significant regression of LGE over time and full functional recovery; these findings would suggest that acute LGE does not always represent scar [Dall'armellina 2011, Engblom 2009, Ibrahim 2009, Kramer 2000]. Secondly, it was shown that early gadolinium enhancement can detect salvageable myocardium [Matsumoto 2011], indicating that the kinetics of gadolinium may play an important role in assessing area at risk in relation to the imaging time. It is also well known that the area of injury detected by T2W-CMR encompasses both irreversibly injured myocardium and salvageable myocardium at-risk,[Aletras 2006] and that it may

evolve in the early days post acute MI with significant variation in the resulting calculated volume of salvaged myocardium [Dall'armellina 2011]. Furthermore, the concept that T2W positive imaging findings represent the area at risk has also been challenged recently [Friedrich 2011] due to the pitfalls of the technique (such as artefacts due to through plane motion or to stationary blood [Keegan 2006]), although newer T2prep bright blood sequence may overcome most of the limitations inherent to fast spin echo based techniques [Kellman 2007, Payne 2011]. Finally, there are important issues with the threshold-based methods widely used to post-process oedema and LGE images. Firstly, there is considerable scope for error depending on the threshold used. Secondly, it remains unclear whether or not an arbitrary signal intensity threshold realistically reflects the tissue changes occurring in the myocardium (big distortions can arise from changing thresholds) [Kwong 2011, Wince 2010].

Given these challenges and the heterogeneous composition of the acutely injured myocardium, a method that can objectively and directly quantify the extent and severity of acute ischemic injury would be highly desirable. Pre-contrast T1-mapping may be such a tool: compared to T2W and LGE, the main advantage of T1 mapping is that it provides measurements of absolute T1 relaxation times for each pixel, with high resolution. [Messroghli 2004, Piechnik 2010]. Although T1 mapping is not exempt from the need for thresholding when sizing myocardial injury, a threshold-based post-processing method requiring reference ROIs (whether in remote myocardium or skeletal muscle) is not required. This makes quantitative techniques such as T1-mapping less prone to subjectivity and error.

In experimental models of acute MI, elevations of absolute T1 values have been demonstrated in areas of increased water content exceeding the area of infarction by histological assessment [Higgins 1983, Williams 1980]. Other studies suggested that further increases in T1 values occur with prolonged ischemia due to larger concentrations of other water constituents [Williams 1980]. These studies indicate the potential of T1 mapping to detect areas of myocardial ischemia in humans.

Until recently, techniques for T1 mapping of the myocardium were limited by poor spatial and/or temporal resolution, which restricted their clinical applicability [Flacke 2001, Wacker 1999]. Messroghly et al., were the first to clinically validate a T1 mapping technique (MOLLI), with high spatial resolution which could be acquired in one single breathold [Messroghli 2006] demonstrated increased T1 values in areas of positive LGE following acute MI [Goldfarb 2007, Messroghli 2007].

However, previous T1 mapping techniques (such as MOLLI)[Messroghli 2004] were of limited use in clinical practice, particularly in acutely ill patients, due to long breath-holds and inability to work well with increased heart rates. We have recently developed and validated a new pre-contrast T1 mapping sequence (Shortened Modified Look-Looker Inversion recovery (ShMOLLI) [Piechnik 2010] , which is highly suitable for examining patients with acute MI, because it not only allows for significantly shorter breath-hold time, but also provides a more accurate estimate of long T1 values at higher heart rates [Piechnik 2010]. Furthermore the T1 values can be directly assessed during the CMR scan without the need for post-processing or exogenous contrast.

6.2 Aims

Using this powerful new technique, the aims of this study were to investigate whether in patients with acute myocardial infarction, pre-contrast T1-mapping [Piechnik 2010] (1) detects acute myocardial injury, (2) is able to quantify the severity of myocardial damage when compared to standard techniques such as LGE and T2W, and (3) has the ability to predict long term functional recovery.

6.3. Methods

Patient population

This prospective study was undertaken in a single tertiary centre. The local ethics committee approved the study protocol, and all patients gave written informed consent. Patients presenting with first occurrence of acute myocardial infarction (MI) between December 2009 and October 2010, were included (refer to methods chapter for inclusion and exclusion criteria) (Out of these only 3 patients were included in previous chapters as well.) Acute clinical management was at the discretion of the responsible physician, with the intention to reflect contemporary practice and guidelines (including use of aspiration catheters; glycoprotein IIb / IIIa receptor inhibitors and high-dose clopidogrel loading).

CMR

Patients underwent CMR 12 - 48 hours after the onset of chest pain and at 6 months. STEMI patients underwent primary PCI prior to CMR in the acute setting. CMR examinations were performed on a 3 Tesla MR scanner (TIM-Trio, Siemens Healthcare, Erlangen, Germany) using a spine and a phased array 6-channel flexible surface coils. Short axis cine images covering the length of the ventricle excluding the LV outflow tract

were acquired as previously reported. [Dall'armellina 2011] Slices matching the cine positions were acquired using T2W (T2prep SSFP, see Methods' chapter for details), T1 mapping and LGE imaging (see methods chapter for details) (Figure 6.1). ShMOLLI T1 maps were generated from 5-7 SSFP images with variable inversion preparation time as described previously[Piechnik 2010]. Typical acquisition parameters were: TE / TR = 1.07 / 2.14 msec, flip angle = 35º, FOV = 340 x 255 mm, matrix size =192 x 144, 107 phase encoding steps, actual experimental pixel size = 1.8 x1.8 mm, interpolated pixel size = 0.9 x 0.9 mm, GRAPPA = 2, 24 reference lines, cardiac delay time TD = 500 msec and 206 msec acquisition time for single image, phase partial Fourier 6/8. If necessary, shimming and centre frequency adjustments were performed before T2W-imaging and T1-mapping to generate images free from off-resonance artefacts.

All patients were in sinus rhythm during the CMR scan. The scan time needed to acquire a short axis stack with full coverage of the ventricle was about 2 min using ShMOLLI versus 4 min using T2W.

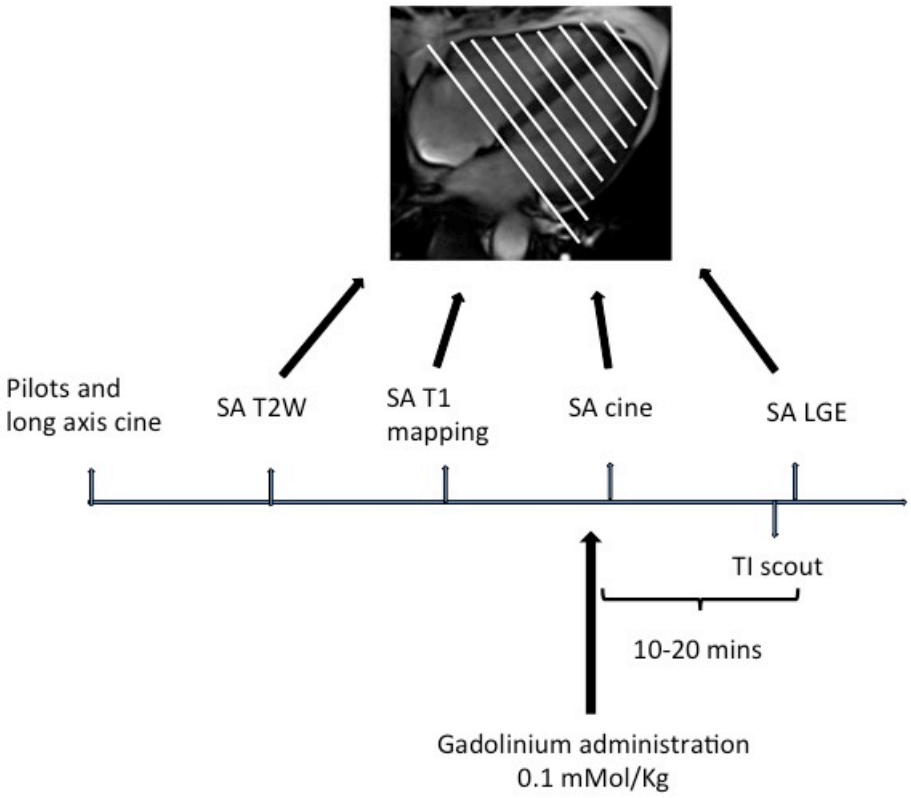


Figure 6.1. CMR protocol. Four different CMR techniques were included: T2W imaging for assessment of oedema, T1 mapping, functional cine imaging and late gadolinium enhancement for assessment of necrosis. Following the acquisition of pilot and long axis images, matching short axis slices covering the full length of the ventricle were acquired using each of the different techniques. T2W and T1 mapping acquisitions were performed prior to the administration of contrast. Following gadolinium, cine imaging was performed. Ten-fifteen minutes post contrast and after the inversion time was meticulously adjusted for optimal nulling of remote normal myocardium, late gadolinium enhancement imaging was completed.

Image analysis

Quantification of LV volumes and ejection fraction (EF) was performed as previously described using Argus software (Version 2002B, Siemens Medical Solutions) [Karamitsos 2007].

All matching short axis images covering the LV and acquired using each of the techniques (T2W, LGE and T1 maps) were manually contoured using an in-house software MC-ROI (IDL v.6.1, www.ittvis.com) to outline the endo- and epicardium. For the comparisons among acute T1 mapping, T2W and LGE, we excluded apical slices due to partial volume effects, slices including the LVOT and slices with off-resonance artefacts. Each slice was segmented in a 6 equiangular segment model with the RV-LV junction as reference point. For analysis purposes, the slices acquired with different techniques were all matched for slice position and radially aligned to the positions of the papillary muscles and the LV-RV junction.

The signal intensity threshold indicating oedema / LGE was set at 2 standard deviations above the mean intensity of reference ROI placed in remote unaffected myocardium as previously described [Berry]. Although different thresholds have previously been applied [Friedrich 2008], there is no standardization and agreement: we used 2 SD for both techniques to avoid introducing systematic errors by applying different thresholds for T2W versus LGE (i.e. 2SD versus 5SD) and overestimating the area of salvaged myocardium [Wince 2010]. Per segment, we derived the average T1 values and the signal intensity normalized to the signal intensity of the remote myocardium both for LGE and T2W. The coefficient of variation (CV = standard

deviation/mean) of T2W signal intensities and T1 values were assessed in remote unaffected myocardium to detect the variability of measurements.

The injured fractions by LGE and oedema both segmental (volume of injured myocardium within a segment/ volume of the segment) and global (volume of injured myocardium within the LV/ LV mass) were assessed. Salvaged myocardial index was derived from the volume of acute oedema and the final infarct size (LV volume of LGE at 6 m). Microvascular obstruction (MO) / haemorrhage was identified as the low intensity core if present on all analysed CMR sequences and both were included in the measurements of LV myocardial damaged volume by LGE, T2W and T1 mapping. Segments with MO were also analysed separately and delineated manually if simultaneously present on corresponding LGE, T1 mapping and T2W slices.

Wall motion abnormalities and LGE were assessed semi quantitatively by an experienced observer (E.D.) as described below. For regional function, segments were scored: 1 = normal; 2 = hypokinetic; 3 = akinetic or 4 = dyskinetic. The wall motion score index (WMSI = sum of segmental scores divided by the number of segments scored) was calculated as previously described. [Dall'armellina 2008] The extent of LGE within each segment was estimated visually and categorized according to the percentage hyperenhanced area of each segment (damaged area/segmental area): [Kim 2000] 0 = no LGE; 1 = 1 - 25% LGE; 2 = 26 - 50% LGE; 3 = 51 - 75% LGE and 4 = > 75%.

Statistical Analyses

The normal distribution was confirmed using the Kernell density plot. Mean (SD) values and median (interquartile range) were calculated for continuous variables. Unpaired student t-test was used for comparison of continuous variables collected at

single time point (EF, WMSI, Troponin I). A random-effects linear regression model was used to describe the association between LGE, T2W (volumes of damaged measured as percentage) and T1 values (average relaxation time measured in msec), controlling for clustering of segments within each subject. The overall fit of the model was investigated using χ^2 ratio test. Receiver operating characteristic (ROC) analysis was performed to identify cutoff values of T1 relaxation times and T2 SI ratio for detecting focal acute changes; this was achieved by using focal LGE scoring (LGE score $\geq$ 1) as the "true positive" surrogate marker for acute myocardial injury in this clinical setting, compared to segments with no LGE (LGE score = 0) in controls as the "true negative". Statistical significance of the differences between ROC curves was assessed using the method of DeLong et al.[Delong 1988]. To analyse the presence of significant difference in T1 values in manually drawn ROIs in region of microvascular obstruction, ANOVA analyses were performed with Bonferroni post-hoc comparisons. A logistic regression model was used to predict the improvement of function at 6 months using as variables acute T1values and acute segmental damage fraction by LGE in matching patients with the same degree of damage based on LGE scoring. All statistical tests were two-tailed, and P-values of less than 0.05 were considered statistically significant.

6.4 Results

Patient characteristics are presented in Table 6.1. Of the 43 patients enrolled, one patient could not complete the CMR protocol due to claustrophobia and one scan had to be excluded due to artefacts rendering the images non-analysable. Thus, a total of 41 patients (mean ± SD age, 56 ± 8 years, 78% with an ST elevation MI [STEMI]) were scanned within 24 hours post symptoms onset; out of these, 7 patients did not undergo the

6 m follow up scan (4 were excluded following CABG or staged PCI, and 3 refused to come back).

CMR findings

A total of 129 slices acquired acutely were suitable for analysis (on average 3.1 ± 0.9 slices per patient with a range of 1 to 5). Out of the resulting 774 segments, a total of 100 segments (13%) were excluded from analysis due to: (i) SSFP off resonance artefacts on T1 mapping or T2W images (70 segments) and (ii) presence of outflow tract (30 segments) on LGE or cine images.

The CMR findings are summarised in Table 6.2. All patients showed positive oedema and LGE. In acute setting, all patients had at least one LV dysfunctional segment; the global ejection fraction was at the lower end of normal (51% ± 11%). The relative mean volume of LGE in acute decreased significantly by 6 months ($P < 0.01$) with a corresponding significant improvement in regional wall motion ($P < 0.01$).

Table 6.1. Baseline characteristics of the study population

Patient characteristics	All N = 41	STEMI N=32 (78%)	NSTEMI N=9 (22%)	P-value
Age	**56 ± 8**	56 ± 8	55 ± 8	**0.8**
Sex	**3:38 (F: M)**	2:30 (F : M)	1:8 (F: M)	
Risk Factors [No (%)]				
Smoking	**14 (35)**	13 (40)	1 (11)	**0.13**
Hypertension	**15 (37)**	9 (28)	7 (78)	**0.17**
Diabetes	**4 (10)**	1 (3)	3 (34)	**0.03**
Family history	**15 (37)**	12(37)	3 (34)	**1.0**
Hyperlipidaemia	**16 (40)**	10 (31)	5 (56)	**0.25**
Previous angina	**4**	2	2	**0.2**
Presenting characteristics				
Troponin I (12 hours post admission) (mg / mL)	**32 ± 20**	38 ± 15	9 ± 7	**<0.01**
Median (IQR) Time from onset of symptoms to procedure (hrs)	**3 (2.2, 9)**	2.6 (2.0, 4.2)	24 (13, 36)	**0.0001**
Culprit coronary artery [No (%)]				
LAD	**21 (52)**	17(53)	4 (44)	**1.0**
LCx	**4 (10)**	2 (6)	2 (22)	**0.3**
RCA	**17 (42)**	14 (40)	3 (33)	**0.15**
N of vessel diseased, n (%)				
0	**1**	0	1	**0.22**
1	**25 (61)**	24 (75)	1 (11)	**0.001**
2	**7 (17)**	5 (16)	3 (33)	**0.3**
3	**7 (17)**	3 (9)	4 (45)	**0.03**
Drug therapy n (%)				
Aspirin	**41 (100)**	32 (100)	9 (100)	**1**
Glycoprotein IIb / IIIa inhibitor	**33 (80)**	32 (100)	1 (11)	**<0.001**
Clopidogrel	**41(100)**	32 (100)	9 (100)	**1**
β-Blockers	**41 (100)**	32 (100)	9 (100)	**1**
Heparin	**41 (100)**	32 (100)	9 (100)	**1**

Table 6.2. CMR findings

Variable	ALL (N=41)	STEMI (N =32)	NSTEMI (N=9)	P-value (NSTEMI vs STEMI)
EF	48 ± 9	46 ± 8	58 ± 10	<0.001
EDV	153 ± 36	157 ± 36	142 ± 39	0.2
ESV	81 ± 30	86 ± 30	65 ± 29	<0.01
SV	73 ± 15	72 ± 15	79 ± 17	<0.05
WMSI	1.6 ± 0.3	1.6 ± 0.3	1.4 ± 0.2	0.02
Oedema (T2W), LV% (Acute)	47 ±14%	51 ± 12%	34 ± 10 %	0.00015
LGE, LV % (acute)	38 ± 16%	41±14 %	25 ± 12 %	0.0006
MO positive	7 (17%)	6 (18%)	1 (11%)	1
	N=34	**N=28**	**N=6**	
EF (6m)	58 ± 11	56 ±11	66 ± 3	0.1
WMSI (6m)	1.3 ± 0.2	1.3 ± 0.35	1.2 ± 0.2	0.2
LGE, LV% (6m)	28 ± 14%	30 ± 14 %	21 ± 14 %	0.1
Myocardial salvaged index (T2W)*	37 ± 27 %	41 ± 23 %	17 ± 37 %	0.3

* myocardial salvage index was calculated using the final infarct size at 6m

T1 values in areas of acute myocardial injury by LGE and T2W

Representative examples of T2W, LGE and T1 mapping from a STEMI and a NSTEMI patient are shown in Figure 6.2, Panel A and B respectively. Increased T1 values are shown in areas of myocardium co-localized with areas of LGE and increased signal intensities on T2W-CMR; in the NSTEMI patient, T1values are increased in an area larger than the one enhanced by LGE.

In order to investigate the accuracy of T1 measurements in comparison to T2W, we first assessed the variability of the T1-values in remote unaffected myocardial segments with no ischemic injury (as confirmed by LGE, T2W or wall motion) and compared it to the signal intensities in T2W imaging of corresponding segments. The average T1 value (± SD) in unaffected myocardium was the same for STEMI and NSTEMI (1189 ± 60 msec and 1176 ± 38 msec respectively, P=0.16), with values similar to volunteers at 3T [Piechnik 2010] (1200 ± 59 msec) with a coefficient of variation (CV) significantly lower compared to T2W (6% versus 14% respectively, $P < 0.0001$).

In order to assess the relationship between areas of injury depicted by T2W or LGE and areas of increased T1 values on T1-mapping, we then investigated the correlation between absolute T1 values and the signal intensity of LGE and / or T2W on a segmental basis. As shown in Figure 1 Panels C and D, increased signal intensity on LGE images correlated with increased absolute T1 values ($r = 0.71$, $P < 0.001$) and with T2W signal intensities ($r = 0.70$, $P < 0.001$) in matching segments, indicating co-localization of injured myocardium. Similarly, a strong correlation was shown between T1 values and T2W signal intensities, with T1 values ranging between 1078 msec and 1624 msec (1257 ± 97 msec – mean ± SD) in the acutely ischemic segments. The T1 measurements in

acutely ischemic segments were significantly different compared to T1 values in normal unaffected segments (1257 ± 97 msec vs 1200 ± 59 msec, $P<0.01$).

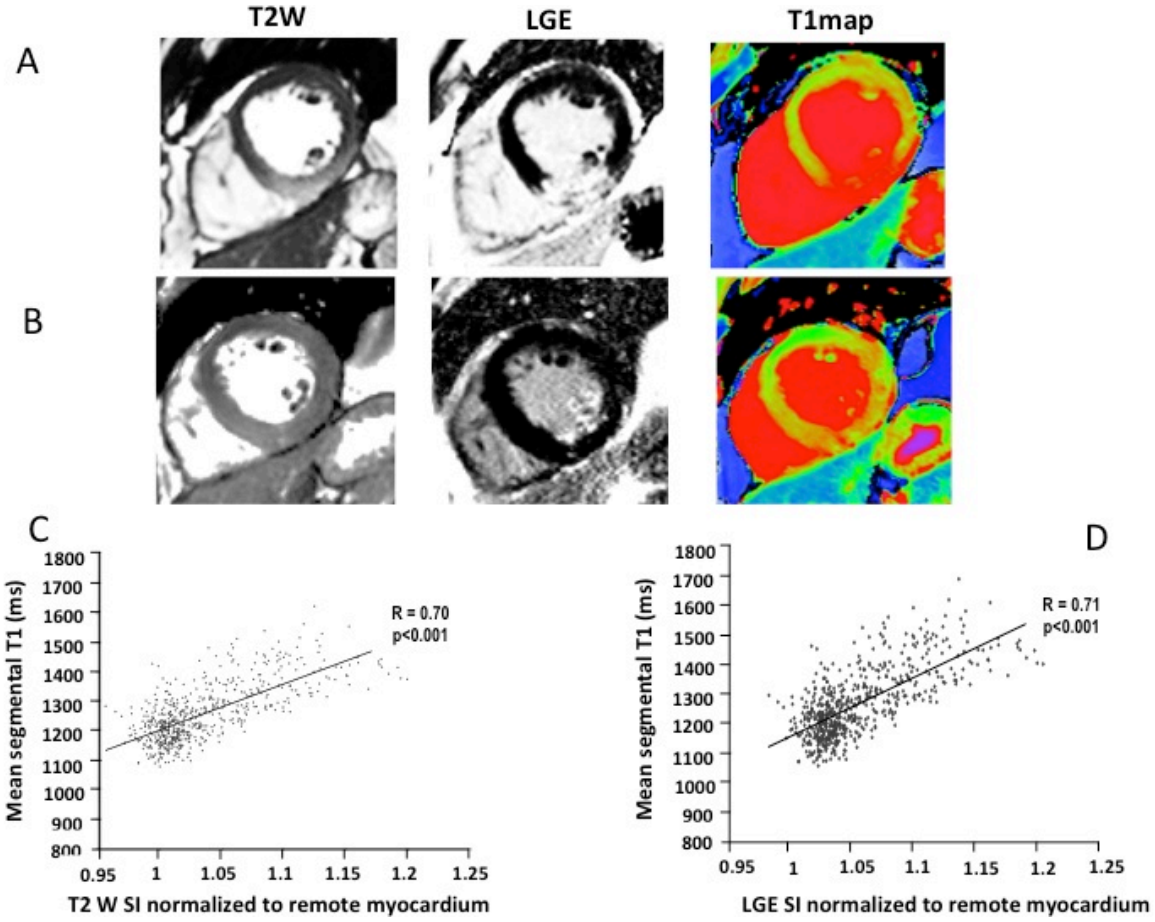


Figure 6.2 Panels A and B. Representative CMR images. Oedema images (left column), acute LGE images (center), and ShMOLLI T1-mapping (right column) are displayed. Two sets of images (Panels A and Panels B) corresponding to two separate patients are shown. *Top panels (A): a case of transmural inferior STEMI:* both oedema (T2W) and LGE depict an area of increased signal intensity; in the same region T1 mapping depicts significantly increased T1 values (shown in red) compared to the remote unaffected myocardium (normal T1 values shown in green). *Lower panels (B), a case of subendocardial NSTEMI* : Although the T2 W images show only a mild increase in brightness, there is an area of increased T1 values exceeding the area of LGE enhancement. Of note the peak troponin I was significantly different in the two patients (peak troponin I 50 mg / mL in the STEMI patient vs. 7 mg / mL in the NSTEMI patient). **Panels C and D**: **Correlation between T1 values and T2W normalized SI (Panel C) and between T1 values and LGE normalized SI (Panel D).** The SI of LGE (on the X axis, panel C) and T2W (on X axis Panel D), both normalized to the remote unaffected myocardium, are shown to correlate strongly with T1 values.

Diagnostic performance of T1 mapping in detecting acute injury in acute myocardial infarction

Figure 6.3 illustrates the diagnostic performance of T1-mapping compared to the T2W technique in detecting acute myocardial injury against acute LGE manual scoring as the gold standard based on ROC analysis. In STEMI patients, both techniques performed equally (T1 mapping area under the curve 0.90 ± 0.01 vs. T2W area under the curve 0.89 ± 0.01, P = 0.34) (Figure 6.3, Panel A). In order to investigate whether the diagnostic performance of T1 mapping could be better in patients with smaller infarcts, we performed ROC analyses in the subgroup of NSTEMI patients. In these patients T1 mapping showed improved detection of myocardial injury compared to T2W (T1 mapping area under the curve 0.91 ± 0.02 vs. T2W area under the curve 0.81 ± 0.04, P = 0.004).

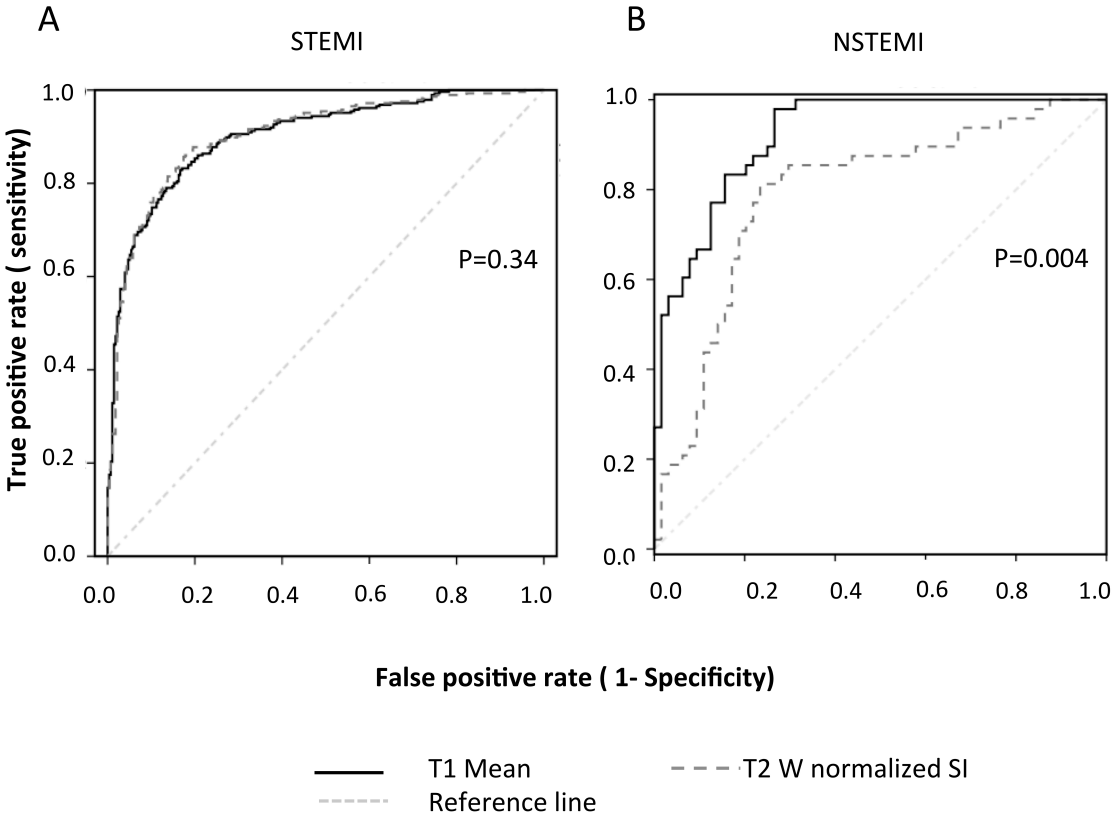


Figure 6.3. Receiver Operating Curves showing the diagnostic performance of T1-mapping compared toT2W in detecting acute injury in MI as derived from late gadolinium enhancement (LGE) scoring. In STEMI patients with acute myocardial infarction, the area under the curve for T2W (dashed line) was not significantly different from T1 mapping (solid line) indicating an equally good diagnostic performance of the two techniques (Panel A). In NSTEMI patients, the area under the curve for T2W (dashed line) was significantly smaller than that for T1 mapping (P = 0.004) indicating a significantly better diagnostic performance of T1 mapping.

Relation between absolute T1 values and the extent of myocardial injury

In order to explore the potential of quantitative T1-mapping to assess the extent of acute ischemic injury on a segmental basis against the current gold standards of LGE and oedema imaging, we investigated the relationship between average segmental T1 values and the volumetric lesion fraction (by LGE and T2W) (Figure 6.4 Panel A and B). For this analysis, segments with MO were excluded (see below paragraph on T1s in MO). A significant relationship between the segmental extent of myocardial injury as defined by LGE and T1 values was found ($P < 0.001$). Increasing T1 values clearly distinguished 20% increments in segmental LGE fractions. A significant relationship was also found between segmental fractions of oedema assessed by T2W and T1 values ($P < 0.001$); however, there was an overlap in T1 values in segments with intermediate extent of oedema (41% to 80% segmental fraction).

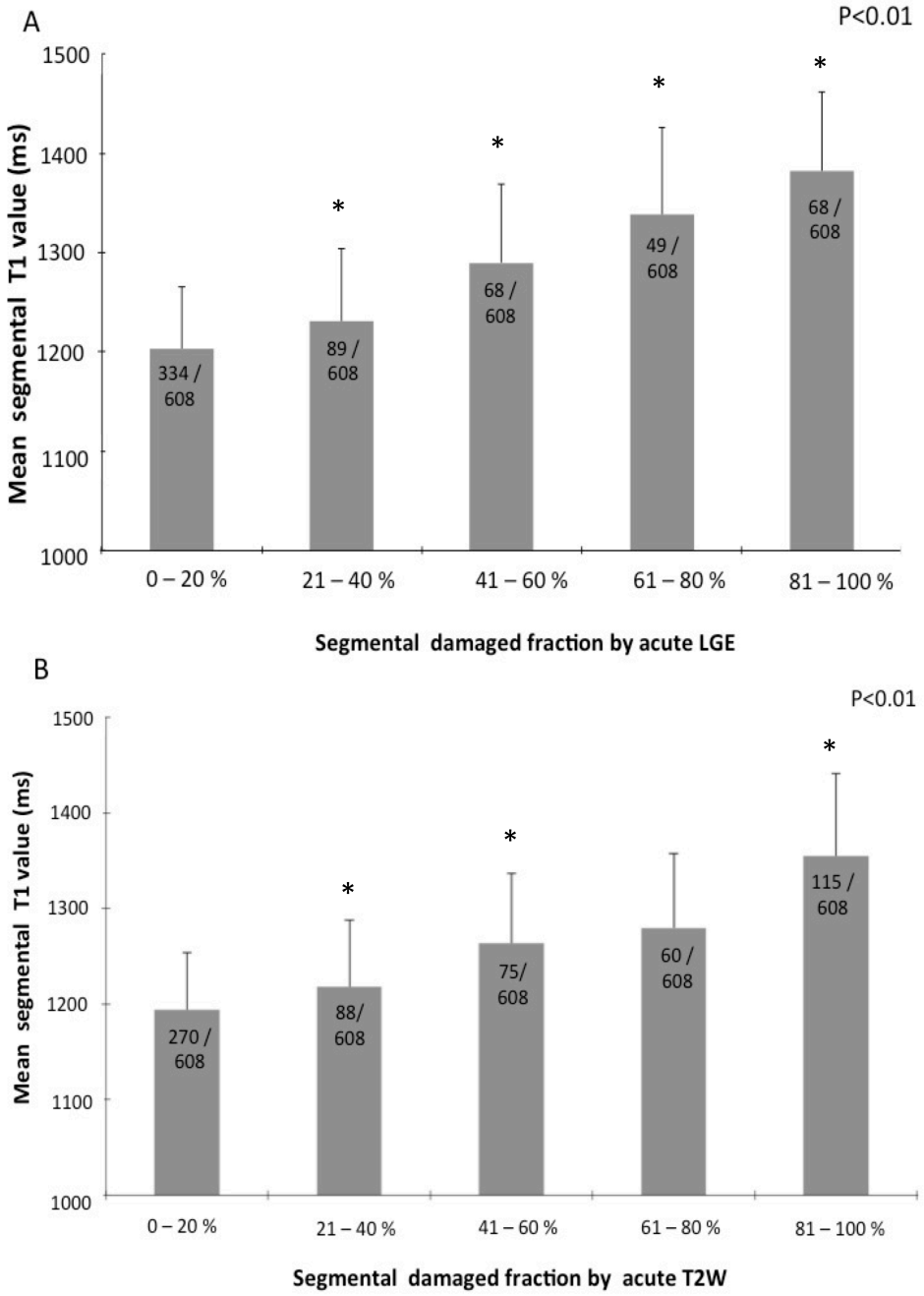


Figure 6.4. Assessment of severity of injury by T1-mapping: relationship withT2W and LGE. Increasing T1 values distinguish increasingly larger segmental extent of injury, assessed by either LGE or T2W with T1 depicting 20% increments in LGE/T2W lesion extent. [Each * asterisk indicate the significant difference (P<0.01) in T1 values in each LGE/T2W category from the precedent one]. Although the overall relationship between T1 and T2 W is still significant (P<0.01 for the trend), there is an overlap in T1 values for segments with T2W segmental damaged fraction between 41 and 80%. Lesions with MO have been excluded from this analysis.

To investigate whether quantitative characterization of myocardial tissue in MI reflects not only myocardial damage by LGE but also functional contractile impairment, we assessed the correlation between T1 values and both regional and global systolic function (Figure 6.5, Panel A and B).

The association between the degree of regional functional impairment (either normal, hypokinetic or akinetic) and increasingly higher T1 values was significant ($P<0.01$ for the trend): while T1 values were within normal range in normally functioning segments (1196 ± 85 msec) they increased significantly in hypokinetic segments (1299 ± 90 msec), reaching maximal values (1368 ± 83 msec) in akinetic segments. Furthermore, we found a highly significant correlation between global myocardial T1 values and LV ejection fraction.

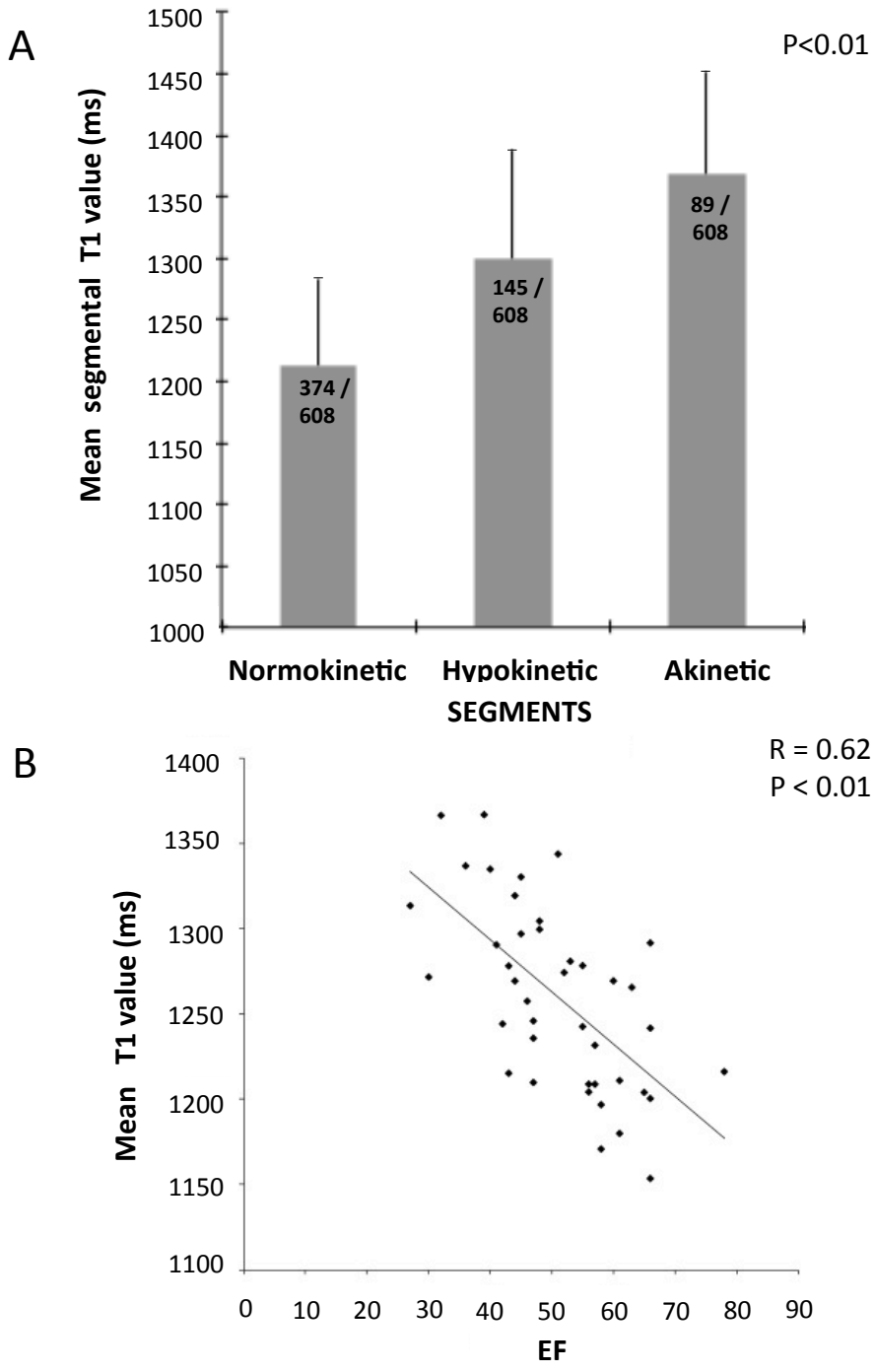


Figure 6.5. Assessment of severity of injury by T1-mapping: relationship with regional and global function. Panel A shows the relationship between T1 values and the extent of regional wall motion abnormalities (P < 0.01 for the trendcorre). A highly significant negative correlation between mean LV T1 values and LV ejection fraction was also found (Panel B).

Salvaged myocardium assessment by T1 mapping

In order to match, on a like-for-like basis, the relative LV mass of acutely damaged myocardium by T1 mapping with the one assessed by T2W and to derive comparable values of salvaged myocardium, we used a threshold of 10% (close to 2 standard deviations) above the previously established T1 values in normal controls [Piechnik 2010]. By empirically choosing 10% above the mean normal T1, the relative LV mass of acutely damaged myocardium was 43 ± 19 % by T1 mapping versus 47 ± 14 % by T2W, P = 0.2. The derived salvaged index using the final infarct size by LGE at 6 months was: 37 ± 24% by T1 mapping versus 37 ± 27% by T2W (P = 0.88).

Characterization of microvascular obstruction by T1 mapping

Overall, 7 patients showed evidence of MO on LGE imaging (6 with STEMI and 1 NSTEMI). A typical case is shown in Figure 6.6. On average, T1 values in the core of MO were significantly higher than in the remote myocardium (1267 ± 52 msec vs 1194 ± 47 msec, P = 0.002), but significantly lower than in the surrounding injured myocardium within the LGE positive myocardium (1403 ± 80 msec, P < 0.01 versus remote myocardium and MO) (Figure 6.6, Panel C).

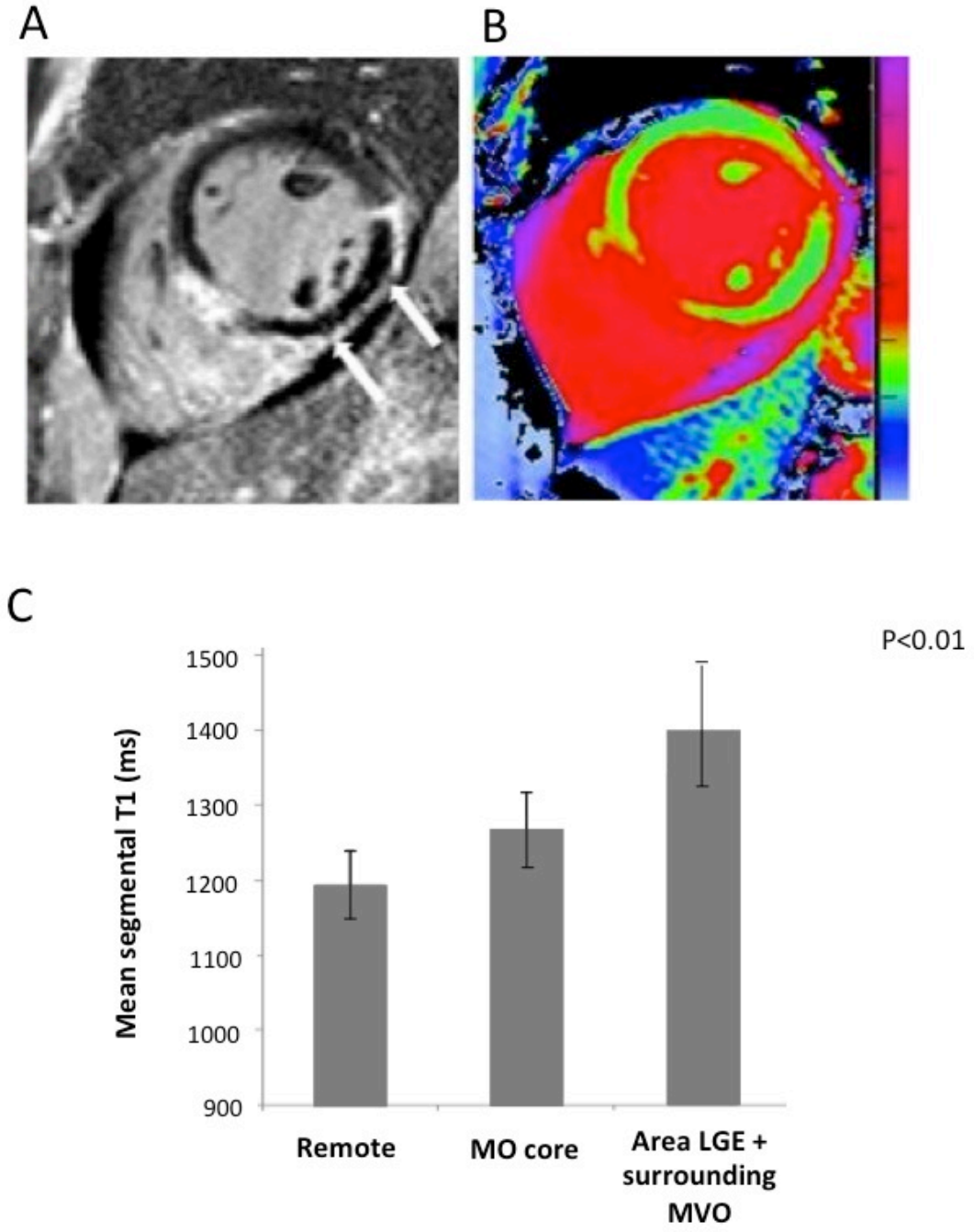


Figure 6.6. Quantitative assessment of microvascular obstruction by T1-mapping. Panel A shows a case of microvascular obstruction as depicted by LGE. The corresponding T1-map is shown in Panel B. The dark core of MO in the LGE image (arrows) is depicted by T1 values (Panel B) in the color range similar to remote myocardium (green). The surrounding injured myocardium (bright on LGE) shows high T1 values (red). Panel C shows quantitative analyses of the 7 cases with MO. T1 values in the MO regions are significantly lower than in the surrounding LGE-positive myocardium.

Likelihood of functional recovery at 6 months by acute T1 mapping

T1 values correlate with the extent of segmental LGE in the acute setting. In order to assess whether acute T1 values predict functional recovery at 6 months, we assessed the ability of acute T1 values and of the acute LGE segmental fraction to predict the likelihood of long-term segmental wall motion improvement in 198 acutely dysfunctioning segments (excluding MO). As shown in Figure 6.7, Panel A, there was a significant association between acute T1 values and the improvement of function at 6 months ($P < 0.0004$ for the trend): virtually all dysfunctional segments with only slightly increased T1s in acute setting recovered function at 6 months, while for values higher than 1422 msec (top 2 quintiles), the percentage of segments which improved wall motion at 6 months decreased to 60%. The relationship between acute LGE and improvement of function was also significant overall ($P < 0.004$). However, while the relationship between functional recovery and T1 was essentially linear, by using acute LGE (Figure 6.7, Panel B), the likelihood of improvement for those segments with intermediate LGE (between 25% and 75%), did not correlate with the amount of damage.

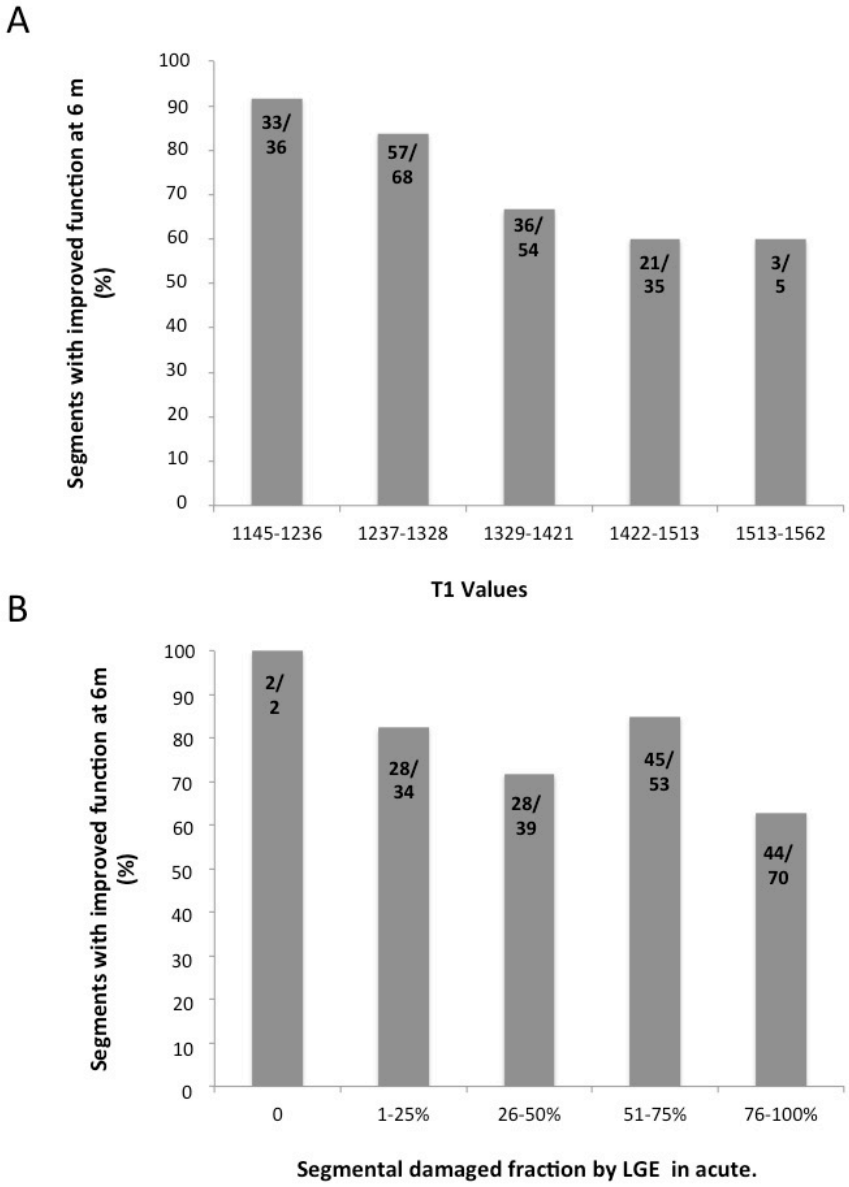


Figure 6.7. Likelihood of functional improvement at 6 m by T1 mapping and acute LGE in dysfunctional segments. Data are shown for 198 segments, which were dysfunctional acutely. Panel A shows the significant association between the likelihood of recovery of function of acutely dysfunctional segments and the T1 values in acute ($P < 0.0004$ fro the trend). Panel B shows the association between the likelihood of recovery of function of acutely dysfunctional segments and the segmental damaged fraction by LGE in acute ($P < 0.004$ for the trend). While the relationship between functional recovery and T1 was essentially linear, by using acute LGE (Panel B) the likelihood of improvement for segments with intermediate LGE did not correlate with the amount of damage. No MO segments were included in this analysis.

6.5 Discussion

The main findings of our study are: 1) quantitative T1 mapping is a more robust technique compared to T2W as T1 measurements show a significantly lower variability than T2W, their acquisition is faster with a better spatial resolution (reconstructed pixel size of 0.9 x 0.9 mm/experimental pixel size 1.8 x 1.8 mm versus 2.1 x 1.6 mm) 2) non contrast T1 mapping accurately detect acutely injured myocardium in MI patients when compared to T2W and LGE as markers of acute injury; 3) the diagnostic performance of T1-mapping is at least as good as that of T2W CMR for detecting acute myocardial injury, 4) non-contrast T1-mapping allows assessment of the extent of acute myocardial damage on a segmental level 5) myocardial salvage index can be calculated based on T1 mapping with similar results compared to T2W 6) T1 values are strongly related to the likelihood of functional improvement at 6 months.

We believe that the results of this study are of direct clinical relevance. For the first time we report on the potential use of quantitative pre-contrast T1-mapping techniques to further improve our ability to characterize the presence and extent of acute myocardial injury and to determine reversible myocardial injury and salvaged myocardium by CMR. The current CMR imaging techniques used to assess acute ischemic injury, T2W and LGE imaging, have important limitations in relation to: a) their clinical applicability in acute ill patients not always capable to hold their breath; b) the accurate assessment of the injury due to inherent issues such as variability of the measurements because of image gradients, partial volume effects and threshold dependent postprocessing. In comparison to the initial T1 mapping techniques limited in resolution, the novel shortened T1 mapping allows for faster acquisition compared to

standard T2W and LGE techniques, and it is a more robust technique with less variability in T1 measurements at improved spatial resolution. Furthermore, both LGE and T2W are semi-quantitative methods which rely on the use of an arbitrary threshold, usually set at 2 SD above remote 'normal' myocardium, to delineate areas of myocardial oedema and / or scarring [Wince 2010]. However, the use of a reference ROI in the remote myocardium may lead to false negative findings when systemic processes globally affect the heart. Secondly, it is unclear whether this arbitrary threshold of 2 SD (rather than 3 SD or 5SD) accurately reflects myocardial tissue changes occurring early after myocardial infarction [Wince 2010]. Thirdly, post processing is time-consuming and not always suitable to applications in acute setting. Being T1 mapping a quantitative technique, the value of "normal myocardium" can be established and used as reference without having to identify a reference ROI. This makes this technique less prone to errors even if thresholds to assess the amount of injury will still be needed. As every intensity based imaging technique, the need for an arbitrary choice of threshold is inevitable; in fact using T1 mapping across different field strengths and systems from different vendors, establishing an absolute value for normal tissue versus abnormal is impossible and using a threshold, actually makes it robust to different field strengths (as discussed in the limitations paragraph).

We recently showed that, due to the dynamic pathophysiological tissue changes occurring very early after an acute ischemic event, there is a significant variability in acute CMR imaging findings, and consequently in derived clinical prognostic indices such as salvageable myocardium [Dall'armellina 2011]. These issues often make the interpretation of CMR findings in acute MI difficult. A novel CMR technique, which

would allow for a more detailed and quantitative characterization of acutely injured myocardium, would thus be highly desirable. Our findings suggest that quantitative T1-mapping techniques are a suitable tool for this A recently validated improved technique (ShMOLLI)[Piechnik 2010] allows for fast acquisition of high resolution pre-contrast T1-maps even at patients with high heart rates and therefore it is well suited for imaging ACS patients [Piechnik 2010].

This is the first study in patients with ACS that has used T1-mapping at 3 Tesla to assess the presence and the extent of acute ischemic injury compared to accepted gold standard measurements of salvageable myocardium such as T2W and LGE-CMR. To the best of our knowledge, no other T1 mapping studies have been conducted at 3T; however previous work conducted at 1.5T CMR by Messroghli et al.[Messroghli 2007] demonstrated that pre-contrast T1 mapping can detect acute myocardial infarction with high sensitivity and specificity (96% and 91%, respectively), against LGE as the gold standard. Goldfarb et al.[Goldfarb 2007] also showed increased T1 values in LGE positive myocardial infarcts up to 1 month after the acute event. However, in both these studies, oedema imaging by T2W CMR was not performed [Goldfarb 2007, Messroghli 2007]. As shown in previous animal studies, the mechanism underlying the increase in T1 values in acutely ischemic myocardium is likely related to the increase in tissue water content, which has been shown to exceed the area of infarction by histological assessment [Williams 1980] [Brown 1984]. We confirm these experimental findings in the clinical setting, as we demonstrated higher T1 values in areas of oedematous myocardium within 24 hours after an acute ischemic event. Our results also indicate that quantitative T1-mapping measurements correlate well with T2W measurements, but show significantly

lower variability than T2W-CMR. Therefore, T1-mapping may be superior to T2W-CMR for assessment of acute myocardial injury in MI. Although only in a small number of patients, this is further supported by the better diagnostic performance of T1-mapping compared to T2W-CMR in detecting small areas of acute myocardial injury in patients with NSTEMI. Recently published data from our department, also demonstrate the highest accuracy of T1 mapping in identifying myocardial oedema in patients with positive oedema and no LGE.[Ferreira 2012] Further investigations will be needed to understand whether the superior sensitivity of T1 mapping in detecting oedema also hold true for small amount of injury.

Our results also indicate that T1-mapping allows for the assessment of the extent of *segmental* injury in the acute setting [Higgins 1983]. This is further supported by the relationship between T1 values and contractile function. The impairment of contractile function in regions with high T1 values is due to severe myocardial damage. The assessment of irreversible injury in the early days following an acute ischemic event is challenging due to several issues. Recently published data [Dall'armellina 2011, Engblom 2009, Ibrahim 2010, Kramer 2000], showed a rapid reduction in LGE volumes occurring in the days following the acute event and have therefore challenged the view that acute LGE equals to stable irreversible injury but may rather reflect a dynamic process resulting from the healing mechanism of the acute injury. Therefore, acute LGE (within 7 days of acute MI) might not be a reliable predictor of functional recovery in this setting. Furthermore, Matsumoto et al[Matsumoto 2011] recently validated early gadolinium enhancement imaging to assess area at risk, indicating that the imaging time to assess irreversible injury acutely is critical and poorly defined. Others have suggested that, to

obtain an accurate assessment of the irreversible injury, late gadolinium should be acquired 20 minutes post injection with consequent prolongation of the acquisition protocol and limited applicability in unstable acutely infarcted patients [Andrew E 2011]. Based on our findings, high T1 values in acutely ischemic myocardium reflect both, areas positive for T2W and for LGE. Previous reports in experimental models have shown that, following prolonged ischemia, T1 values may increase above and beyond the corresponding increase in water content; this may be related to a more severe degree of cellular injury with consequent release of intracellular ions into the extracellular space [Williams 1980]. In keeping with these experimental findings, our results indicate that the likelihood of improvement in function at 6 months *decreases* with incremental increases of T1 values. Based on these results, T1 mapping may be considered a better predictor of recovery of function compared to acute LGE although, the predictive value of T1 mapping does not reach the predictive value of chronic LGE [Kim 2000]. Clearly, acute T1 mapping reflects the sum of reversible and irreversible injury while chronic LGE represents irreversible injury only, therefore a better relationship with 6 months functional improvement is expected for the latter [Kim 2000, Selvanayagam 2004]. However, information on chronic LGE findings is not available when assessing patients acutely. Further studies will be needed to assess the potential of T1 mapping to depict the changes occurring in the myocardium in the early days post MI and their predictive value.

Finally, we demonstrated that T1 values are significantly lower in areas of MO compared to T1 values in infarcted areas without MO. This is likely to a combination of blood degradation products (haemorrhage) and reduced water content, which both result in lower T1 values compared to infarcts without MO. The prognostic value of

MO/haemorrhage as a predictor of adverse LV remodelling [Mather 2011, Wu 1998] is well recognized. Further work is needed to better characterize areas of MO with non-contrast T1-mapping and to determine whether additional prognostic information can be derived by ShMOLLI T1-mapping in this setting.

6.6 Limitations

Even though T1 mapping is an inherently quantitative method providing pixel-wise absolute T1 values, the lack of invasive tissue sampling only permits comparisons between arbitrary chosen thresholds. We chose 1271 msec as the closest value to replicate the common 2SD threshold used in T2W oedema imaging. The use of an arbitrary choice is unavoidable in signal intensity based imaging methods and it makes the method robust to different fields and acquisition sequences [Piechnik 2010]. However, a 10% threshold might still change, and further investigation (possibly with histologic comparison) will be needed to fully address this issue.

Also, at 3T we encountered frequent SSFP off-resonance artefacts despite shim correction, and 10% of ShMOLLI segments had to be excluded from analysis. This limitation is strictly related to high-field imaging: in fact the incidence of these artefacts is expected to be lower at 1.5T allowing for application in clinical routine practice. Secondly, T2 mapping is a promising new CMR technique for assessing acute myocardial injury, [Giri 2009] which was not included in this study. We did, however, compare our T1 mapping approach with a novel, state-of-the-art T2prep-SSFP sequence shown to be superior to traditional T2W STIR imaging and widely considered a gold standard for oedema imaging in the acute setting. Thirdly, the 6 months follow up was not performed in 17% of our acute population. Although a complete follow up would have been

desirable, the final sample size used to assess the relationship between T1 values in acute and long term functional improvement was adequate based on 80% power calculation with an accuracy of 0.05. Finally, we do not provide histopathological confirmation of our findings and the precise mechanisms leading to increase T1 values in acute myocardial injury warrant further investigation.

6.7 Conclusions

Increased pre-contrast T1 values depict areas of acutely injured myocardium with a diagnostic accuracy at least as good if not superior to T2W. In patients with acute MI, incremental increases in T1 values delineate the severity of the extent myocardial injury and predict functional recovery at 6 months. Although further investigations will be needed, our results suggest that pre-contrast T1 mapping may represent a valuable alternative to standard oedema and scar imaging methods with particular usefulness in the assessment of reversible myocardial injury and salvaged myocardium with no need for post-processing.

Chapter 7: General conclusions and outlook

Patients with acute coronary syndrome are investigated as early as possible in order to improve medical management and address treatment. CMR is emerging as a non-invasive tool, which may play a role in early diagnosis by allowing for characterization of acutely injured myocardium. Recent developments have provided clinician with sequences to accurately detect reversible injury in ACS. New CMR T2W techniques (bright blood T2-prep SPSS) have been shown to be superior compared to the standard conventional ones (black blood T2W TSE or STIR) at 1.5T because less prone to artefacts due to motion and signal intensity gradients. These new techniques have also the important advantage to be free breathing and therefore more suitable for acute sick patients.

We started by implementing a short 3T CMR protocol for applications in acute patients including novel CMR bright blood technique (T2-prep SPSS) to assess myocardial oedema following ischemic injury. In the first chapter of results we validated this new technique at 3T and we demonstrated that, although the images are normalised by a proton density map, a signal intensity gradient across the myocardium still exists. We identified the range of signal intensities within the variation due to the gradient and we established a signal intensity threshold to analyse the images. This will be of particular use for reference in both clinical and research studies.

We then moved on to application of this technique at 3T in the clinical setting. In order to assess the efficacy of treatments to improve outcomes by increasing salvaged myocardium assessed by CMR, we felt the need for standardising the imaging time. We acquired a detailed database including CMR imaging at different time points from the

ACS patient admission up to 6 months later. We found relevant dynamic changes happening in the underlying myocardial tissue in the early hours post myocardial infarction as part of the healing process. We established that the optimal imaging time for oedema is anytime up to 5-7 days from the event. We also found that the assessment of scar at 24 hours post MI might be hampered by the coexistence of oedema and it may not reflect the actual final scar. This is keeping with previously published data [Engblom 2009, Ibrahim 2009, Kramer 2000]. Our findings have important clinical relevance as they set the timing for optimal oedema imaging for future clinical trials. Following publication of our results, other studies have shown that the peri-infarct zone can be detected on early contrast enhanced CMR within 2 minutes from injection of gadolinium; these findings indicated that early gadolinium can depict ischemic but salvaged myocardium [Matsumoto 2011]. Therefore the kinetics of gadolinium may play an important role in the assessment of scar versus reversible injury in acute ischemia. There is a general consensus in the scientific community on the need for a detail investigation of the correct imaging timing to avoid hybrid data and being able to recognise the two different pathophysiological processes.

By using the acute CMR protocol including the T2W method established in this thesis, we then moved on to assess the pathological and functional significance of bystander disease in acute coronary syndrome and compared these to 6 months follow up findings. We used T2W oedema and LGE imaging acutely to identify myocardial injury downstream non-culprit plaques. We found that in patients with multivessel disease undergoing PCI, the angiographic assessment alone may fail in identifying the real culprit

vessel; the medical approach and invasive treatment to multivessel NSTEMI patients may benefit of invasive tools to assess the plaques and of CMR to stratify patients and identify myocardial injury. By scanning again the patients at 6 months, we also showed no new LGE downstream of non-culprit plaques suggesting that in NSTEMI with negative acute CMR in territories associated with remote plaques, an aggressive secondary prevention might be needed rather than an invasive approach including stenting.

Finally, due to the existing limitations of current techniques which rely on signal intensity threshold based methods to assess myocardial oedema, we established pre-contrast T1 mapping techniques to assess acute myocardial injury in ACS. We demonstrated how T1 mapping is feasible and more suitable for acute sick patients thanks to the short breath-holds need to acquire an image; furthermore T1 mapping provides T1 values on a voxel by voxel basis and we established a correlation between higher T1 values and the increasing severity of injury as assessed by LGE and oedema. This is relevant for clinical and research applications for two main reasons: 1) pre contrast T1 mapping allows for assessment of acute injury also in patients with impaired kidney function who are at risk of collateral effects due to gadolinium administration and elimination 2) new techniques based on quantitative assessment of injury independent of thresholds based methods will allow for better understanding of the ischemic tissue changes land a more accurate assessment of reversible versus irreversible injury.

Building on the cardiovascular magnetic imaging protocol developed here for the acute patients including the new T1 mapping techniques, we plan to extend the work presented in this thesis by incorporating other CMR measurements (such as quantitative myocardial perfusion) and new CMR techniques. We aim to match acute imaging by

CMR with acute invasive measurements in patients presenting with ACS. By investigating the existing correlations between acute CMR findings and invasive measurements such as OCT and IMR, we will have a better understanding of the pathophysiological mechanisms. We believe that this knowledge will be extremely helpful to predict the remodelling of the heart in patients with acute myocardial ischemia; more importantly it will provide us with a rationale for the introduction of specific pharmacologic treatments or pre/post conditioning in ACS in the ultimate aim of improving patients prognosis.

Finally we plan also to include molecular imaging: we will approach this by working in the experimental field and introducing new contrast agents targeting molecules /cells involved in the acute inflammatory processes.

We believe that the CMR will play a central role in acute imaging of patients with ACS and will provide further scientific knowledge to ultimately improve patients' prognosis.

References

Abdel-Aty H, Zagrosek A, Schulz-Menger J, Taylor AJ, Messroghli D, Kumar A, Gross M, Dietz R, Friedrich MG. Delayed enhancement and t2-weighted cardiovascular magnetic resonance imaging differentiate acute from chronic myocardial infarction. *Circulation*. 2004;109:2411-2416

Abdel-Aty H, Cocker M, Meek C, Tyberg JV, Friedrich MG. Edema as a very early marker for acute myocardial ischemia: A cardiovascular magnetic resonance study. *J Am Coll Cardiol*. 2009;53:1194-1201

Aletras AH, Tilak GS, Natanzon A, Hsu L-Y, Gonzalez FM, Hoyt RF, Jr., Arai AE. Retrospective determination of the area at risk for reperfused acute myocardial infarction with t2-weighted cardiac magnetic resonance imaging: Histopathological and displacement encoding with stimulated echoes (dense) functional validations. *Circulation*. 2006;113:1865-1870

Aletras AH, Kellman P, Derbyshire JA, Arai AE. Acut2e tse-ssfp: A hybrid method for t2-weighted imaging of edema in the heart. *Magn Reson Med*. 2008;59:229-235

Anderson JL, Adams CD, Antman EM, Bridges CR, Califf RM, Casey DE, Jr., Chavey WE, 2nd, Fesmire FM, Hochman JS, Levin TN, Lincoff AM, Peterson ED, Theroux P, Wenger NK, Wright RS, Smith SC, Jr., Jacobs AK, Halperin JL, Hunt SA, Krumholz HM, Kushner FG, Lytle BW, Nishimura R, Ornato JP, Page RL, Riegel B. Acc/aha 2007 guidelines for the management of patients with unstable angina/non-st-elevation myocardial infarction: A report of the american college of cardiology/american heart association task force on practice guidelines (writing committee to revise the 2002 guidelines for the management of patients with unstable angina/non-st-elevation myocardial infarction) developed in collaboration with the american college of emergency physicians, the society for cardiovascular angiography and interventions, and the society of thoracic surgeons endorsed by the american association of cardiovascular and pulmonary rehabilitation and the society for academic emergency medicine. *J Am Coll Cardiol*. 2007;50:e1-e157

Andrew E A. Gadolinium can depict area at risk and myocardial infarction: A double-edged sword? *JACC: Cardiovascular Imaging*. 2011;4:619-621

Arai AE. Using magnetic resonance imaging to characterize recent myocardial injury: Utility in acute coronary syndrome and other clinical scenarios. *Circulation*. 2008;118:795-796

Atar D, Petzelbauer P, Schwitter Jr, Huber K, Rensing B, Kasprzak JD, Butter C, Grip L, Hansen PR, S¸selbeck T, Clemmensen PM, Marin-Galiano M, Geudelin B, Buser PT. Effect of intravenous fx06 as an adjunct to primary percutaneous coronary intervention for acute st-segment elevation myocardial infarction: Results of the f.I.R.E. (efficacy of fx06 in the prevention of myocardial reperfusion injury) trial. *Journal of the American College of Cardiology*. 2009;53:720-729

Baer FM, Theissen P, Schneider CA, Voth E, Sechtem U, Schicha H, Erdmann E. Dobutamine magnetic resonance imaging predicts contractile recovery of chronically dysfunctional myocardium after successful revascularization. *J Am Coll Cardiol*. 1998;31:1040-1048

Basso C, Corbetti F, Silva C, Abudureheman A, Lacognata C, Cacciavillani L, Tarantini G, Marra MP, Ramondo A, Thiene G, Iliceto S. Morphologic validation of reperfused hemorrhagic myocardial infarction by cardiovascular magnetic resonance. *The American Journal of Cardiology*. 2007;100:1322-1327

Beek AM, K¸hl HP, Bondarenko O, Twisk JWR, Hofman MBM, van Dockum WG, Visser CA, van Rossum AC. Delayed contrast-enhanced magnetic resonance imaging for the prediction of regional functional improvement after acute myocardial infarction. *Journal of the American College of Cardiology*. 2003;42:895-901

Berry C, Zalewski A, Kovach R, Savage M, Goldberg S. Surface electrocardiogram in the detection of transmural myocardial ischemia during coronary artery occlusion. *The American Journal of Cardiology*. 1989;63:21-26

Berry C, Kellman P, Mancini C, Chen MY, Bandettini WP, Lowrey T, Hsu LY, Aletras AH, Arai AE. Magnetic resonance imaging delineates the ischemic area-at-risk and myocardial salvage in patients with acute myocardial infarction. *Circ Cardiovasc Imaging*. 2010;3:527-535

Bilheimer DW, Buja LM, Parkey RW, Bonte FJ, Willerson JT. Fatty acid accumulation and abnormal lipid deposition in peripheral and border zones of experimental myocardial infarcts. *J Nucl Med*. 1978;19:276-283

Bøtker HE, Kharbanda R, Schmidt MR, Bøttcher M, Kaltoft AK, Terkelsen CJ, Munk K, Andersen NH, Hansen TM, Trautner S, Lassen JF, Christiansen EHj, Krusell LR, Kristensen SD, Thuesen L, Nielsen SS, Rehling M, Sørensen HT, Redington AN, Nielsen TT. Remote ischaemic conditioning before hospital admission, as a complement to angioplasty, and effect on myocardial salvage in patients with acute myocardial infarction: A randomised trial. *The Lancet*. 2010;375:727-734

Bove CM, DiMaria JM, Voros S, Conaway MR, Kramer CM. Dobutamine response and myocardial infarct transmurality: Functional improvement after coronary artery bypass grafting--initial experience. *Radiology*. 2006;240:835-841

Brown JJ, Peck WW, Gerber KH, Higgins CB, Strich G, Slutsky RA. Nuclear magnetic resonance analysis of acute and chronic myocardial infarction in dogs: Alterations in spin-lattice relaxation times. *American Heart Journal*. 1984;108:1292-1297

Buja LM. Myocardial ischemia and reperfusion injury. *Cardiovascular Pathology*. 2005;14:170-175

Canby RC, Reeves RC, Evanochko WT, Elgavish GA, Pohost GM. Proton nuclear magnetic resonance relaxation times in severe myocardial ischemia. *J Am Coll Cardiol*. 1987;10:412-420

Cerqueira MD, Weissman NJ, Dilsizian V, Jacobs AK, Kaul S, Laskey WK, Pennell DJ, Rumberger JA, Ryan T, Verani MS. Standardized myocardial segmentation and nomenclature for tomographic imaging of the heart: A statement for healthcare professionals from the cardiac imaging committee of the council on clinical cardiology of the american heart association. *Circulation*. 2002;105:539-542

Choi KM, Kim RJ, Gubernikoff G, Vargas JD, Parker M, Judd RM. Transmural extent of acute myocardial infarction predicts long-term improvement in contractile function. *Circulation*. 2001;104:1101-1107

Cury RC, Shash K, Nagurney JT, Rosito G, Shapiro MD, Nomura CH, Abbara S, Bamberg F, Ferencik M, Schmidt EJ, Brown DF, Hoffmann U, Brady TJ. Cardiac magnetic resonance with t2-weighted imaging improves detection of patients with acute coronary syndrome in the emergency department. *Circulation*. 2008;118:837-844

Dall'Armellina E, Morgan TM, Mandapaka S, Ntim W, Carr JJ, Hamilton CA, Hoyle J, Clark H, Clark P, Link KM, Case D, Hundley WG. Prediction of cardiac events in patients with reduced left ventricular ejection fraction with dobutamine cardiovascular magnetic resonance assessment of wall motion score index. *Journal of the American College of Cardiology*. 2008;52:279-286

Dall'Armellina E, Karamitsos TD, Neubauer S, Choudhury RP. Cmr for characterization of the myocardium in acute coronary syndromes. *Nat Rev Cardiol*. 2010;7:624-636

Dall'Armellina E, Karia N, Lindsay AC, Karamitsos TD, Ferreira V, Robson MD, Kellman P, Francis JM, Forfar C, Prendergast B, Banning AP, Channon KM, Kharbanda RK, Neubauer S, Choudhury RP. Dynamic changes of edema and late gadolinium enhancement after acute myocardial infarction and their relationship

to functional recovery and salvage index. *Circulation: Cardiovascular Imaging*. 2011

de Roos A, Doornbos J, van der Wall E, van Voorthuisen A. Mr imaging of acute myocardial infarction: Value of gd-dtpa. *Am. J. Roentgenol.* 1988;150:531-534

de Roos A, van Rossum AC, van der Wall E, Postema S, Doornbos J, Matheijssen N, van Dijkman PR, Visser FC, van Voorthuisen AE. Reperfused and nonreperfused myocardial infarction: Diagnostic potential of gd-dtpa--enhanced mr imaging. *Radiology*. 1989;172:717-720

DeLong ER, DeLong DM, Clarke-Pearson DL. Comparing the areas under two or more correlated receiver operating characteristic curves: A nonparametric approach. *Biometrics*. 1988;44:837-845

Eitel I, Desch S, Sareban M, Fuernau G, Gutberlet M, Schuler G, Thiele H. Prognostic significance and magnetic resonance imaging findings in aborted myocardial infarction after primary angioplasty. *American Heart Journal*. 2009;158:806-813

Eitel I, Kubusch K, Strohm O, Desch S, Mikami Y, de Waha S, Gutberlet M, Schuler G, Friedrich MG, Thiele H. Prognostic value and determinants of a hypointense infarct core in t2-weighted cardiac magnetic resonance in acute reperfused st-elevation‚äìmyocardial infarction / clinical perspective. *Circulation: Cardiovascular Imaging*. 2011;4:354-362

Engblom H. Rapid initial reduction of hyperenhanced myocardium after reperfused first myocardial infarction suggests recovery of the peri-infarction zone: One year follow up by mri. *Circulation cardiovascular imaging*. 2009;2:47-55

Ferreira VM, Piechnik SK, Dall'armellina E, Karamitsos TD, Francis JM, Choudhury RP, Friedrich MG, Robson MD, Neubauer SM. Non-contrast t1-mapping detects acute myocardial edema with high diagnostic accuracy: A comparison to t2-weighted cardiovascular magnetic resonance. *Journal of cardiovascular magnetic resonance : official journal of the Society for Cardiovascular Magnetic Resonance*. 2012;14:42

Fieno DS, Hillenbrand HB, Rehwald WG, Harris KR, Decker RS, Parker MA, Klocke FJ, Kim RJ, Judd RM. Infarct resorption, compensatory hypertrophy, and differing patterns of ventricular remodeling following myocardial infarctions of varying size. *J Am Coll Cardiol*. 2004;43:2124-2131

Flacke SJ, Fischer SE, Lorenz CH. Measurement of the gadopentetate dimeglumine partition coefficient in human myocardium in vivo: Normal distribution and elevation in acute and chronic infarction1. *Radiology*. 2001;218:703-710

Francone M, Bucciarelli-Ducci C, Carbone I, Canali E, Scardala R, Calabrese FA, Sardella G, Mancone M, Catalano C, Fedele F, Passariello R, Bogaert J, Agati L. Impact of primary coronary angioplasty delay on myocardial salvage, infarct size, and microvascular damage in patients with st-segment elevation myocardial infarction: Insight from cardiovascular magnetic resonance. *Journal of the American College of Cardiology*. 2009;54:2145-2153

Francone M, Bucciarelli-Ducci C, Carbone I, Canali E, Scardala R, Calabrese FA, Sardella G, Mancone M, Catalano C, Fedele F, Passariello R, Bogaert J, Agati L. Impact of primary coronary angioplasty delay on myocardial salvage, infarct size, and microvascular damage in patients with st-segment elevation myocardial infarction: Insight from cardiovascular magnetic resonance. *J Am Coll Cardiol*. 2009;54:2145-2153

Friedrich MG, Abdel-Aty H, Taylor A, Schulz-Menger J, Messroghli D, Dietz R. The salvaged area at risk in reperfused acute myocardial infarction as visualized by cardiovascular magnetic resonance. *J Am Coll Cardiol*. 2008;51:1581-1587

Friedrich MG. Myocardial edema--a new clinical entity? *Nat Rev Cardiol*. 2010;7:292-296

Friedrich MG, Kim HW, Kim RJ. T2-weighted imaging to assess post-infarct myocardium at risk. *JACC: Cardiovascular Imaging*. 2011;4:1014-1021

Ganame J, Messalli G, Dymarkowski S, Rademakers FE, Desmet W, Van de Werf F, Bogaert J. Impact of myocardial haemorrhage on left ventricular function and remodelling in patients with reperfused acute myocardial infarction. *Eur Heart J*. 2009;30:1440-1449

Garcia-Dorado D, Oliveras J, Gili J, Sanz E, Perez-Villa F, Barrabes J, Carreras MJ, Solares J, Soler-Soler J. Analysis of myocardial oedema by magnetic resonance imaging early after coronary artery occlusion with or without reperfusion. *Cardiovasc Res*. 1993;27:1462-1469

Gerber BL, Garot J, Bluemke DA, Wu KC, Lima JA. Accuracy of contrast-enhanced magnetic resonance imaging in predicting improvement of regional myocardial function in patients after acute myocardial infarction. *Circulation*. 2002;106:1083-1089

Ghugre NR, Ramanan V, Pop M, Yang Y, Barry J, Qiang B, Connelly KA, Dick AJ, Wright GA. Quantitative tracking of edema, hemorrhage, and microvascular obstruction in subacute myocardial infarction in a porcine model by mri. *Magnetic Resonance in Medicine*. 2011:n/a-n/a

Giri S, Chung YC, Merchant A, Mihai G, Rajagopalan S, Raman SV, Simonetti OP. T2 quantification for improved detection of myocardial edema. *J Cardiovasc Magn Reson*. 2009;11:56

Go LO, Murry CE, Richard VJ, Weischedel GR, Jennings RB, Reimer KA. Myocardial neutrophil accumulation during reperfusion after reversible or irreversible ischemic injury. *Am J Physiol*. 1988;255:H1188-1198

Goldfarb JW, Arnold S, Han J. Recent myocardial infarction: Assessment with unenhanced t1-weighted mr imaging. *Radiology*. 2007;245:245-250

Goldstein JA, Demetriou D, Grines CL, Pica M, Shoukfeh M, O'Neill WW. Multiple complex coronary plaques in patients with acute myocardial infarction. *N Engl J Med*. 2000;343:915-922

Graham MM, Faris PD, Ghali WA, Galbraith PD, Norris CM, Badry JT, Mitchell LB, Curtis MJ, Knudtson ML. Validation of three myocardial jeopardy scores in a population-based cardiac catheterization cohort. *American Heart Journal*. 2001;142:254-261

Greenwood JP, Younger JF, Ridgway JP, Sivananthan MU, Ball SG, Plein S. Safety and diagnostic accuracy of stress cardiac magnetic resonance imaging vs exercise tolerance testing early after acute st elevation myocardial infarction. *Heart*. 2007;93:1363-1368

Hasche ET, Fernandes C, Freedman SB, Jeremy RW. Relation between ischemia time, infarct size, and left ventricular function in humans. *Circulation*. 1995;92:710-719

Hazlewood CF, Chang DC, Nichols BL, Woessner DE. Nuclear magnetic resonance transverse relaxation times of water protons in skeletal muscle. *Biophys J*. 1974;14:583-606

Hedstrom E, Engblom H, Frogner F, Astrom-Olsson K, Ohlin H, Jovinge S, Arheden H. Infarct evolution in man studied in patients with first-time coronary occlusion in comparison to different species - implications for assessment of myocardial salvage. *J Cardiovasc Magn Reson*. 2009;11:38

Higgins CB, Herfkens R, Lipton MJ, Sievers R, Sheldon P, Kaufman L, Crooks LE. Nuclear magnetic resonance imaging of acute myocardial infarction in dogs: Alterations in magnetic relaxation times. *Am J Cardiol*. 1983;52:184-188

Hochman JS, Reynolds HR, D≈æav√≠k Vr, Buller CE, Ruzyllo W, Sadowski ZP, Maggioni AP, Carvalho AC, Rankin JM, White HD, Goldberg S, Forman SA, Mark DB, Lamas GA. Long-term effects of percutaneous coronary intervention of

the totally occluded infarct-related artery in the subacute phase after myocardial infarction / clinical perspective. *Circulation*. 2011;124:2320-2328

Holmes JW, Yamashita H, Waldman LK, Covell JW. Scar remodeling and transmural deformation after infarction in the pig. *Circulation*. 1994;90:411-420

Hombach V, Grebe O, Merkle N, Waldenmaier S, Hoher M, Kochs M, Wohrle J, Kestler HA. Sequelae of acute myocardial infarction regarding cardiac structure and function and their prognostic significance as assessed by magnetic resonance imaging. *Eur Heart J*. 2005;26:549-557

Hudsmith LE, Peterson SE, Tayler DJ, Francis JM, Clarke K, Joseph BS, Robson MD, Nebauer S. Determination of cardiac volumes and mass with flash and ssfp cine sequences at 1.5 vs. 3 tesla: A validation study. *Journal of Magnetic Resonance Imaging*. 2006;24:312-318

Huey BL, Beller GA, Kaiser DL, Gibson RS. A comprehensive analysis of myocardial infarction due to left circumflex artery occlusion: Comparison with infarction due to right coronary artery and left anterior descending artery occlusion. *Journal of the American College of Cardiology*. 1988;12:1156-1166

Ibrahim T, Makowski MR, Jankauskas A, Maintz D, Karch M, Schachoff S, Manning WJ, Schomig A, Schwaiger M, Botnar RM. Serial contrast-enhanced cardiac magnetic resonance imaging demonstrates regression of hyperenhancement within the coronary artery wall in patients after acute myocardial infarction. *J Am Coll Cardiol Img*. 2009;2:580-588

Ibrahim T, Hackl T, Nekolla SG, Breuer M, Feldmair M, Schomig A, Schwaiger M. Acute myocardial infarction: Serial cardiac mr imaging shows a decrease in delayed enhancement of the myocardium during the 1st week after reperfusion. *Radiology*. 2010;254:88-97

Ichikawa Y, Sakuma H, Suzawa N, Kitagawa K, Makino K, Hirano T, Takeda K. Late gadolinium-enhanced magnetic resonance imaging in acute and chronic myocardial infarction. Improved prediction of regional myocardial contraction in the chronic state by measuring thickness of nonenhanced myocardium. *J Am Coll Cardiol*. 2005;45:901-909

Iles L, Pfluger H, Phrommintikul A, Cherayath J, Aksit P, Gupta SN, Kaye DM, Taylor AJ. Evaluation of diffuse myocardial fibrosis in heart failure with cardiac magnetic resonance contrast-enhanced t1 mapping. *Journal of the American College of Cardiology*. 2008;52:1574-1580

Ingkanisorn WP, Rhoads KL, Aletras AH, Kellman P, Arai AE. Gadolinium delayed enhancement cardiovascular magnetic resonance correlates with clinical measures of myocardial infarction. *J Am Coll Cardiol*. 2004;43:2253-2259

Jennings RB, Schaper J, Hill ML, Steenbergen C, Jr., Reimer KA. Effect of reperfusion late in the phase of reversible ischemic injury. Changes in cell volume, electrolytes, metabolites, and ultrastructure. *Circulation research*. 1985;56:262-278

Jennings RB, Murry CE, Steenbergen C, Jr., Reimer KA. Development of cell injury in sustained acute ischemia. *Circulation*. 1990;82:II2-12

Jung B, Markl M, Foll D, Hennig J. Investigating myocardial motion by mri using tissue phase mapping. *Eur J Cardiothorac Surg*. 2006;29 Suppl 1:S150-157

Kannel WB, Abbott RD. Incidence and prognosis of unrecognized myocardial infarction. An update on the framingham study. *The New England journal of medicine*. 1984;311:1144-1147

Karamitsos TD, Hudsmith LE, Selvanayagam JB, Neubauer S, Francis JM. Operator induced variability in left ventricular measurements with cardiovascular magnetic resonance is improved after training. *J Cardiovasc Magn Reson*. 2007;9:777-783

Karolle BL, Carlson RE, Aisen AM, Buda AJ. Transmural distribution of myocardial edema by nmr relaxometry following myocardial ischemia and reperfusion. *Am Heart J*. 1991;122:655-664

Keegan J, Gatehouse PD, Prasad SK, Firmin DN. Improved turbo spin-echo imaging of the heart with motion-tracking. *J Magn Reson Imaging*. 2006;24:563-570

Kellman P, Andrew CL, Li-Yueh H, Yiu-Cho C, Orlando PS, Elliot RM, Andrew EA. Motion-corrected free-breathing delayed enhancement imaging of myocardial infarction. *Magnetic Resonance in Medicine*. 2005;53:194-200

Kellman P, Aletras AH, Mancini C, McVeigh ER, Arai AE. T2-prepared ssfp improves diagnostic confidence in edema imaging in acute myocardial infarction compared to turbo spin echo. *Magn Reson Med*. 2007;57:891-897

Kerensky RA, Wade M, Deedwania P, Boden WE, Pepine CJ. Revisiting the culprit lesion in non‚äìq-wave myocardial infarction: Results from the vanqwish trial angiographic core laboratory. *Journal of the American College of Cardiology*. 2002;39:1456-1463

Kim HW, Klem I, Shah DJ, Wu E, Meyers SN, Parker MA, Crowley AL, Bonow RO, Judd RM, Kim RJ. Unrecognized non-q-wave myocardial infarction: Prevalence and prognostic significance in patients with suspected coronary disease. *PLoS Med*. 2009;6:e1000057

Kim RJ, Fieno DS, Parrish TB, Harris K, Chen E-L, Simonetti O, Bundy J, Finn JP, Klocke FJ, Judd RM. Relationship of mri delayed contrast enhancement to irreversible injury, infarct age, and contractile function. *Circulation*. 1999;100:1992-2002

Kim RJ, Wu E, Rafael A, Chen EL, Parker MA, Simonetti O, Klocke FJ, Bonow RO, Judd RM. The use of contrast-enhanced magnetic resonance imaging to identify reversible myocardial dysfunction. *N Engl J Med*. 2000;343:1445-1453

Kim RJ, Manning WJ. Viability assessment by delayed enhancement cardiovascular magnetic resonance: Will low-dose dobutamine dull the shine? *Circulation*. 2004;109:2476-2479

Klein C, Schmal TR, Nekolla SG, Schnackenburg B, Fleck E, Nagel E. Mechanism of late gadolinium enhancement in patients with acute myocardial infarction. *J Cardiovasc Magn Reson*. 2007;9:653-658

Klocke FJ. Cardiac magnetic resonance measurements of area at risk and infarct size in ischemic syndromes. *J Am Coll Cardiol*. 2010;55:2489-2490

Kloner RA, Ganote CE, Jennings RB. The "no-reflow" phenomenon after temporary coronary occlusion in the dog. *J Clin Invest*. 1974;54:1496-1508

Knight RA, Ordidge RJ, Helpern JA, Chopp M, Rodolosi LC, Peck D. Temporal evolution of ischemic damage in rat brain measured by proton nuclear magnetic resonance imaging. *Stroke*. 1991;22:802-808

Korosoglou G, Lehrke S, Wochele A, Hoerig B, Lossnitzer D, Steen H, Giannitsis E, Osman NF, Katus HA. Strain-encoded cmr for the detection of inducible ischemia during intermediate stress. *J Am Coll Cardiol Img*. 2010;3:361-371

Kotani J-i, Mintz GS, Castagna MT, Pinnow E, Berzingi CO, Bui AB, Pichard AD, Satler LF, Suddath WO, Waksman R, Laird JR, Kent KM, Weissman NJ. Intravascular ultrasound analysis of infarct-related and non‚äìinfarct-related arteries in patients who presented with an acute myocardial infarction. *Circulation*. 2003;107:2889-2893

Kramer CM, Rogers WJ, Jr., Mankad S, Theobald TM, Pakstis DL, Hu YL. Contractile reserve and contrast uptake pattern by magnetic resonance imaging and functional recovery after reperfused myocardial infarction. *Journal of the American College of Cardiology*. 2000;36:1835-1840

Kuntz ID, Jr., Brassfield TS, Law GD, Purcell GV. Hydration of macromolecules. *Science*. 1969;163:1329-1331

Kushner FG, Hand M, Smith SC, Jr, King SB, III, Anderson JL, Antman EM, Bailey SR, Bates ER, Blankenship JC, Casey DE, Jr, Green LA, Hochman JS, Jacobs AK, Krumholz HM, Morrison DA, Ornato JP, Pearle DL, Peterson ED, Sloan MA, Whitlow PL, Williams DO. 2009 focused updates: Acc/aha guidelines for the management of patients with st-elevation myocardial infarction (updating the 2004 guideline and 2007 focused update) and acc/aha/scai guidelines on percutaneous coronary intervention (updating the 2005 guideline and 2007 focused update): A report of the american college of cardiology foundation/american heart association task force on practice guidelines. *Circulation*. 2009;120:2271-2306

Kwong RY, Schussheim AE, Rekhraj S, Aletras AH, Geller N, Davis J, Christian TF, Balaban RS, Arai AE. Detecting acute coronary syndrome in the emergency department with cardiac magnetic resonance imaging. *Circulation*. 2003;107:531-537

Kwong RY, Farzaneh-Far A. Measuring myocardial scar by cmr. *JACC. Cardiovascular imaging*. 2011;4:157-160

Larose E, RodÈs-Cabau J, Pibarot P, Rinfret S, Proulx G, Nguyen CM, DÈry J-P, Gleeton O, Roy L, NoÎl B, Barbeau G, Rouleau J, Boudreault J-R, Amyot M, De LarochelliËre R, Bertrand OF. Predicting late myocardial recovery and outcomes in the early hours of st-segment elevation myocardial infarction: Traditional measures compared with microvascular obstruction, salvaged myocardium, and necrosis characteristics by cardiovascular magnetic resonance. *Journal of the American College of Cardiology*. 2010;55:2459-2469

Larose E, Tizon-Marcos H, RodÈs-Cabau J, Rinfret S, DÈry J-P, Nguyen CM, Gleeton O, Boudreault J-R, Roy L, NoÎl B, Proulx G, Rouleau J, Barbeau G, LarochelliËre RD, Bertrand OF. Improving myocardial salvage in late presentation acute st-elevation myocardial infarction with proximal embolic protection. *Catheterization and Cardiovascular Interventions*. 2010;76:461-470

Lee WW, Marinelli B, van der Laan AM, Sena BF, Gorbatov R, Leuschner F, Dutta P, Iwamoto Y, Ueno T, Begieneman MP, Niessen HW, Piek JJ, Vinegoni C, Pittet MJ, Swirski FK, Tawakol A, Di Carli M, Weissleder R, Nahrendorf M. Pet/mri of inflammation in myocardial infarction. *Journal of the American College of Cardiology*. 2012;59:153-163

Lima JAC, Judd RM, Bazille A, Schulman SP, Atalar E, Zerhouni EA. Regional heterogeneity of human myocardial infarcts demonstrated by contrast-enhanced mri : Potential mechanisms. *Circulation*. 1995;92:1117-1125

Mather A, Lockie T, Nagel E, Marber M, Perera D, Redwood S, Radjenovic A, Saha A, Greenwood J, Plein S. Appearance of microvascular obstruction on high

resolution first-pass perfusion, early and late gadolinium enhancement cmr in patients with acute myocardial infarction. *Journal of Cardiovascular Magnetic Resonance*. 2009;11:33

Mather AN, Fairbairn TA, Ball SG, Greenwood JP, Plein S. Reperfusion haemorrhage as determined by cardiovascular mri is a predictor of adverse left ventricular remodelling and markers of late arrhythmic risk. *Heart*. 2011;97:453-459

Matsumoto H, Matsuda T, Miyamoto K, Shimada T, Mikuri M, Hiraoka Y. Peri-infarct zone on early contrast-enhanced cmr imaging in patients with acute myocardial infarction. *JACC: Cardiovascular Imaging*. 2011;4:610-618

Messroghli DR, Radjenovic A, Kozerke S, Higgins DM, Sivananthan MU, Ridgway JP. Modified look-locker inversion recovery (molli) for high-resolution t1 mapping of the heart. *Magnetic resonance in medicine : official journal of the Society of Magnetic Resonance in Medicine / Society of Magnetic Resonance in Medicine*. 2004;52:141-146

Messroghli DR, Plein S, Higgins DM, Walters K, Jones TR, Ridgway JP, Sivananthan MU. Human myocardium: Single-breath-hold mr t1 mapping with high spatial resolution--reproducibility study. *Radiology*. 2006;238:1004-1012

Messroghli DR, Walters K, Plein S, Sparrow P, Friedrich MG, Ridgway JP, Sivananthan MU. Myocardial t1 mapping: Application to patients with acute and chronic myocardial infarction. *Magnetic resonance in medicine : official journal of the Society of Magnetic Resonance in Medicine / Society of Magnetic Resonance in Medicine*. 2007;58:34-40

Miller S, Helber U, Kramer U, Hahn U, Carr J, Stauder N, Hoffmeister H, Claussen C. Subacute myocardial infarction: Assessment by stir t2-weighted mr imaging in comparison to regional function. *Magnetic Resonance Materials in Physics, Biology and Medicine*. 2001;13:8-14

Montalescot G, Dallongeville J, Van Belle E, Rouanet S, Baulac C, Degrandsart A, Vicaut E. Stemi and nstemi: Are they so different? 1 year outcomes in acute myocardial infarction as defined by the esc/acc definition (the opera registry). *European Heart Journal*. 2007

Moon JCC, Perez De Arenaza D, Elkington AG, Taneja AK, John AS, Wang D, Janardhanan R, Senior R, Lahiri A, Poole-Wilson PA, Pennell DJ. The pathologic basis of q-wave and non-q-wave myocardial infarction: A cardiovascular magnetic resonance study. *J Am Coll Cardiol*. 2004;44:554-560

Nacif MS, Arai AE, Lima JA, Bluemke DA. Gadolinium-enhanced cardiovascular magnetic resonance: Administered dose in relationship to united states food and drug administration (fda) guidelines. *Journal of cardiovascular magnetic*

resonance : official journal of the Society for Cardiovascular Magnetic Resonance. 2012;14:18

Naghavi M, Libby P, Falk E, Casscells SW, Litovsky S, Rumberger J, Badimon JJ, Stefanadis C, Moreno P, Pasterkamp G, Fayad Z, Stone PH, Waxman S, Raggi P, Madjid M, Zarrabi A, Burke A, Yuan C, Fitzgerald PJ, Siscovick DS, de Korte CL, Aikawa M, Juhani Airaksinen KE, Assmann G, Becker CR, Chesebro JH, Farb A, Galis ZS, Jackson C, Jang IK, Koenig W, Lodder RA, March K, Demirovic J, Navab M, Priori SG, Rekhter MD, Bahr R, Grundy SM, Mehran R, Colombo A, Boerwinkle E, Ballantyne C, Insull W, Jr., Schwartz RS, Vogel R, Serruys PW, Hansson GK, Faxon DP, Kaul S, Drexler H, Greenland P, Muller JE, Virmani R, Ridker PM, Zipes DP, Shah PK, Willerson JT. From vulnerable plaque to vulnerable patient: A call for new definitions and risk assessment strategies: Part i. *Circulation*. 2003;108:1664-1672

Nassenstein K, Breuckmann F, Bucher C, Kaiser G, Konorza T, Schafer L, Konietzka I, de Greiff A, Heusch G, Erbel R, Barkhausen J. How much myocardial damage is necessary to enable detection of focal late gadolinium enhancement at cardiac mr imaging? *Radiology*. 2008;249:829-835

Neizel M, Lossnitzer D, Korosoglou G, Schaufele T, Lewien A, Steen H, Katus HA, Osman NF, Giannitsis E. Strain-encoded (senc) magnetic resonance imaging to evaluate regional heterogeneity of myocardial strain in healthy volunteers: Comparison with conventional tagging. *J Magn Reson Imaging*. 2009;29:99-105

Niccoli G, Burzotta F, Galiuto L, Crea F. Myocardial no-reflow in humans. *Journal of the American College of Cardiology*. 2009;54:281-292

O'Regan DP, Ahmed R, Karunanithy N, Neuwirth C, Tan Y, Durighel G, Hajnal JV, Nadra I, Corbett SJ, Cook SA. Reperfusion hemorrhage following acute myocardial infarction: Assessment with t2* mapping and effect on measuring the area at risk. *Radiology*. 2009;250:916-922

Ochiai K, Shimada T, Murakami Y, Ishibashi Y, Sano K, Kitamura J, Inoue S, Murakami R, Kawamitsu H, Sugimura K. Hemorrhagic myocardial infarction after coronary reperfusion detected in vivo by magnetic resonance imaging in humans: Prevalence and clinical implications. *J Cardiovasc Magn Reson*. 1999;1:247-256

Ortiz-Perez JT, Meyers SN, Lee DC, Kansal P, Klocke FJ, Holly TA, Davidson CJ, Bonow RO, Wu E. Angiographic estimates of myocardium at risk during acute myocardial infarction: Validation study using cardiac magnetic resonance imaging. *European Heart Journal*. 2007;28:1750-1758

Ortiz-PÈrez JT, Lee DC, Meyers SN, Davidson CJ, Bonow RO, Wu E. Determinants of myocardial salvage during acute myocardial infarction: Evaluation with a

combined angiographic and cmr myocardial salvage index. *JACC: Cardiovascular Imaging*. 2010;3:491-500

Payne AR, Casey M, McClure J, McGeoch R, Murphy A, Woodward R, Saul A, Bi X, Zuehlsdorff S, Oldroyd KG, Tzemos N, Berry C. Bright blood t2 weighted mri has higher diagnostic accuracy than dark blood stir mri for detection of acute myocardial infarction and for assessment of the ischemic area-at-risk and myocardial salvage. *Circulation: Cardiovascular Imaging*. 2011;4:210-219

Pennell DJ, Sechtem UP, Higgins CB, Manning WJ, Pohost GM, Rademakers FE, van Rossum AC, Shaw LJ, Yucel EK. Clinical indications for cardiovascular magnetic resonance (cmr): Consensus panel report. *Eur Heart J*. 2004;25:1940-1965

Phrommintikul A, Abdel-Aty H, Schulz-Menger J, Friedrich MG, Taylor AJ. Acute oedema in the evaluation of microvascular reperfusion and myocardial salvage in reperfused myocardial infarction with cardiac magnetic resonance imaging. *European Journal of Radiology*. 2010;74:e12-17

Piechnik S, Ferreira V, Dall'Armellina E, Cochlin L, Greiser A, Neubauer S, Robson M. Shortened modified look-locker inversion recovery (shmolli) for clinical myocardial t1-mapping at 1.5 and 3 t within a 9 heartbeat breathhold. *Journal of Cardiovascular Magnetic Resonance*. 2010;12:69

Piper HM, Garcna-Dorado D, Ovize M. A fresh look at reperfusion injury. *Cardiovasc Res*. 1998;38:291-300

Porto I, Selvanayagam JB, Van Gaal WJ, Prati F, Cheng A, Channon K, Neubauer S, Banning AP. Plaque volume and occurrence and location of periprocedural myocardial necrosis after percutaneous coronary intervention: Insights from delayed-enhancement magnetic resonance imaging, thrombolysis in myocardial infarction myocardial perfusion grade analysis, and intravascular ultrasound. *Circulation*. 2006;114:662-669

Raman SV, Simonetti OP, Winner Iii MW, Dickerson JA, He X, Mazzaferri Jr EL, Ambrosio G. Cardiac magnetic resonance with edema imaging identifies myocardium at risk and predicts worse outcome in patients with non-st-segment elevation acute coronary syndrome. *Journal of the American College of Cardiology*. 2010;55:2480-2488

Rehwald WG, Fieno DS, Chen E-L, Kim RJ, Judd RM. Myocardial magnetic resonance imaging contrast agent concentrations after reversible and irreversible ischemic injury. *Circulation*. 2002;105:224-229

Reimer KA, Lowe JE, Rasmussen MM, Jennings RB. The wavefront phenomenon of ischemic cell death. 1. Myocardial infarct size vs duration of coronary occlusion in dogs. *Circulation*. 1977;56:786-794

Reimer KA, Jennings RB. The changing anatomic reference base of evolving myocardial infarction. Underestimation of myocardial collateral blood flow and overestimation of experimental anatomic infarct size due to tissue edema, hemorrhage and acute inflammation. *Circulation*. 1979;60:866-876

Reimer KA, Jennings RB, Tatum AH. Pathobiology of acute myocardial ischemia: Metabolic, functional and ultrastructural studies. *Am J Cardiol*. 1983;52:72A-81A

Ricciardi MJ, Wu E, Davidson CJ, Choi KM, Klocke FJ, Bonow RO, Judd RM, Kim RJ. Visualization of discrete microinfarction after percutaneous coronary intervention associated with mild creatine kinase-mb elevation. *Circulation*. 2001;103:2780-2783

Rogers WJ, Jr., Kramer CM, Geskin G, Hu YL, Theobald TM, Vido DA, Petruolo S, Reichek N. Early contrast-enhanced mri predicts late functional recovery after reperfused myocardial infarction. *Circulation*. 1999;99:744-750

Rosen BD, Lima JA, Nasir K, Edvardsen T, Folsom AR, Lai S, Bluemke DA, Jerosch-Herold M. Lower myocardial perfusion reserve is associated with decreased regional left ventricular function in asymptomatic participants of the multi-ethnic study of atherosclerosis. *Circulation*. 2006;114:289-297

Sabia P, Abbott R, Afrookteh A, Keller M, Touchstone D, Kaul S. Importance of two-dimensional echocardiographic assessment of left ventricular systolic function in patients presenting to the emergency room with cardiac-related symptoms. *Circulation*. 1991;84:1615-1624

Saeed M, Bremerich J, Wendland MF, Wyttenbach R, Weinmann HJ, Higgins CB. Reperfused myocardial infarction as seen with use of necrosis-specific versus standard extracellular mr contrast media in rats. *Radiology*. 1999;213:247-257

Sardella G, Mancone M, Bucciarelli-Ducci C, Agati L, Scardala R, Carbone I, Francone M, Di Roma A, Benedetti G, Conti G, Fedele F. Thrombus aspiration during primary percutaneous coronary intervention improves myocardial reperfusion and reduces infarct size: The expira (thrombectomy with export catheter in infarct-related artery during primary percutaneous coronary intervention) prospective, randomized trial. *Journal of the American College of Cardiology*. 2009;53:309-315

Schulz-Menger J, Gross M, Messroghli D, Uhlich F, Dietz R, Friedrich MG. Cardiovascular magnetic resonance ofacute myocardial infarction at a very early stage. *Journal of the American College of Cardiology*. 2003;42:513-518

Selvanayagam JB, Kardos A, Francis JM, Wiesmann F, Petersen SE, Taggart DP, Neubauer S. Value of delayed-enhancement cardiovascular magnetic resonance imaging in predicting myocardial viability after surgical revascularization. *Circulation*. 2004;110:1535-1541

Selvanayagam JB, Porto I, Channon K, Petersen SE, Francis JM, Neubauer S, Banning AP. Troponin elevation after percutaneous coronary intervention directly represents the extent of irreversible myocardial injury: Insights from cardiovascular magnetic resonance imaging. *Circulation*. 2005;111:1027-1032

Setser RM, O'Donnell TP, Smedira NG, Sabik JF, Halliburton SS, Stillman AE, White RD. Coregistered mr imaging myocardial viability maps and multi, äìdetector row ct coronary angiography displays for surgical revascularization planning: Initial experience1. *Radiology*. 2005;237:465-473

Steenbergen C, Hill ML, Jennings RB. Volume regulation and plasma membrane injury in aerobic, anaerobic, and ischemic myocardium in vitro. Effects of osmotic cell swelling on plasma membrane integrity. *Circ Res*. 1985;57:864-875

Stone GW, Maehara A, Lansky AJ, de Bruyne B, Cristea E, Mintz GS, Mehran R, McPherson J, Farhat N, Marso SP, Parise H, Templin B, White R, Zhang Z, Serruys PW. A prospective natural-history study of coronary atherosclerosis. *N Engl J Med*. 2011;364:226-235

Stribling WK, Kontos MC, Abbate A, Cooke R, Vetrovec GW, Dai D, Honeycutt E, Wang TY, Lotun K. Left circumflex occlusion in acute myocardial infarction (from the national cardiovascular data registry). *The American Journal of Cardiology*. 2011;108:959-963

Tarantini G, Cacciavillani L, Corbetti F, Ramondo A, Marra MP, Bacchiega E, Napodano M, Bilato C, Razzolini R, Iliceto S. Duration of ischemia is a major determinant of transmurality and severe microvascular obstruction after primary angioplasty: A study performed with contrast-enhanced magnetic resonance. *J Am Coll Cardiol*. 2005;46:1229-1235

van Gaal WJ, Banning AP. Percutaneous coronary intervention and the no-reflow phenomenon. *Expert Rev Cardiovasc Ther*. 2007;5:715-731

Verhaert D, Thavendiranathan P, Giri S, Mihai G, Rajagopalan S, Simonetti OP, Raman SV. Direct t2 quantification of myocardial edema in acute ischemic injury. *JACC. Cardiovascular imaging*. 2011;4:269-278

Wacker CM, Bock M, Hartlep AW, Beck G, van Kaick G, Ertl G, Bauer WR, Schad LR. Changes in myocardial oxygenation and perfusion under pharmacological stress with dipyridamole: Assessment using t*2 and t1 measurements. *Magnetic*

resonance in medicine : official journal of the Society of Magnetic Resonance in Medicine / Society of Magnetic Resonance in Medicine. 1999;41:686-695

Wagner A, Mahrholdt H, Holly TA, Elliott MD, Regenfus M, Parker M, Klocke FJ, Bonow RO, Kim RJ, Judd RM. Contrast-enhanced mri and routine single photon emission computed tomography (spect) perfusion imaging for detection of subendocardial myocardial infarcts: An imaging study. *The Lancet*. 2003;361:374-379

Weinmann HJ, Laniado M, Mutzel W. Pharmacokinetics of gddtpa/dimeglumine after intravenous injection into healthy volunteers. *Physiol Chem Phys Med NMR*. 1984;16:167-172

Wellnhofer E, Olariu A, Klein C, Grafe M, Wahl A, Fleck E, Nagel E. Magnetic resonance low-dose dobutamine test is superior to scar quantification for the prediction of functional recovery. *Circulation*. 2004;109:2172-2174

Whalen DA, Jr., Hamilton DG, Ganote CE, Jennings RB. Effect of a transient period of ischemia on myocardial cells. I. Effects on cell volume regulation. *The American journal of pathology*. 1974;74:381-397

Willerson JT, Scales F, Mukherjee A, Platt M, Templeton GH, Fink GS, Buja LM. Abnormal myocardial fluid retention as an early manifestation of ischemic injury. *Am J Pathol*. 1977;87:159-188

Williams ES, Kaplan JI, Thatcher F, Zimmerman G, Knoebel SB. Prolongation of proton spin lattice relaxation times in regionally ischemic tissue from dog hearts. *Journal of nuclear medicine : official publication, Society of Nuclear Medicine*. 1980;21:449-453

Wince WB, Kim RJ. Molecular imaging: T2-weighted cmr of the area at risk--a risky business? *Nature reviews. Cardiology*. 2010;7:547-549

Wisenberg G, Prato FS, Carroll SE, Turner KL, Marshall T. Serial nuclear magnetic resonance imaging of acute myocardial infarction with and without reperfusion. *Am Heart J*. 1988;115:510-518

Wu KC, Zerhouni EA, Judd RM, Lugo-Olivieri CH, Barouch LA, Schulman SP, Blumenthal RS, Lima JAC. Prognostic significance of microvascular obstruction by magnetic resonance imaging in patients with acute myocardial infarction. *Circulation*. 1998;97:765-772

Wu KC, Kim RJ, Bluemke DA, Rochitte CE, Zerhouni EA, Becker LC, Lima JA. Quantification and time course of microvascular obstruction by contrast-enhanced

echocardiography and magnetic resonance imaging following acute myocardial infarction and reperfusion. *J Am Coll Cardiol*. 1998;32:1756-1764

Xu J, Song Y, Hahn J-Y, Chang S-A, Lee S-C, Choe Y, Choi S-H, Choi J-H, Lee S, Oh J, Gwon H-C. Comparison of magnetic resonance imaging findings in non-st-segment elevation versus st-segment elevation myocardial infarction patients undergoing early invasive intervention. *The International Journal of Cardiovascular Imaging (formerly Cardiac Imaging)*. 2011:1-11

Yan AT, Shayne AJ, Brown KA, Gupta SN, Chan CW, Luu TM, Di Carli MF, Reynolds HG, Stevenson WG, Kwong RY. Characterization of the peri-infarct zone by contrast-enhanced cardiac magnetic resonance imaging is a powerful predictor of post-myocardial infarction mortality. *Circulation*. 2006;114:32-39

Index of Figures

Figure 1.1. Normal CMR findings in the absence of a flow-limiting coronary stenosis. The figure shows a normal coronary vessel, a microvessel, and myocardium. CMR images representing normal findings are shown for a | T2W imaging, and b | LGE imaging. [Dall'armellina 2010] 21
Figure 1.2. CMR findings in the presence of a flow-limiting coronary stenosis. A flow-limiting stenosis leads to downstream microvessel and myocardial changes, including swollen myocytes and initial swelling of endothelial cells. a| As a result of ischemia, initial changes in the myocardium owing to increased myocardial oedema (arrow) are shown on T2W imaging. b| No sign of irreversible damage is depicted by LGE imaging. [Dall'armellina 2010]..... 23
Figure 1.3 Myocardial inflammatory processes following coronary occlusion. A coronary vessel with a complicated plaque may cause long-term lack of oxygen, leading to ultrastructural changes and swelling of the endothelial cells in the capillaries and myocytes. The disruption of the endothelium in the capillaries results in increased content of interstitial water. Oncosis of the myocytes and early stages of myocardial necrosis, including inflammation and infiltration of macrophages, will also occur. a | increased signal intensity on T2W images as a result of myocardial oedema (arrows). b | Presence of myocardial scar (arrows) is revealed by LGE imaging. 26
Figure 1.4. Complicated reperfused myocardial infarction. Following restoration of the patency of the vessel, a release of mediators of inflammation and oxidative stress causes damage of the endothelium with loss of function and structural integrity of the endothelial barrier. The combination of increased pressure and loss of structural integrity of the microvessels leads to increased interstitial oedema together with accumulation of polymorphonuclear leukocytes and platelets and extravasation of red blood cells (hemorrhage). These events lead to an obstruction of the microvessels. a | CMR T2W images show the presence of oedema (white arrows). Furthermore, a hypo intense area is consistent with presence of hemorrhage (black arrows), which determines a lack of surrounding perfusion resulting in little contrast penetration on LGE images. b | Microvascular obstruction is depicted by CMR after infusion of gadolinium as a dark core in the hyper enhanced area. Abbreviations: PMN, polymorphonuclear leukocyte; RBC, red blood cell; VCAM, vascular cell adhesion molecule. [Dall'armellina 2010]..... 33
Figure 2.1 Study protocols for (A) STEMI and (B) NSTEMI. Imaging time points (TP) in relation to the acute MI and primary percutaneous coronary intervention (PPCI)/ angiogram and coronary intervention. For each TP, the CMR data acquired is given. 45
Figure 2.2 Cardiovascular magnetic resonance in ACS. An example of an acute imaging protocol applied in a case of acute inferior myocardial infarction is shown here. The execution of the CMR protocol begins with the acquisition of

short-axis T2W oedema imaging, which reveals bright signal in the inferior wall (black arrows in top panel). Matching T1 mapping short axis images are acquired pre administration of gadolinium contrast agent. Within a minute post infusion of the contrast agent early gadolinium imaging can be also performed (not shown here). Functional short-axis images are acquired before the late gadolinium images. As shown in the figure, impairment of regional wall motion is present in the systolic frame at the level of the inferior wall. At the end, 10 to 20 minutes post gadolinium infusion, the presence of co-localized hyper enhancement is also evident on the LGE images (black arrows in bottom panel) in keeping with the other the imaging findings. 47

Figure 2.3 Strategy for obtaining short axis images in the same tridimensional orientation. The white lines on the localiser, long-axis and short axis pilots, and long axis cine indicate the slice positions for obtaining the subsequent views demarcated by the black arrows. (Abbreviations= HLA, horizontal long axis; VLA, vertical long axis; SA, short axis) 49

Figure 2.4. Improvement of image quality by shimming and frequency adjustment. On panel A, example of an off-resonance artefact (black arrow) and ringing artefact (red arrow). After performing shimming and frequency adjustment, the image quality has improved with no more artefacts visible. 51

Figure 2.5: Standardized Myocardial 17 segment model (segment number given in each segment) and Nomenclature for Tomographic Imaging of the heart. Adapted from A Statement for Healthcare Professionals From the Cardiac Imaging Committee of the Council on Clinical Cardiology of the American Heart Association [Cerqueira 2002]. 55

Figure 2.6: Bland-Altman chart illustrating the Inter observer variability for T2W continuous measurements of oedema (% LV myocardium) on 20 patients. Bias is 0.5 with a SD of 7.6, and 95% limits of agreements from -14.3 to 15.3 57

Figure 3.1. Assessment of change in signal intensity (S.I.) between affected bright myocardium and adjacent or remote unaffected myocardium. The oedematous myocardium (here indicated as OEDEMA ROI) was manually identified by drawing an ROI. The adjacent myocardium was identified as 1 or 2 depending on the anatomical position (either anticlockwise =1 or clockwise =2). The remote myocardium was the most distant from the oedema ROI..... 66

Figure 3.2 Phantom experiments to investigate the signal homogeneity of T2-prep SSFP sequence at 3T. Panels a and b: axial images across homogeneous phantom without (a) and with (b) correction for coil-sensitivity. Panel c and d: corresponding profiles across the isocentre in x (c) and y (d) direction. The grey trace corresponds to the uncorrected image ("magnitude") while the black trace corresponds to the corrected image from panel b ("normalized"). The coil sensitivity correction results in considerably improved homogeneity across the field of view. 68

Figure 3.3. Example of signal intensity gradient in a short axis image of a volunteer. The 4 ROIs in skeletal muscle are shown (white arrows) together with the corresponding mean ± SD. 70

Figure 3.4: Assessment of myocardial signal intensity (SI) variation in normal volunteers using a 6 equiangular segment model. Panel (A) Signal intensities of the myocardial walls in 3 volunteers in 2 different scans. I.S.=Inferior septum, A.S.= anterior septum, A.W.= anterior wall, L.W.= lateral wall, PL.W. = Posterolateral wall, I.W.= inferior wall. Panel (B). Example of a T2prep SSFP short axis image acquired in a volunteer. The red arrows indicate an area of increased signal intensity at the level of the septum in keeping with an artefact. 72
Figure 3.5: Signal intensities of T2-prep SSFP images of the myocardium in STEMI and NSTEMI patients. Signal intensities were measured in 4 different regions of the myocardium including the zone identified as bright (oedema), a remote region, and regions adjacent to the oedema (1 positioned clockwise and 1 anticlockwise of the oedema area). The signal intensity in the adjacent regions area shown significantly lower than the area with oedema. 75
Figure 4.1. Study protocol. Imaging time points (TP) in relation to the acute myocardial infarction (MI) and primary percutaneous coronary intervention (PPCI). For each TP, the CMR data acquired is given. CMR = cardiovascular magnetic resonance; LGE = late gadolinium enhancement. 84
Figure 4.2. Patient flow. Disposition of patients with STEMI recruited to this study, indicating numbers at each follow-up CMR examination up to six .. x months and reasons for loss from study. 89
Figure 4.3 T2W imaging Inter-observer differences. Bland-Altman chart illustrating the Inter observer variability for T2W continuous measurements of oedema (% LV myocardium) on 20 patients. 90
Figure 4.4. Time course of oedema. **A.** Mean percentage of LV volume positive for myocardial oedema at each time point. The volume of oedema remained stable in the first week post event with a significant decrease at 15 -17 days with near resolution by 6 months. **B.** The time course of oedema and resolution is given for each patient. There was a large range of LV % volume of oedema (0 to 60%). This analysis on an individual level confirms the constancy of oedema measured in the first 5-7 days, that is suggested in Panel A, with marked variation thereafter. Using the objective thresholding methods described in the text, a small number of patients had a substantial volume of apparent residual oedema at 6 months. 92
Figure 4.5. Segments with acute myocardial injury as identified either by presence of late gadolinium (LGE) and/or oedema in patients with STEMI..... 95
Figure 4.6. Impaired segments (% affected) as a function of the extent of segment positive for (A) oedema and (B) LGE at 24H. Segments with acute myocardial injury as identified either by presence of late gadolinium (LGE) and/or oedema. For both oedema and LGE, the probability of segmental dysfunction increased with the fraction of segment affected. For unaffected segments, as expected, a large majority showed normal function. 97
Figure 4.7. (A) Myocardial LGE early (12-48hrs) *vs.* late (6 months) and (B) wall motion improvement abnormalities. A. The myocardial volume (mean % ± SD) positive for LGE, decreased significantly from 12 - 48 hrs to 6 months.

The change in extent of LGE is also shown for each patient. Patients with unchanged LGE at 6 months are shown in gray while those with decreased LGE in black. Eleven patients out of 23 (46%) who underwent CMR at 6 months time, showed a reduction in LGE volume (of 38 ± 14%). In the remaining 13 patients, no reduction in size of the LGE volume was identified (23% ± 14% *vs.* 23% ± 14% respectively). **B.** Segments with improved function at six months (n = 68) broken down by extent of LGE within that segment LGE (none; 1-75% = partial thickness and 76-100% = full thickness) at both 24H and 6M. Across categories, the extent of LGE, measured at 12 - 48 hours (dark bars) was a poor predictor of functional recovery. Significantly, even segments showing full thickness LGE were associated with functional recovery. By contrast, LGE extent at 6 months (light bars) was strongly inversely correlated with improved function in that segment. 99

Figure 4.8. Representative CMR images. Oedema images (left column), acute LGE images (centre), chronic LGE (right column) are displayed. Three separate patients (rows A to C) representing alternative patterns of acute *vs.* chronic CMR features are shown. **A.** Oedema is present in inferior wall; the appearance of LGE is unambiguous as high signal zone that corresponds to the area of oedema, but there is no LGE present at 6 months. **B.** T2W image, on the left, shows oedema in the anterior wall; the acute LGE shows compact enhancement, which is reduced in size by 6 months. **C.** The oedema imaging confirms acute injury. In this example LGE present early persists without significant alteration to the 6 month time point. 100

Figure 4.9. Relationship between the extent of late gadolinium (LGE) and the Troponin I at 48 hrs. The correlation between the LV % of LGE (% LV_{score}) assessed at 6 months and troponin I assessed at 48 hrs ($R^2 = 0.8$; $P < 0.01$) is shown in comparison to the equivalent relationship with LGE measured at 12 - 48 hours ($R^2 = 0.5$, $P < 0.01$). 102

Figure 5.1. Matching angiographic and CMR segmentation analyses. The 16-segments coronary artery scheme (A) and the myocardial 17 segments model of the American Heart association (B) are here shown. Based on the plaque position, we matched the two schemes and we have extracted the correlations between various segments downstream the indexed plaque but also between segments and certain areas (left, right, proximal, distal) of the coronary tree. The legend at the top right shows some of the most representative correlations between anatomical location of the plaque in the vessel and the corresponding segments downstream of the indexed plaque. 116

Figure 5.2. Representation of segments remote and adjacent to injured segments. The scheme shows injury in the anterior wall (black lines). The injured segment adjacent to the injured myocardium is shown in red (red lines) while the remote in blue (blue lines) 118

Statistical analyses 119

Figure 5.3. Segments affected (by oedema and LGE on CMR) downstream the culprit and non culprit vessel in STEMI (Panel A) and NSTEMI (Panel B). In STEMI patients (Panel A), acute myocardial injury either by CMR oedema or LGE was depicted downstream the culprit vessel while virtually no injury was

shown downstream non-culprit stenosis. The number of segments positive for oedema was significantly larger than the number of segments positive for LGE. In the NSTEMI patients (Panel B), CMR showed acute oedema or LGE downstream both culprit and non-culprit vessels. While, the territory positive for oedema downstream the culprit was significantly larger than LGE, the area downstream the non-culprit by oedema was equivalent to the one LGE positive. (Adjacent segments have been excluded from these analyses). 127
Figure 5.4 Angiographic and corresponding acute CMR findings in STEMI (Panel A) and NSTEMI patients (Panel B). As showed in Panel A, most of the STEMI patients had single vessel disease at the angiogram. The CMR showed positive findings downstream in the culprit vessel territory in all patients. Most of the NSTEMI patients had multivessel disease: in 28% of these CMR showed positive acute findings downstream from a non –culprit plaque (Panel B). 128
Figure 5.5. Representative example of a patient with multivessel disease and acute injury by CMR in a territory downstream a vessel different from the one identified as culprit. On panels A, B and C, CMR images of acute oedema and LGE show acute myocardial injury in the inferior septum and inferior wall pertaining to the RCA. On the angiogram (Panels D and E) the RCA was occluded and the vessel identified as culprit and treated was the left anterior descending (LAD). 130
Figure 5.6. Representative case of a NSTEMI patient with multi-vessel disease and positive CMR downstream the non-culprit. As shown in Panel A and B, both oedema and acute LGE CMR show acute myocardial damage in the inferior wall downstream the right coronary artery (RCA). The angiogram (Panels C and D) revealed a significant stenosis at the level of the mid circumflex (Panel A) identified as the culprit plaque and two plaques of 48% and 31% stenosis in the proximal and mid RCA (Panel D). 131
Figure 5.7 Representative examples of acute myocardial injury by CMR in regions other than downstream the culprit or non-culprit vessels. T2W CMR (Panel A) depicted oedema in the inferior wall (red arrow) while the LGE imaging (Panel B) is negative. The angiogram shows single vessel disease with the culprit plaque located in the distal LCx (red arrow on Panel C) 132
Figure 5.8. Representative examples of acute myocardial injury by CMR in a patients with normal coronaries Both oedema (Panel A) and LGE imaging (Panel B) reveal acute injury in the inferior septum. However the angiogram (Panel C and D) showed normal coronaries. 133
Figure 5.9. A case of multivessel disease patient with positive acute oedema and LGE by CMR, both in the inferior and lateral (Panels A and B). At 6 months the LGE shows minor persistent positive findings in the lateral territory (Panel C). On the angiogram (Panels D to F) the circumflex was identified as culprit vessel and treated, while the LAD (mid) and the RCA (proximal and distal) were identified as non-culprit. 136
Figure 6.1. CMR protocol. Four different CMR techniques were included: T2W imaging for assessment of oedema, T1 mapping, functional cine imaging and late gadolinium enhancement for assessment of necrosis. Following the

acquisition of pilot and long axis images, matching short axis slices covering the full length of the ventricle were acquired using each of the different techniques. T2W and T1 mapping acquisitions were performed prior to the administration of contrast. Following gadolinium, cine imaging was performed. Ten-fifteen minutes post contrast and after the inversion time was meticulously adjusted for optimal nulling of remote normal myocardium, late gadolinium enhancement imaging was completed. 147

Figure 6.2 Panels A and B. Representative CMR images. Oedema images (left column), acute LGE images (center), and ShMOLLI T1-mapping (right column) are displayed. Two sets of images (Panels A and Panels B) corresponding to two separate patients are shown. *Top panels (A): a case of transmural inferior STEMI:* both oedema (T2W) and LGE depict an area of increased signal intensity; in the same region T1 mapping depicts significantly increased T1 values (shown in red) compared to the remote unaffected myocardium (normal T1 values shown in green). *Lower panels (B), a case of subendocardial NSTEMI* : Although the T2 W images show only a mild increase in brightness, there is an area of increased T1 values exceeding the area of LGE enhancement. Of note the peak troponin I was significantly different in the two patients (peak troponin I 50 mg / mL in the STEMI patient vs. 7 mg / mL in the NSTEMI patient). **Panels C and D**: **Correlation between T1 values and T2W normalized SI (Panel C) and between T1 values and LGE normalized SI (Panel D).** The SI of LGE (on the X axis, panel C) and T2W (on X axis Panel D), both normalized to the remote unaffected myocardium, are shown to correlate strongly with T1 values. 156

Figure 6.3. Receiver Operating Curves showing the diagnostic performance of T1-mapping compared toT2W in detecting acute injury in MI as derived from late gadolinium enhancement (LGE) scoring. In STEMI patients with acute myocardial infarction, the area under the curve for T2W (dashed line) was not significantly different from T1 mapping (solid line) indicating an equally good diagnostic performance of the two techniques (Panel A). In NSTEMI patients, the area under the curve for T2W (dashed line) was significantly smaller than that for T1 mapping (P = 0.004) indicating a significantly better diagnostic performance of T1 mapping. 158

Figure 6.4. Assessment of severity of injury by T1-mapping: relationship withT2W and LGE. Increasing T1 values distinguish increasingly larger segmental extent of injury, assessed by either LGE or T2W with T1 depicting 20% increments in LGE/T2W lesion extent. [Each * asterisk indicate the significant difference (P<0.01) in T1 values in each LGE/T2W category from the precedent one]. Although the overall relationship between T1 and T2 W is still significant (P<0.01 for the trend), there is an overlap in T1 values for segments with T2W segmental damaged fraction between 41 and 80%. Lesions with MO have been excluded from this analysis. 160

Figure 6.5. Assessment of severity of injury by T1-mapping: relationship with regional and global function. Panel A shows the relationship between T1 values and the extent of regional wall motion abnormalities (P < 0.01 for the

trendcorre). A highly significant negative correlation between mean LV T1 values and LV ejection fraction was also found (Panel B). 162
Figure 6.6. Quantitative assessment of microvascular obstruction by T1-mapping. Panel A shows a case of microvascular obstruction as depicted by LGE. The corresponding T1-map is shown in Panel B. The dark core of MO in the LGE image (arrows) is depicted by T1 values (Panel B) in the color range similar to remote myocardium (green). The surrounding injured myocardium (bright on LGE) shows high T1 values (red). Panel C shows quantitative analyses of the 7 cases with MO. T1 values in the MO regions are significantly lower than in the surrounding LGE-positive myocardium. 164
Figure 6.7. Likelihood of functional improvement at 6 m by T1 mapping and acute LGE in dysfunctional segments. Data are shown for 198 segments, which were dysfunctional acutely. Panel A shows the significant association between the likelihood of recovery of function of acutely dysfunctional segments and the T1 values in acute ($P < 0.0004$ fro the trend). Panel B shows the association between the likelihood of recovery of function of acutely dysfunctional segments and the segmental damaged fraction by LGE in acute ($P < 0.004$ for the trend). While the relationship between functional recovery and T1 was essentially linear, by using acute LGE (Panel B) the likelihood of improvement for segments with intermediate LGE did not correlate with the amount of damage. No MO segments were included in this analysis. 166

Index of Tables

Table 1.1 Summary of imaging techniques used in cardiac magnetic resonance to assess myocardial tissue changes and function. 20
Table 2.1. List of the data obtained analysing SA images acquired using different sequences 53
Table 2.2. Reproducibility of LGE quantification (% of LV myocardium) assessed with Bland-Altman test on 10 patients. 57
Table 3.1. Signal intensities in areas of oedema versus adjacent and remote myocardium in patients with acute myocardial infarction (both STEMI and NSTEMI) 73
T**able 3.2**. Signal intensities in affected and non-affected areas of the myocardium in patients grouped by location of the injured myocardium in the heart. Signal intensities of the oedematous regions are highlighted in grey. 77
Table 4.1. Patient characteristics 87
Table 4.2. CMR findings. 93
Table 4.3. List of segments included In CMR analyses at each time point. 94
Table 5.1. Patients' characteristics 120
Table 5.2. Angiographic findings 123
Table 5.3. CMR findings 124
Table 5.4. Distribution of segments positive for oedema on acute CMR and segments downstream the vessels on the angiogram. 126
Table 5.5. Distribution of segments positive for LGE on acute CMR and segments downstream the vessels on the angiogram 126
Table 5.6. Patients with lack of correspondence between CMR findings and angiographic findings 134
Table 6.1. Baseline characteristics of the study population 152
Table 6.2. CMR findings 153